Photovoltaics International

THE TECHNOLOGY RESOURCE FOR PV PROFESSIONALS

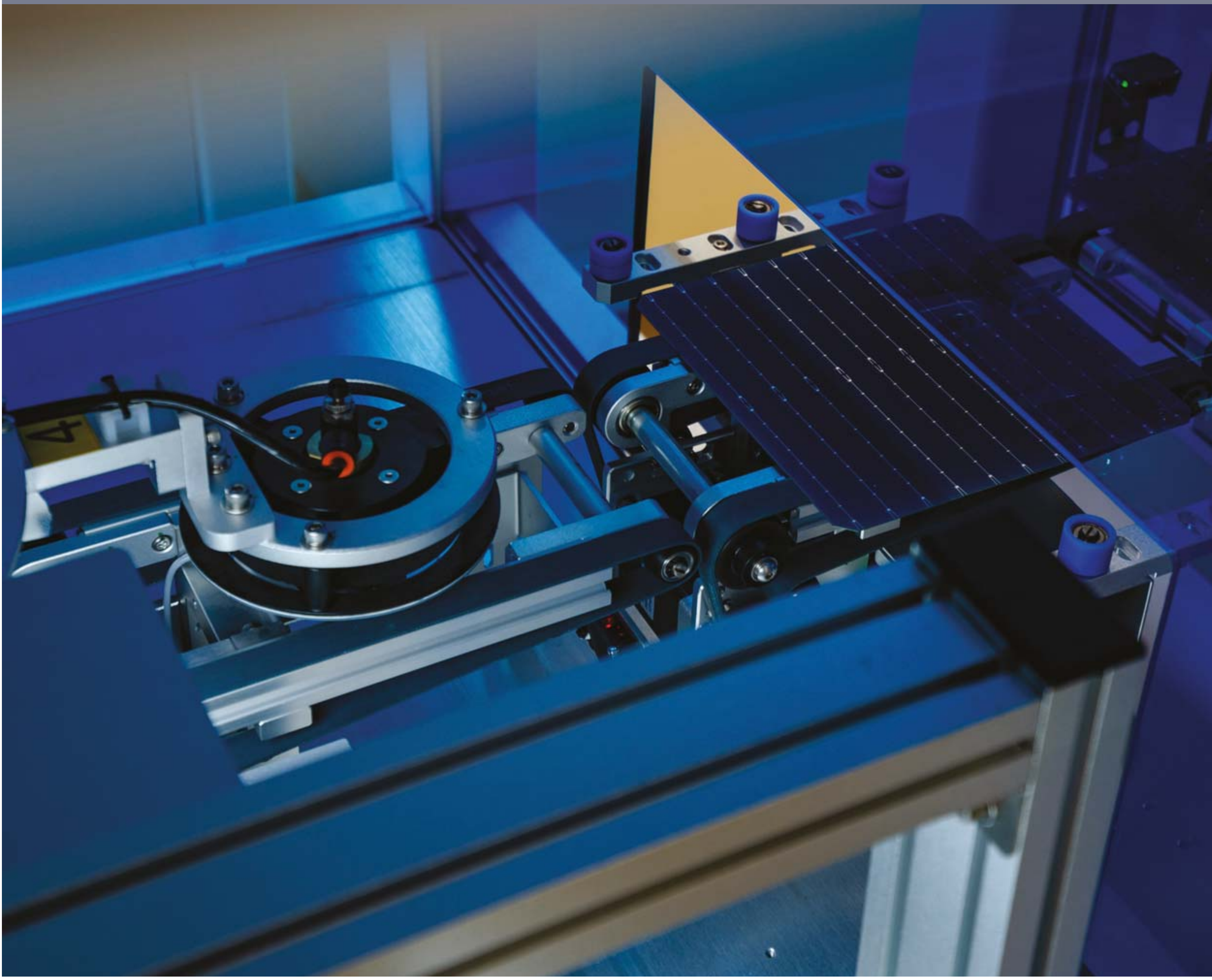

Edition 47

Future PV technologies
Cell efficiency records versus industrial reality

TOPCon's technology roadmap
LONGi discusses the route to TOPCon cell efficiency of 25.5%

PERC production
Fraunhofer ISE explores ways of increasing industrial throughput

The rise of ECAs
How industry trends and new technologies are driving conductive adhesives

Ni/Cu plating requirements
UNSW reviews fabrication technologies for mass production of Ni/Cu plated contacts

www.pv-tech.org
PVTECH .ORG

JA SOLAR

DeepBlue, Infinite Potential

DeepBlue 3.0 Series

DEEP BLUE 3.0 Light	DEEP BLUE 3.0	DEEP BLUE 3.0 Pro
415W+	550W+	560W+

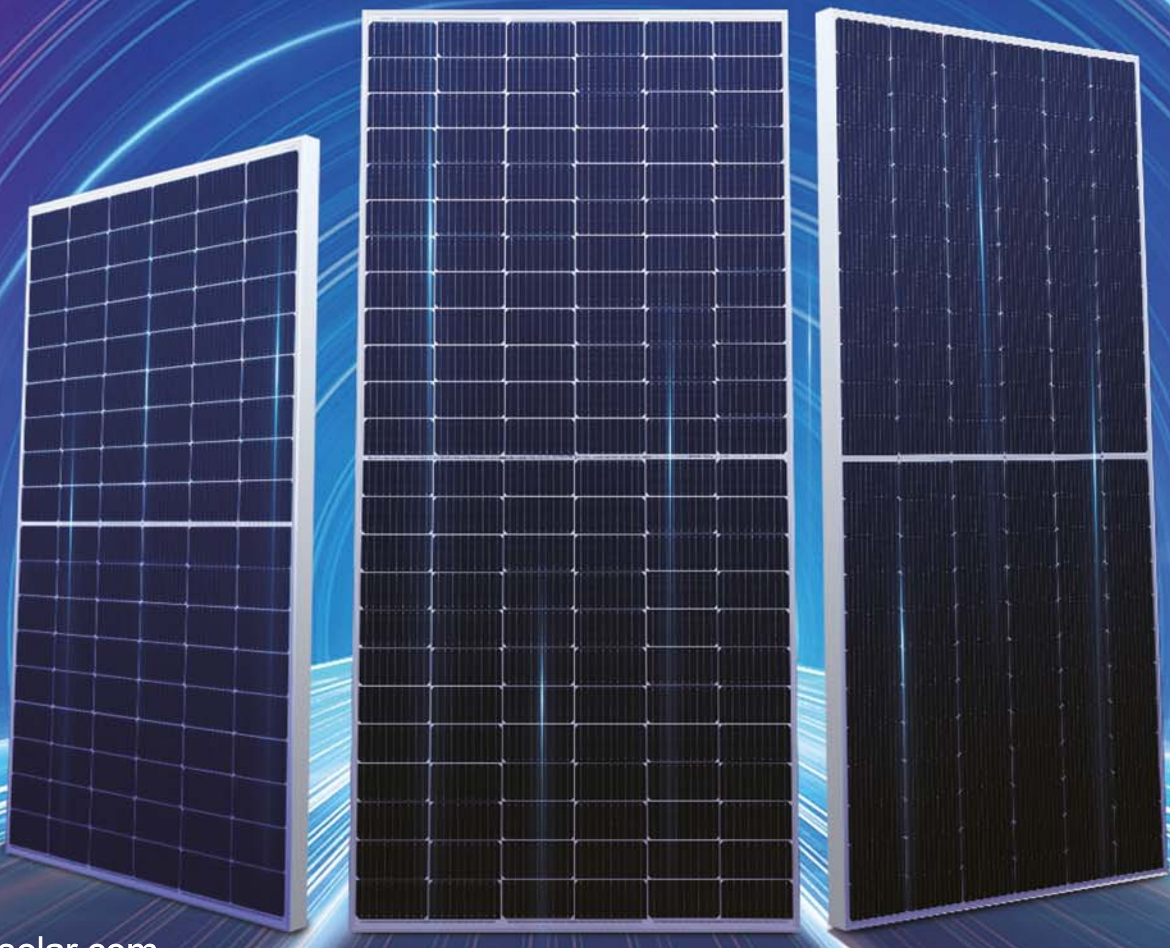

www.jasolar.com

Photovoltaics International

Published by:
Solar Media Ltd.,
123 Buckingham Palace Rd
Victoria, London SW1W 9SH
United Kingdom
T: +44 (0) 207 871 0122
T: +44 (0) 7827 885311
E info@pv-tech.org
www.pv-tech.org

Publisher: **David Owen**

Editor in Chief: **Liam Stoker**
Technical Publishing Director: **Mark Osborne**
Commissioning Editor: **Adam Morrison**
Sub-Editor: **Steve D. Brierley**
Design: **Tina Davidian**
Production: **Daniel H Brown, Sarah-Jane Lee**
Sales Director: **David Evans**
Account Managers: **Adam Morrison, Graham Davie, Lili Zhu**

Cover image: Jolywood

Printed by Buxton Press

Photovoltaics International
Forty Seventh Edition
November 2021
Photovoltaics International is a six monthly journal published in February and September each year.

Distributed in the USA by Mail Right International, 1637 Stelton Road B4, Piscataway, NJ 08854.

ISSN: 1757-1197

USPS Information
USPS Periodical Code: 025 313

Periodicals Postage Paid at
New Brunswick, NJ
Postmaster: Send changes to:
Photovoltaics International,
Solar Media Ltd., C/o 1637 Stelton Road,
B-4, Piscataway, NJ 08854, USA

Foreword

Welcome to Photovoltaics International 47. When we last published a volume of PVI in May of this year, we'd been covering news of supply chain volatility and manufacturing constraints for approximately three months. At the time it was considered that said volatility would be short-lived, an otherwise momentary blip on PV's path to pricing dominance over other energy generation technologies.

But, some six months later, the industry still finds itself gripped by material prices. Recent months have seen polysilicon prices spike once more, while the cost of other materials and components including silver, aluminium, glass and encapsulants soar as well.

All of this has occurred at a time of a step change, both for global power systems – which are turning to solar PV at a near frenetic speed – and indeed within the solar upstream, which is hurtling along its technology roadmap, perhaps quicker than previously anticipated.

It was evident earlier this year that module makers were turning to n-type en masse. Most of the 'Solar Module Super League' members demonstrated some form of n-type product at this year's SNEC exhibition in China and, since then, n-type – and particularly TOPCon – products have begun to be released.

In PVI47, you can read why the industry is shifting to n-type and TOPCon at such speed. LONGi – one of those module makers to have launched a TOPCon module this year – documents the efficiency limits of TOPCon solar cells and what the roadmap looks like for the industry to reach them.

With so much talk of n-type, you could be forgiven for thinking that mono PERC manufacturing is all but finished. But is the talk of its demise greatly exaggerated? While most industry observers conclude that PV manufacturing will have shifted predominantly to n-type by 2025, there will still be a sizeable market share for p-type mono PERC for much of the remaining decade and, in a paper produced by Fraunhofer ISE for this journal, you can read how research is uncovering ways of increasing the throughput of industrial PERC production.

And there are words of caution for the industry from ISC Konstanz Radovan Kopecek and Joris Libal, who discuss here the recent tranche of broken cell efficiency records and what they actually mean for industrial, scale manufacturing.

As 2021 concludes, it's fair to say that swathes of solar's upstream industry will not look back on it as one to remember. The next year will, however, begin with significant promise for solar PV and, as the pages of this journal will attest to, this is an industry ready to grasp it with both hands.

Thank you for reading, and we hope you enjoy the journal.

Liam Stoker
Editor in chief
Solar Media Ltd.

Editorial Advisory Board

Photovoltaics International's primary focus is on assessing existing and new technologies for "real-world" supply chain solutions. The aim is to help engineers, managers and investors to understand the potential of equipment, materials, processes and services that can help the PV industry achieve grid parity. The Photovoltaics International advisory board has been selected to help guide the editorial direction of the technical journal so that it remains relevant to manufacturers and utility-grade installers of photovoltaic technology. The advisory board is made up of leading personnel currently working first-hand in the PV industry.

Our editorial advisory board is made up of senior engineers from PV manufacturers worldwide. Meet some of our board members below:

Prof Armin Aberle, CEO, Solar Energy Research Institute of Singapore (SERIS), National University of Singapore (NUS)

Prof Aberle's research focus is on photovoltaic materials, devices and modules. In the 1990s he established the Silicon Photovoltaics Department at the Institute for Solar Energy Research (ISFH) in Hamelin, Germany. He then worked for 10 years in Sydney, Australia as a professor of photovoltaics at the University of New South Wales (UNSW). In 2008 he joined NUS to establish SERIS (as Deputy CEO), with particular responsibility for the creation of a Silicon PV Department.

Dr. Markus Fischer, Director R&D Processes, Hanwha Q Cells

Dr. Fischer has more than 15 years' experience in the semiconductor and crystalline silicon photovoltaic industry. He joined Q Cells in 2007 after working in different engineering and management positions with Siemens, Infineon, Philips, and NXP. As Director R&D Processes he is responsible for the process and production equipment development of current and future c-Si solar cell concepts. Dr. Fischer received his Ph.D. in Electrical Engineering in 1997 from the University of Stuttgart. Since 2010 he has been a co-chairman of the SEMI International Technology Roadmap for Photovoltaic.

Dr. Thorsten Dullweber, Head of PV Department at the Institute for Solar Energy Research Hamelin (ISFH)

Dr. Thorsten Dullweber is leading the PV Department and the R&D Group Industrial Solar Cells at ISFH. His research work focuses on high efficiency industrial-type PERC and bifacial PERC+ silicon solar cells, where he co-authored more than 100 Journal and Conference publications. Before joining ISFH in 2009, Thorsten worked as project leader for DRAM memory chips at Infineon Technologies AG. He received his Ph. D. degree in 2002 for research on Cu(In,Ga)Se2 thin film solar cells. Thorsten is member of the Scientific Committees of the EU-PVSEC and SNEC conferences.

Dr. Wei Shan, Chief Scientist, JA Solar

Dr. Wei Shan has been with JA Solar since 2008 and is currently the Chief Scientist and head of R&D. With more than 30 years' experience in R&D in a wider variety of semiconductor material systems and devices, he has published over 150 peer-reviewed journal articles and prestigious conference papers, as well as six book chapters.

Florian Clement, Head of Group, MWT solar cells/printing technology, Fraunhofer ISE

Dr. Clement received his Ph.D in 2009 from the University of Freiburg. He studied physics at the Ludwigs-Maximilian-University of Munich and the University of Freiburg and obtained his diploma degree in 2005. His research is focused on the development, analysis and characterization of highly efficient, industrially feasible MWT solar cells with rear side passivation, so called HIP-MWT devices, and on new printing technologies for silicon solar cell processing.

Dr. Jochen Rentsch, Head of department "Production technology – Surfaces and Interfaces", Fraunhofer Institute for Solar Energy Systems (ISE), Germany

Dr. Rentsch received his Ph.D degree in physics in 2005 from the Albert-Ludwigs University of Freiburg, Germany. He studied physics at the Technical University of Braunschweig and the University of Sussey (Brighton, UK) and obtained his diploma degree in 2002.

His current work focusses on the acquisition and management of public and industrial funded projects, the publication and licensing of R&D results, the transfer of processes and cell structures in the PV industry as well as consultancy on and auditing of PV manufacturing facilities worldwide.

Finlay Colville, Head of Market Intelligence, Solar Media

Finlay Colville joined Solar Media in June 2015 as head of its new Solar Intelligence activities. Until October 2014, he was vice president and head of solar at NPD Solarbuzz. Widely recognised as a leading authority on the solar PV industry, he has presented at almost every solar conference and event worldwide, and has authored hundreds of technical blogs and articles in the past few years. He holds a BSc in Physics and a PhD in nonlinear photonics.

Photovoltaics International remains the solar PV industry's only independent technical journal, carrying papers written by recognised industry experts and leaders in their field, highlighting technological innovation and manufacturing excellence to drive the sector forward. The PVI advisory board therefore plays a critical role in ensuring that the themes and topics covered in each volume of the journal are truly representative. Members of PVI publisher Solar Media's publishing team liaise with the advisory board on a regular basis and ahead of each volume of the journal to establish industry trends, qualify the journal's selection of papers and guarantee technical relevance. For more information on the Photovoltaics International advisory board, contact info@pv-tech.org.

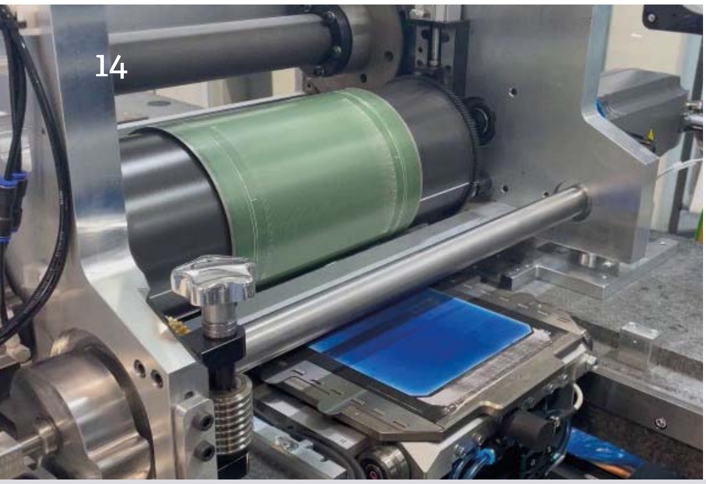

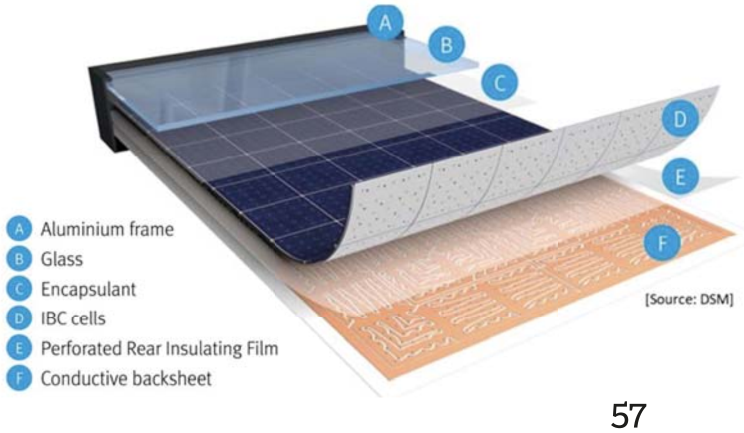

Contents

3 Foreword

4 Editorial Advisory Board

8 Products

10 News

Section 1: **Cell Processing**

14 Increasing the throughput of industrial PERC production
Marius Meßmer, Andreas Wolf, Martin Zimmer, Fabian Meyer, Georg Hoppe, Andreas Lorenz, Sebastian Tepner, Daniel Ourinson, Gernot Emanuel, Sebastian Nold, Baljeet Goraya & Florian Clement, Fraunhofer Institute for Solar Energy Systems (ISE), Freiburg, Germany

27 TOPCon solar cells – Technology roadmap for 25.5%-efficiency industrial manufacturing
Xinxing Xu, Zhaowei Wang, Hongbo Tong & Hua Li, Longi Green Energy Technology Co., Ltd., Xi'an, Shaanxi, China

37 Future industrial solar PV technologies: Record cell efficiency announcements versus industrial reality
Radovan Kopecek & Joris Libal, International Solar Energy Research Center ISC Konstanz, Germany

45 Technology requirements for Ni/Cu plating metallization in commercial PV
Yuan-Chih Chang[1], Sisi Wang[1], Rong Deng[1], Xiaoli Li[2], Beibei Zhu[3], Shaoyuan Li[4] & Jingjia Ji[1]
[1]School of Photovoltaic and Renewable Engineering, University of New South Wales, Sydney, Australia; [2]Shenzhen Institute of Advanced Technology, Chinese Academy of Sciences, China; [3]School of Materials Science and Engineering, Southeast University, China; [4]Faculty of Metallurgical and Energy Engineering, Kunming University of Science and Technology, China

Section 2: **PV Modules**

57 The sun is rising on conductive adhesives
Daniel Tune[1], Torsten Rössler[2], Gernot Oreski[3], Carolyn Carriere[4], Christina Kaiser[2], Tudor Timofte[1], Nils Klasen[2,5], Julian Weber[2], Bengt Jäckel[6], Stephan Großer[6], Matthias Pander[6], Marko Turek[6], Marco Galiazzo[7], Ignacia Devoto[1,8], Thomas Fischer[9], Ingo Ullmann[1], Dominik Rudolph[1] & Andreas Halm[1]
[1]International Solar Energy Research Center ISC Konstanz, Germany; [2]Fraunhofer Institute for Solar Energy Systems ISE, Freiburg, Germany; [3]Polymer Competence Center Leoben PCCL, Leoben, Austria; [4]French Alternative Energies and Atomic Energy Commission CEA, France: [5]Institute for Applied Materials – Materials and Biomechanics IAM-WMB, Karlsruhe Institute of Technology KIT, Germany; [6]Fraunhofer Center for Silicon Photovoltaics CSP, Halle (Saale), Germany; [7]Applied Materials, Inc., Santa Clara, California, USA; [8]Faculty of Natural Sciences II, Martin Luther University, Halle-Wittenberg, Germany; [9]teamtechnik GmbH, Freiberg, Germany

78 Subscription / Advertisers Index

Control every step
of your PV value chain.

Secure quality.
Improve processes.
Save costs.

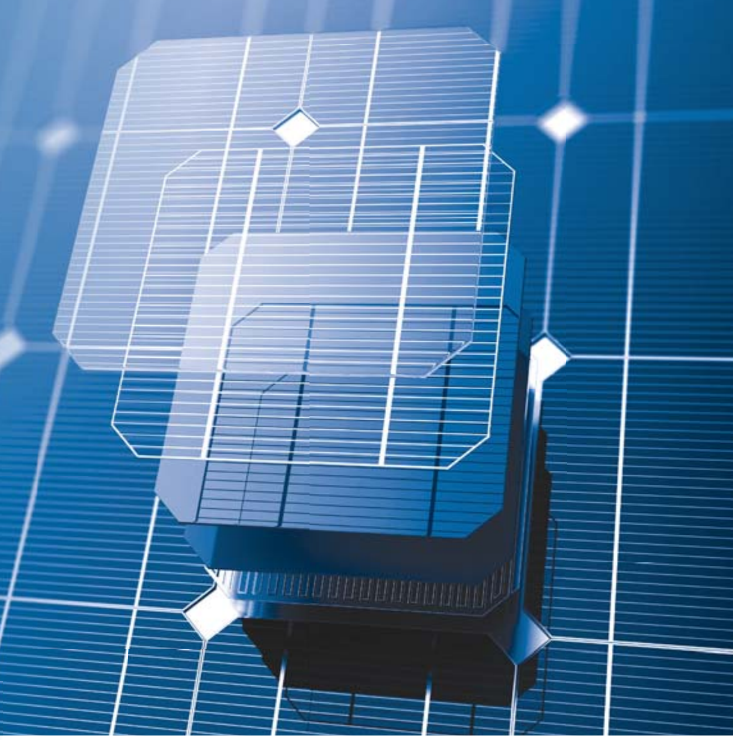

FabEagle® MES

FabEagle® MES – your software for manufacturing operations.

- PRODUCTION VISUALISATION
- ONLINE PROCESS VISUALISATION
- WORK ORDER MANAGEMENT
- WORK PLAN MANAGEMENT
- PRODUCTION CONTROL
- RECIPE MANAGEMENT
- MATERIAL TRACKING
- MACHINE & PROCESS DATA
- REPORTING
- ONLINE-SPC
- EVENT MANAGEMENT
- MAINTENANCE MANAGEMENT
- LOGBOOK/DAILY MACHINE LOG
- LONG TERM ARCHIVING

Find out more about our products and solutions:

www.kontron-ais.com
info@kontron-ais.com

www.k-ais.de/mes

kontron S&T Group

Kontron AIS GmbH

THE BENCHMARK IN INDUSTRIAL SOFTWARE

Product reviews

Cell Processing: **3D-Micromac**

3D-Micromac introduces new laser system for half- and shingled-cell cutting in photovoltaic manufacturing

Product outline: 3D-Micromac has launched an advanced laser cutting system specifically for half-cut and shingled solar cells. Dubbed the microCELL MCS, the advanced laser system has been designed to meet the global solar market's demands for enhanced module power output and service life by minimising power losses and allowing for high mechanical strength of cut cells.

Problem: The cutting of solar cells into half- or triple-cut versions has become a key strategy for PV manufacturers, enabling significant gains in power output and mechanical strength at the module level. This trend has been accompanied by a shift to larger full-cell module formats and associated increases in power ratings. Cutting cells into two or three, as well as shingling, compensates for increased power losses associated with the higher cell currents produced by larger area wafers, with cell cutting set to remain at the heart of PV manufacturing. This has placed considerable importance on effective and precise cutting technologies capable of catering for PV manufacturers' needs.

Solution: The microCELL MCS system uses 3D-Micromac's patented thermal laser separation (TLS) process for cell separation. The ablation-free technique guarantees improved edge quality and, as a result, the separated cells have up to 30% higher mechanical strength when compared to those subjected to ablative laser processes, enabling reduced power degradation over the resultant module's life cycle. By reducing edge recombination losses and allowing for cutting edge passivation, TLS has been shown to achieve module power gains of at least 2W.

German manufacturer Heckert Solar has purchased two microCELL MCS systems for its plants in Thuringia (LWD Solar) and Chemnitz.

Platform: The microCELL MCS includes a one-pass contactless dicing process, which provides higher mechanical stability compared with conventionally processed cells. While it has inherent flexibility on the number of cell cuts, with half-cut cells being the standard configuration, the system is able to produce up to six-cut cells without decreasing throughput.

The system can produce more than 6,000 wafers per hour and is also upgradeable, allowing for easy integration of additional laser modules to increase the number of cell cuts if required. Furthermore, it is futureproofed to accommodate wafer sizes of up to M12/G12 (210mm) and is suitable for cells with temperature-sensitive coatings or depositions, including heterojunction cells.

Availability: The 3D-Micromac microCELL MCS is available now.

Cell Processing: **Exateq**

Exateq's Batch Wet Bench q612 – ready for 1 GW

Product outline: Exateq's q600 platform has been revised to accept wafer sizes up to M12/G12, including half cut cells. Appropriate carriers are manufactured by and available from exateq. Based on 600 wafers per batch and a throughput capability of 12,000 wafers per hour, the plus one system can support a production line of up to 1GW

Problem: All of exateq's wet bench platforms were designed at a time when M4 was the maximum conceivable wafer size. When M6 (166mm) was introduced, the platforms were already able to accept this size too. Only a few months after the industry had accepted this size and was making necessary adaptations, 210mm (M12/G12) was stipulated as the new and next wafer size. No existing equipment was capable of handling such a jump in size, meaning the industry has had to invest into new production lines.

Solution: What used to be a q400, exateq's platform and wet bench for 400 w/h, became a q406 as its maximum capability was M6. A new platform was created for M12: q412. Likewise with the q600, capable of 12,000 w/h and operating in the field for four years already, and the q612 has had to be created.

This step-up in wafer size causes the wet bench to be extended by 25%. A typical q412 texturing system for SHJ application is beyond 20 metres in length, while customized q612 systems ended up touching the 30 metre mark. Considering that respective tanks hold up to 1m³ of solution, this is new to the PV industry.

As production does not accept prolonged downtimes, there is a need to ensure that supply, disposal and make-up capabilities are sufficient for this much larger volume.

The q612 has a nominal throughput of 12,000 w/h and beyond, equating to respective annual power outputs of 800MW up to 1GW, subject to wafer efficiency.

Applications: While texturing systems are the most popular, all conceivable processes can be transferred to a q612.

Platform: New platforms are the q412 and q612, a derivative thereof is the qX10 where the tank size is adapted to M10 wafers to reduce CoO, if this is deemed to be the maximum wafer size. The actual output depends on the process requirements and their translation into the wet bench design. q400 systems in operation achieve more than 7000 w/h, so far q600 systems have not been pushed to their limit. The latest q612 designs focus on a throughput of around 12,000 w/h.

Maximum wafer size	M6	M10	M12
400 w/batch	q406	q410	q412
600 w/batch	q606	q610	q612

Obviously, with M12 cells manufactured in production R&D has to get up to the same capability which exateq picked up immediately by offering a q2512. This can be a manual, semi-automatic or fully automatic lab wet bench with tanks accepting 25 wafers of M12 size. With it still being very compact it is popular with research institutes.

Beyond all this, the new designs could be a basis for 200mm/8" semiconductor applications.

Availability: Last quarter of 2021 onwards.

Product reviews

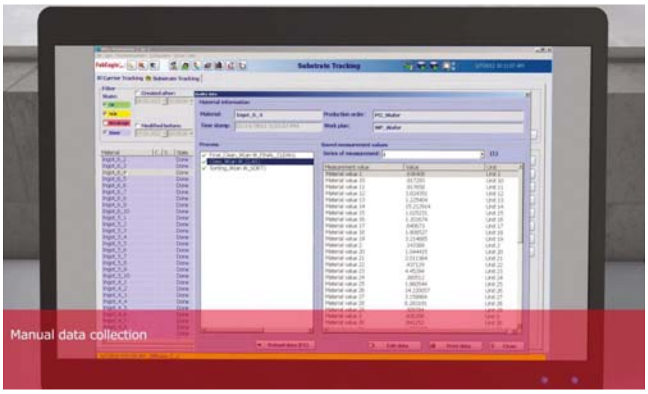

Cell Processing: **Kontron AIS**

Kontron AIS delivers FabEagle MES solution to PV manufacturers to secure quality, optimise processes and save costs

Product Outline: Kontron AIS is supporting PV manufacturers with a standardised Manufacturing Execution System (MES) for production control, material track and trace and equipment performance tracking, covering all processes from crystal growing over wafer and solar cell production to module assembly. The MES has proven its ability to secure quality, optimise manufacturing processes and save costs across the PV industry for over 15 years.

Problem: The challenge is to integrate an MES system which allows a PV manufacturer to closely control every step of the value chain. This requires a full vertical integration of manufacturing processes like crystal growing, wafering, solar cell processing and solar module assembly.

Manufacturers install such MES to achieve traceability for all products from raw silicon through crystal, ingot, wafer, solar cell up to the finished solar module. The goal is to keep track of all transactions and operations to determine precisely what was done to the product, when it was processed, at which equipment and under which conditions.

Solution: Process and equipment data acquisition is conducted using various standard compliant equipment interfaces like SECS, PV2, XML, OPC-UA and S7. These interfaces are used to reliably communicate the equipment state, material movement, process parameter and equipment data.

Material and carrier interlock commands are used to prevent material mishandling and to enforce the orderly execution of steps in work plans. Product yield is improved, and scrap reduced by enforcing the execution of the work plan and tightly controlling and monitoring manual and automatic material processing.

Material tracking and tracing data ensures besides correct inventory data and end-to-end backward and forward genealogy. Backward tracking starts from the finished solar module relating it back to solar cells, wafers, ingot, crystal, raw silicon and related consumables to build a module. Forward tracking starts from raw silicon tracking it to all the finished solar modules that were produced using a certain silicon lot.

Real-time connection to the ERP system is used to continuously exchange master data, work orders, production progress and quality information to keep track of semi-finished and finished product inventory and the associated consumption of raw material and consumables.

The acquired equipment data is used to calculate KPIs like OEE. This allows closely monitoring and improving equipment performance.

Applications: Crystal growing (e.g. Czochralski process) including silicon commissioning with recipe handling, different raw silicon types, dopant, seeds, crucible, hot zone part tracking, re-charge scenarios, multiple crystal unloads, scrap handling, manual data collection, yield and inventory tracking, cropping, automatic and manual lifetime, resistivity measurement, tracking of cropped parts and scrap recycling of silicon including etching and sorting.

Wafering processes including inspection, mounting, squaring, chamfering, slicing, singulation, pre- and final cleaning, classification and sorting.

Solar cell processing, batch and single wafer processes including texturing, diffusion, CVD, PVD, PECVD, printing, classification and sorting, transport system tracking, virtual wafer tracking and consumable tracking.

Solar module assembly processes including glass washing, stringing, matrix layup, inspection and rework, lamination, framing, junction box mount, flashing and palletising.

Platform: Integrates seamlessly in local IT infrastructure or public cloud environments

Availability: Available worldwide now.

PV Modules: **JinkoSolar**

JinkoSolar's next-generation n-type ultra-high efficiency Tiger Neo Modules

Product Outline: JinkoSolar has launched a new series of ultra-efficient Tiger Neo Modules. The new module adopts n-type tunnel oxidised passivated contact (TOPCon) technology with further enhancements in performance, power, energy density and reliability. The new module delivers a maximum power output of up to 620W in mass production, with an ultra-high efficiency of up to 22.30%.

Problem: The solar cell efficiency of PERC is approaching its limits of 24.5%, and new cell technology is needed to deliver breakthroughs in conversion efficiency, power output and levelised cost of energy (LCOE). With higher efficiency and a higher bifacial factor, lower degradation, lower working temperature and better low-irradiance performance, n-type TOPCon technology is touted to be the next-generation mainstream technology after mono PERC.

Solution: JinkoSolar adheres to a philosophy of high power and high efficiency, and the company is to enhance both by integrating n-type TOPCon technology, M10 (182mm) silicon wafers, a 78-cell specification, multiple busbars and stitch welding technology. JinkoSolar claims its N-type TOPCon technology provides about 5% to 6% more efficiency than mono PERC and about 3% to 4% more energy generation. The Tiger Neo module has an ultra-high efficiency of up to 22.30%, a bifacial factor of up to 85% compared with ~70% for p-type, and a lower temperature coefficient of -0.30%/ compared with -0.35%/ for p-type. Thanks to a reduced LID and LeTID risk, JinkoSolar provides a 30-year linear power output warranty, with first-year degradation of less than 1% and power output guaranteed to be no less than 87.40% of nominal power output after 30 years.

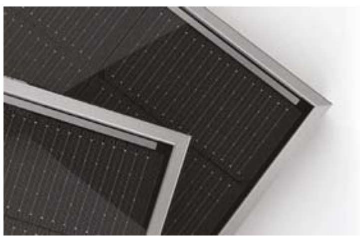

Applications: Large-scale utility, industrial and commercial distributed generation, and residential PV applications.

Platform: The Tiger Neo monofacial module measures 2465mm*1134mm*35mm and weighs 30.6kg in the 156 half-cut monocrystalline cell configuration, with module power range of 595~615W.

Availability: Mass production starts from Q1 2022.

News

Fraunhofer ISE and M10 industries unveil new matrix shingle technology

Credit: Fraunhofer ISE

Fraunhofer ISE said the technology was best suited for integrated solar applications and facades.

The Fraunhofer Institute for Solar Energy Systems ISE and M10 Industries have unveiled a new matrix shingle technology for connecting solar cells which is claimed to produce modules 2 – 6% more efficient than those using conventionally connected half-cut cells. Under the approach, the stringer arranges shingle solar cells in an offset fashion likened to how bricks are laid in a masonry wall. This arrangement boosts the efficiency of the module while also improving shading tolerance, the duo said. Fraunhofer ISE said the technology goes "one step further" than conventional shingled solar module technologies, wherein individual cells are overlapped in a shingle arrangement to reduce the space between solar cells of a string, resulting in smaller currents and higher efficiencies. The matrix arrangement allows for a more complete use of the entire module area, producing modules which are up to 6% more efficient than modules using conventionally connected half-cut solar cells. Meanwhile, the matrix also allows for current to flow around shaded areas of the module, potentially doubling the amount of power a module can produce while under partial shading.

POLICY

US trade agency promotes four-year extension of Section 201 tariffs

The US International Trade Commission (ITC) has recommended that President Joe Biden extend tariffs on imported crystalline silicon PV cells and modules for another four years. In a report explaining its decision, the ITC said that although the domestic industry is making a "positive adjustment" to import competition, the safeguard measure "continues to be necessary to prevent or remedy serious injury". The tariffs are currently due to expire in February. The commission recommends that Biden maintains the duty on imports of cell and modules – currently at 15% – but with the rate decreasing by just 0.25 percentage points as of 7 February 2022, and then continuing to drop by the same rate in each of the following three years. It also suggests maintaining a tariff exemption for the first 2.5GW of cells imported annually. The ITC said in the report that given the industry's "already poor financial condition", as well as the impediments that the domestic sector has faced to its adjustment efforts, such as the bifacial exclusion and COVID-19, an extension of less than four years "would not appear to be sufficient for the industry's efforts to adjust to import competition".

A-SMACC members 'evaluating all options' after AD/CVD petition rejection

US solar manufacturers behind the controversial anti-circumvention petition have said they are "evaluating all options" and could refile petitions in the future. Following a decision by the US Department of Commerce to throw out a petition alleging circumvention of anti-dumping and countervailing duties (AD/CVD) by Chinese solar manufacturers via Southeast Asia-based subsidiaries, American Solar Manufacturers Against Chinese Circumvention (A-SMACC) issued a statement saying the group "strongly disagrees" with Commerce's rationale behind its verdict. "Above all, we will not cede monopoly power to China and to Chinese-owned companies on solar products. U.S. solar manufacturing is recovering, and the future is bright, but we should not have to compete with the unfair trade practices of China and Chinese-owned companies. We should ensure that America, which invented solar technology, leads the next generation of solar manufacturing, R&D, and deployment," the statement read.

India planning more than five-fold increase in funding for PLI solar manufacturing scheme

India's government is set to scale up funding for its production-linked incentive (PLI) programme for solar manufacturing as it eyes exports of PV equipment. While the scheme was originally designed to allocate INR 45 billion (US$604 million) over five years to back the domestic development of high-efficiency PV modules, this will be increased to INR 240 billion (US$3.22 billion), said India's minister of new and renewable energy, RK Singh. A petition to sanction additional funds for the programme has been approved in principle by the government, Singh told news agency PTI, adding: "We would be exporting solar equipment."

R&D

US DOE unveils support for advanced materials research

The US Department of Energy (DOE) is to fund the development of advanced materials such as perovskites. Included within a US$40 million package of funding supporting projects aiming to enhance and develop novel solar technologies in October, the DOE revealed it would support a range of research initiatives underway at US universities and research labs. Institutes to receive funding include the likes of Columbia University, National Renewable Energy Laboratory and New York University, amongst others, with topics including encapsulation materials to prevent perovskite degradation and the development of new nanomaterials for use in CadTel modules.

CdTe breakthrough could lead to more efficient solar cells

New insight into how chlorine enhances the performance of cadmium telluride (CdTe) cells could result in even higher efficiencies, according to a team of researchers at Loughborough University in the UK. The group is aiming to understand the role of chlorine in both improving cell efficiency and also in removing defects known as stacking faults. A previous study from the team showed that grain boundaries, where crystals of different orientation join together, are responsible for poor cell efficiency. These grain boundaries have defects that can act as traps for electrons, making these areas 'active'. During the passivation process, the scientists showed chlorine can deactivate some of the traps and make the grain boundaries less active – therefore increasing the efficiency of CdTe. While the missing piece was said to be understanding how the stacking faults disappear, the new research shows that if there is enough chlorine in the grain boundaries, a cascade mechanism is triggered that structurally removes these stacking faults.

PVEL releases new hail test

PV Evolution Labs (PVEL) has released a new hail test for its PV Module Product Qualification Programme (PQP). The hail stress sequence was added to the PQP after concerns from insurers and asset owners about the ability of modules to withstand the impact of severe hail. PVEL took data from nearly 1GW of hail-damaged projects that it has evaluated as well as test results from in-lab experiments.

EFFICIENCY RECORDS

LONGi sets new heterojunction cell efficiency record of 25.82%

LONGi in October 2021 claimed a new record conversion efficiency of 25.82% for its commercial-sized heterojunction (HJT) solar cells. Validated by the Institute for Solar Energy Research (ISFH), the achievement has seen the manufacturer beat a previous record of 25.26%, which it set less than five months prior when it also achieved a record cell efficiency for a p-type monocrystalline bifacial TOPCon solar cell of 25.02%.

JinkoSolar claims new record taking n-type cell conversion efficiency to 25.4%

JinkoSolar laid claim to a new n-type monocrystalline silicon solar cell conversion efficiency record in October 2021, taking that efficiency rating to 25.4%. The record was set by a JinkoSolar-made large-size passivating contact solar cell and independently confirmed by the Japan Electrical Safety and Environment Technology Laboratories (JET). The cell was fabricated on a high-quality Czochralski mono-Si substrate utilising technologies such as ultrafine line metallisation, advanced diffusion, low parasitic absorption material and JinkoSolar's proprietary n-type HOT cell design, which is based on tunnel oxide passivation contact (TOPCon) technology. Various material upgrades were also integrated into the cell process, Jinko said.

Trina Solar sets 210mm PERC cell efficiency record of 23.56%

Trina Solar has achieved a new record efficiency of 23.56% for its mass production 210mm p-type monocrystalline silicon PERC cells. The 'Solar Module Super League' (SMSL) member said the result, recorded in August 2021, was achieved at its State Key Laboratory of PV Science and Technology and had been independently confirmed by the National Center of Supervision and Inspection on Solar Photovoltaic Product Quality.

MATERIALS

Solar Inventions receives US patent for silver cost-saving cell process

New architecture for solar cells that can increase power generation and reduce silver costs is closer to commercialisation after the company behind the technology secured a patent in the US. US-based start-up Solar Inventions said its Configurable Current Cells, or C3, innovation has been awarded a patent from the US Patent and Trademark Office, potentially opening the door to licensing from PV manufacturers. The technology stems from the work of the company's chief technical officer and former Suniva engineer Ben Damiani, who discovered he could create multiple 'lanes' or sub-cells on a single wafer by electrically dividing each cell during the metallisation process. "The benefits are similar to half-cells, also a major solar industry trend, but without requiring cells to be physically broken and rewired," Damiani said.

Daqo begins pilot production at new polysilicon facility

Daqo New Energy has begun pilot production at its new 35,000MT Phase 4B polysilicon production facility, which has been completed ahead of schedule. Daqo expects to significantly ramp up production at the site to a full capacity of 105,000MT per year by the end of Q1 2022. The company has a target of achieving total annual production capacity of 270,000MT by the end of 2024, however in October its CEO Longgen Zhang warned that the pace of polysilicon capacity expansion could slow in the future because of quotas concerning energy consumption in China. Zhang said the company "will continue to execute our three-year plan to expand our production capacity to 270,000MT by the end of 2024" and that it would also "continue to improve our product quality to be market-ready for the next generation N-type technology."

Hanwha buys large stake in REC Silicon, looks to restart US polysilicon production
Hanwha Solutions Corporation has agreed to buy a 16.67% stake in Norwegian polysilicon manufacturer REC Silicon in a deal worth around US$160 million, with the South Korean chemical company looking to reopen REC Silicon's 20,000MT polysilicon factory in the US. Under the deal Hanwha, which wholly owns module maker Q CELLS, will purchase around 70 million shares from REC silicon and Aker Horizons, with each share being worth NOK20 (US$2.28), resulting in a 16.67% stake.

JinkoSolar to invest US$70m in 100,000MT Tongwei polysilicon plant
'Solar Module Super League' manufacturer JinkoSolar is to invest RMB450 million (US$70.3 million) in Tongwei Solar subsidiary Sichuan Yongxiang Energy Technology to help finance a 100,000MT high-purity polysilicon facility. In return for the investment to help construct the plant, Jinko will receive 30,000MT of polysilicon per year and will "share the pro rata profit allocated by the paid-in capital" with Sichuan Yongxiang for the entirety of the joint venture. The initial agreement was announced in November 2020 and, at the time, Tongwei said the contract would run until December 2023.

TBEA planning 400,000MT of polysilicon production in Inner Mongolia
Chinese energy firm TBEA is planning to invest RMB6 billion (US$938 million) to set up a polysilicon production facility with an annual output of 400,000MT in China's Inner Mongolia region. TBEA will build the facility in two phases, each with 200,000MT of output per year. Construction of the first phase is set to begin in the next month and is expected to be completed within 12 months.

WAFERS

TZS launches new 218.2mm wafer size
Tianjin Zhonghuan Semiconductor (TZS) has launched a new 218.2mm-size wafer. Unveiled in early December, the new "super-large" wafers have been initially priced at RMB9.22/pc. TZS said it had launched the new wafer size in response to customer demand for higher-power products, adding that the new size could be produced using the company's existing 210mm wafer lines.

LONGi signs US$1.1bn solar wafer supply deal with DAS Solar
Solar manufacturing leader LONGi Solar has signed a two-year wafer supply deal with Chinese PV manufacturer DAS Solar which could be worth up to US$1.1 billion. The deal will see LONGi supply DAS Solar with around 1.2 billion M10 182mm solar wafers between 2022 and 2023. The contract is in effect repeat business for LONGi, with the business having signed a similarly-sized contract with Quzhou-headquartered DAS Solar in 2019.

CAPACITY EXPANSION

JinkoSolar plots major n-type expansion
'Solar Module Super League' JinkoSolar manufacturer is to pursue a major n-type cell capacity expansion planned for next year, with Jinko intending to finish Q1 2022 with around 16GW of n-type cell capacity. Additionally, JinkoSolar is forecasting that more than 25% of its module shipments next year will be attributable to its n-type TOPCon module range. Speaking to sister publication PV Tech, JinkoSolar vice president Dany Qian further revealed that the SMSL manufacturer expects to ship around 10GW of n-type TOPCon modules in 2022.

Canadian Solar halts solar cell expansions, ramps up module assembly plans
Canadian Solar has warned of solar cell overcapacity next year, slamming the breaks on its own cell manufacturing expansion plans while accelerating on its module assembly roadmap. Canadian Solar chief executive Shawn Qu said the company's manufacturing division was to respond to a projected overcapacity of solar cells next year, while Yan Zhuang, president at CSI Solar, would limit investment in certain areas of the manufacturing chain to "avoid falling into the overcapacity trap". In an updated capacity expansion plan, Canadian Solar said it expected to finish 2021 with around 13.9GW of solar cell manufacturing capacity, up from the 13.3GW of cell capacity it finished Q3 on. However this figure is now not expected to rise at all in 2022. Likewise, CSI expects to finish 2021 with 11.5GW of solar wafering capacity, a figure it also currently expects to finish 2022 on. The division has, however, ramped up its module assembly capacity plans and expected to add nearly 10GW of module assembly between the end of Q3 2021 and the end of 2022, taking its overall module assembly capacity to 32GW by the end of next year. Just over 8GW of module assembly capacity is expected to be added next year.

Tata Group to establish 4GW solar cell facility in Tamil Nadu
Tata Group is planning to set up a 4GW solar cell manufacturing unit in the Indian state of Tamil Nadu. The conglomerate's solar power arm is said to be in the final stages of negotiations with the state government over constructing the facility, which would see the company invest around INR 30 billion (US$403 million). The reported manufacturing expansion follows Tata Power Solar increasing production capacity of solar modules and cells at its Bengaluru facility to 1.1GW earlier in 2021.

THIN FILM

US approves US$500m loan for First Solar's India module production plant

A US development agency has approved up to US$500 million of debt financing for First Solar to support the manufacturer in setting up a thin film module production plant in India. The US International Development Finance Corporation (DFC) will provide the loan for the US-headquartered company's 3.3GWdc module assembly facility in the state of Tamil Nadu that First Solar previously said would require an investment of US$684 million. Ground works were recently completed at the plant, which is due to begin commercial operations in the second half of 2023 and sell most of its output into India's solar market. First Solar CEO Mark Widmar said the DFC's intent to support the facility has the potential to create a "repeatable blueprint for enabling the clean energy ambitions of likeminded nations".

Midsummer awarded US$44m to support Italy thin film factory plans

Swedish thin film solar cell manufacturer Midsummer will receive roughly €38 million (US$44 million) worth of financial incentives to build a 50MW factory in Bari, Italy. Confirmed by Italian authorities in October, the incentives come in the form of grants and soft loans, which make up 35% and 23% of the total project investment of €66 million (US$76.5 million), respectively. The 'soft loans' are provided by the investment arm of the Italian state, Invitalia. Midsummer had already purchased the plant in Bari in southern Italy and can now begin filling it with equipment and recruiting staff.

NanoPV to open manufacturing facility in Georgia, US

Thin film module and solar technology manufacturer NanoPV plans to invest over US$36 million in a manufacturing and distribution facility in Georgia, announced by state Governor Brian Kemp as he praised Georgia's "thriving solar environment". Announced in early October, the commitment will see NanoPV operate in an existing 56,000 square foot facility in Sumter County that will oversee manufacturing, quality control, operations and maintenance (O&M), research and development and marketing activities.

PATENTS

US ITC finds in favour of Solaria in initial ruling over Canadian Solar regarding patent infringement

The US International Trade Commission (ITC) has ruled in favour of US solar manufacturer Solaria in an initial ruling related to alleged patent infringement by Canadian Solar. The ruling relates to two patents covering shingled solar modules and a manufacturing process used to separate photovoltaics strips from cells to be used in shingled solar modules. The patents particularly referenced in the case are US Patent 10,651,33 and 10,763,388. Canadian Solar refuted the claims in 2020, arguing them to be "meritless and unfounded". In an initial determination finding issued in October 2021, an ITC judge found that Canadian Solar violated section 337 of the US Tariff Act 1930 by importing shingled solar modules.

PEROVSKITES

'Mystery' behind perovskite resilience revealed

Researchers from the University of Cambridge claim to have unlocked the mystery behind perovskite's apparent tolerance of defects, with potentially huge implications for the future efficiency of solar PV modules. Using new microscopic methods to visualise perovskite materials and their seeming tolerance to defects in their structure 'for the first time', researchers concluded that two forms of disorder operate in parallel: electronic disorder and chemical disorder. It is the chemical disorder that mitigates the electronic disorder resulting from defects by funnelling the charge carriers away from such "traps", researchers said. "And what we've found is that the chemical disorder – the 'good' disorder in this case – mitigates the 'bad' disorder from the defects by funnelling the charge carriers away from these traps that they might otherwise get caught in," said Kyle Frohna, a PhD student at Cambridge University and lead author on the study, which was published in the scientific journal Nature Nanotechnology.

Saule Technologies perovskite cells reach 25.5% efficiency for IoT applications

Perovskite-based PV manufacturer Saule Technologies said its cells have achieved a 25.5% efficiency for internet of things (IoT) applications. Confirmed by research organisation the Fraunhofer Institute for Solar Energy Systems ISE, the efficiency was reached following testing under 1000 lux illumination by a cold white LED. Poland-based Saule Technologies said its flexible perovskite devices are well suited for powering electronic devices in indoor, low light intensity conditions, making them a solution for various IoT applications.

Toshiba reaches 15.1% power conversion efficiency for polymer film-based perovskite modules

Japanese conglomerate Toshiba said it has developed a new coating method that boosts the power conversation efficiency of large, polymer film-based perovskite modules to a new high. The record 15.1% efficiency was achieved for a 703cm2 module thanks to a one-step meniscus coating method that uses improved ink, film drying processes and production equipment to form a uniform perovskite layer.
This process halves the steps for deposition of the perovskite layer and raises the coating speed to a rate that meets mass production requirements, according to Toshiba.

Increasing the throughput of industrial PERC production

Marius Meßmer, Andreas Wolf, Martin Zimmer, Fabian Meyer, Georg Hoppe, Andreas Lorenz, Sebastian Tepner, Daniel Ourinson, Gernot Emanuel, Sebastian Nold, Baljeet Goraya & Florian Clement, Fraunhofer Institute for Solar Energy Systems (ISE), Freiburg, Germany

Abstract

The development of new ways of increasing the production throughput for passivated emitter and rear cells (PERCs), as the major solar cell technology in the global market, is an area of great interest to the PV community. This paper presents approaches for significantly increasing the throughput of PERC production processes. The main focus is on the tube furnace processes for the emitter formation and oxidation, with the introduction of the High Temperature Stack Oxidation (HiTSOx) approach. Additional approaches that are currently under investigation at Fraunhofer ISE for increasing the throughput for wet-chemical, printing and laser processes will also be briefly outlined.

Introduction

The passivated emitter and rear cell (PERC) structure [1,2] has gained a significant world market share during the last decade, and will remain the mainstream technology in the industry in the coming years [3]. The energy conversion potential of PERC is estimated to be around 24% [4], although high efficiency is not the sole driver for decreasing the cost of ownership (COO). In point of fact, increasing production tool throughput, while maintaining the energy conversion efficiency, is the main driver for decreasing the COO by reducing the CAPEX, the fab area and the labour costs.

“Increasing production tool throughput is the main driver for decreasing the COO.”

The process flow for PERC solar cells requires the implementation of high-throughput approaches for several process tools. This paper presents high-throughput approaches currently under investigation at Fraunhofer ISE, with a focus on the high-temperature processes, the emitter formation and the thermal oxidation. Furthermore, other approaches for some of the remaining process steps in the fabrication of PERC solar cells are outlined, namely wet-chemical processes, metallization, laser contact opening and contact firing.

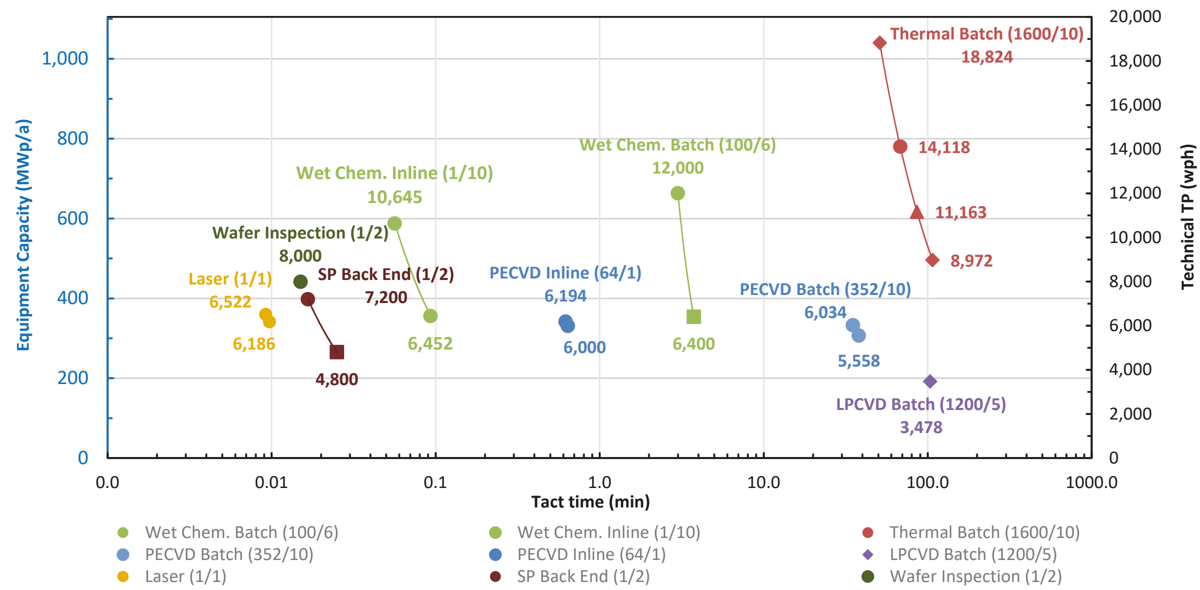

Figure 1. Technical throughput (TP, not including equipment downtime) of the production equipment for M6 wafer format as a function of the tact time t_{tct} for the various state-of-the-art technologies. Batch and inline processes are shown, along with the respective number of wafers processed at the same time (I_{bat}), and the number of parallel lines used (in the case of inline processing) or batches used (in the case of batch processing) (I_{pl}). The indicated equipment capacity in MWp/a is calculated on the basis of an overall equipment efficiency (OEE) of 100% (365 d/a × 24 h/d = 8,760 h/a operation with 100% equipment uptime and 100% yield) and an M6 solar cell efficiency of 23%.

Production equipment throughput

Fig. 1 shows the technical throughput (TP) as a function of the tact time t_{tct} for various production tools/equipment. The different technologies used and the type of processing – batch or inline – are also indicated. The respective number of wafers processed at the same time within a single batch (I_{bat}), and the number of parallel processed batches or the number of parallel lines within the equipment (I_{pl}), are shown in parentheses. For the diffusion/oxidation/anneal, 1,600 wafers per batch with ten possible batches (in this case tubes in the furnace) can be processed.

Also shown in Fig. 1 is the dependency of the technical throughput on batch size and cycle time. Possible ways to increase the production tool throughput are therefore:

- increasing the batch size (I_{bat});
- increasing the number of parallel processed batches within the equipment (I_{pl});
- decreasing the process cycle time (but ultimately decreasing the tact time t_{tct} of subsequent successfully processed batches leaving the equipment).

Emitter formation and oxidation

State-of-the-art emitter formation

The main technology employed in the industrial fabrication of PERC solar cells for the emitter formation is the tube furnace diffusion process using phosphorus oxychloride ($POCl_3$) as a liquid dopant source. The diffusion process usually consists of two process phases as shown in Fig. 2(a).

The first stage of production is a deposition phase, where nitrogen (N_2) flows through the $POCl_3$ bubbler; further, N_2 and oxygen (O_2) contribute to the total gas flow. During this phase, which occurs at a moderate temperature, the phosphosilicate glass (PSG) layer [5,6] grows on the silicon (Si) wafer surface, and already a moderate amount of phosphorus (P) diffuses into the Si wafer.

In the subsequent drive-in phase, the PSG layer still serves as the dopant source. Here, a high O_2 gas flow is often introduced into the process tube [7–9]. For this so-called *in situ oxidation*, the furnace is usually ramped up to temperatures above 850°C [10–12]. With this in situ oxidation, the in-diffusion of phosphorus and the reduction of the phosphorus dose can be controlled as a result of the decoupling of the dopant source. Currently, low pressure (LP) diffusion dominates in production [13]. With this technology, a wafer-to-wafer distance of 2.38mm (for M2 to M6 wafers) is possible, consequently increasing the throughput to 1,200 wafers per process (back-to-back loading), or to 1,600 wafers for the newest generation of production equipment, as seen in Fig. 1. The PERC fabrication then often continues with laser-doping for a selective emitter structure, followed by PSG removal and edge isolation as a combined wet-chemical process.

Subsequently, most production sequences involve a second thermal process for emitter passivation, often denoted as *low-temperature oxidation or annealing* [2], as shown graphically in Fig. 2(a). This process is also performed in a tube furnace similar to that for the diffusion process, but the temperatures are usually well below those for the diffusion [2,15,16]. In this process, gaseous N_2 and O_2 are used [17–19] to grow a thin layer of silicon dioxide (SiO_2) on the silicon surface. In combination with a hydrogen-rich capping layer, this SiO_2 layer serves as surface passivation for the front emitter of the PERC device. The emitter doping profile is barely affected by the thermal oxidation process because of the moderate temperatures usually involved [15,20].

High-throughput approach for emitter formation and oxidation HiTSOx

To achieve a further increase in the throughput of the emitter formation and thermal oxidation, the High Temperature Stack Oxidation (HiTSOx) approach has been introduced by Fraunhofer ISE [14,20,21]. This technique comprises an adapted LP-$POCl_3$ diffusion and a high-throughput thermal oxidation process with stacked wafers.

Fig. 2(b) illustrates graphically the thermal processes of the HiTSOx approach, whereby the $POCl_3$ diffusion process is reduced to just a PSG deposition step. In this step, only the PSG growth and a moderate in-diffusion of phosphorus into the silicon take place; neither in-diffusion nor in situ oxidation is performed during the diffusion. This process results in a lightly doped emitter with a typical sheet resistance R_{sh} in the range 130Ω/sq. < R_{sh} < 170Ω/sq., and with a doping profile that is heavily doped at the surface and very shallow in nature [20]. The additional thermal treatment required for the phosphorus in-diffusion is shifted to the subsequent thermal oxidation process. With this adaptation of the $POCl_3$ diffusion, a significant reduction in process time compared with state-of-the-art diffusion is realized, while keeping the typical load of 1,200 wafers (1,600 in the latest generation) per process.

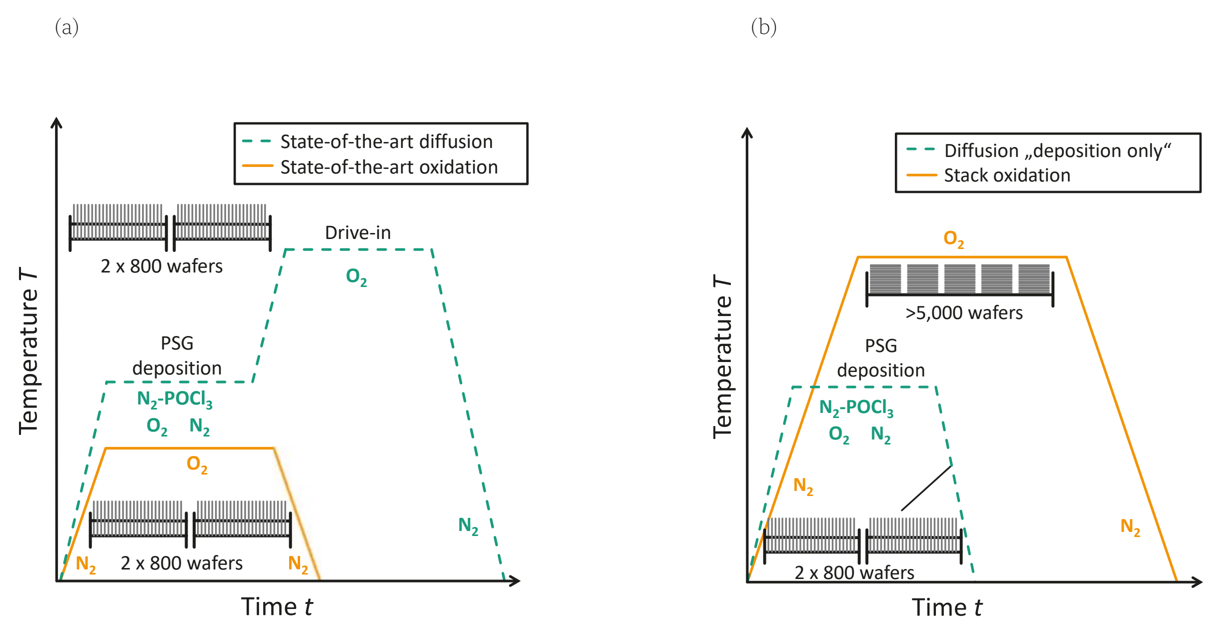

Credit: Meßner et al. [14].

Figure 2. (a) State-of-the-art tube furnace diffusion and oxidation processes as a function of the temperature *T* over time *t*. The assumed throughput of both processes is 1,600 wafers. (b) HiTSOx approach: adapted LP-$POCl_3$ diffusion and high-throughput thermal oxidation using wafer stacks (>5,000 wafers).

After the $POCl_3$ diffusion, the next processes to take place are laser doping, PSG etch and edge isolation; thus, the PERC process sequence itself remains unchanged. The HiTSOx approach then employs a thermal oxidation process with horizontally stacked wafers, with the wafer surfaces in direct contact with each other. The throughput of the thermal oxidation process may thereby be increased significantly, to more than 5,000 wafers per run (also depicted in Fig. 2(b)). However, compared with the state-of-the-art low-temperature oxidation, this high-throughput oxidation process features a higher process temperature, similar to typical drive-in temperature levels, as well as a longer process time to compensate for the omitted drive-in phase in the $POCl_3$ diffusion process. In this stacked thermal oxidation, a simultaneous redistribution and activation of the dopants and surface passivation by thermal oxidation takes place, since the thermal oxide that is grown in this process remains as a passivation layer.

Cost calculation

Fig. 3 presents the COO for the state-of-the-art diffusion and oxidation for PERC solar cells with LP-$POCl_3$ diffusion and low-temperature thermal oxidation (left half), as well as for the HiTSOx approach (right half). The data has been updated from Meßmer et al. [20] using the 'SCost' COO model [22], which conforms with SEMI standards E35 [23] and E10 [24]. This calculation is based on industrial equipment data and process parameters.

The LP-$POCl_3$ diffusion in the HiTSOx approach gives rise to a reduction in the COO from 0.77€ct/wafer to 0.48€ct/wafer. In the case of the thermal oxidation processes, the higher load with 5,000 wafers per process leads to a reduction in the COO from 0.33€ct/wafer for the low-temperature oxidation to 0.18€ct/wafer for the high-temperature stack oxidation. The resulting COO is lower in spite of higher investment costs, assumed to be 30% higher because of the need for adapted process equipment for the wafer handling and for mechanical adaptations to allow for the higher weight load. Nevertheless, HiTSOx increases the throughput of diffusion by a factor of 1.8 and thermal oxidation by a factor of 2.4, and reduces the total COO from 1.11€ct/wafer for the state-of-the-art processing to 0.65€ct/wafer; this equates to a 41% reduction in the COO. As regards the specific power consumption, taking into account the heat capacity of the Si wafers a reduction of approximately 50% is expected because of reduced heat losses [20].

"HiTSOx increases the throughput of diffusion by a factor of 1.8 and thermal oxidation by a factor of 2.4."

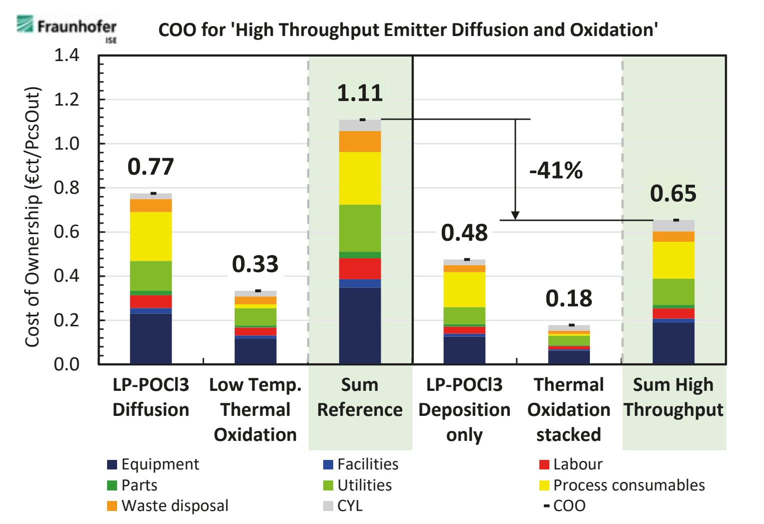

Figure 3. Cost of ownership (COO) calculation for the state-of-the-art process route with LP-$POCl_3$ diffusion (1st bar) and low-temperature thermal oxidation (2nd bar), as well as for the HiTSOx approach with LP-$POCl_3$ deposition only (4th bar) and thermal oxidation using stacked wafers (5th bar). The sum of the COO for the reference state-of-the-art process route is indicated by the 3rd bar, and for the HiTSOx approach by the 6th bar. (Taken from Meßmer et al. [20], but updated to 1,600 wafers (M6) and ten tubes.)

Process characterization

As mentioned earlier, the stack oxidation process is a simultaneous redistribution of dopants and thermal oxide passivation by the SiO_2 growth. In the HiTSOx approach, the thermal oxide grown in the wafer stack remains as a passivation layer in the solar cell.

First, the question arises as to whether the availability of oxygen within the small gap in between the stacked wafers is sufficiently high to grow a thermal oxide layer of uniform thickness. Fig. 4(a) demonstrates that this is indeed the case. The HiTSOx approach yields thicker oxide layers than typical oxidation processes for PERC solar cells [20]. The reasons for this are the higher temperature and the fact that the doping profile is heavily doped at the surface, resulting in an increased oxide growth rate [25,26].

Thermal oxide thickness (d_{Ox}) as a function of sheet resistance after the HiTSOx process sequence has been reported by Meßmer et al. [20], with d_{Ox} in the range 16nm < d_{Ox} < 19nm, decreasing with decreasing R_{sh} as well as surface concentration N_s. Fig. 4(a) shows the spatially resolved oxide thickness for the HiTSOx approach over an M2-sized wafer; the resulting thickness is 19.6nm with a relative standard deviation of σ_{dOx} = 2.6%, which indicates sufficient homogeneity.

The oxide thickness is controllable by adjusting, on the one hand, the diffusion process, and, on the other, the oxidation process parameters, such as oxygen content in the atmosphere [21]. Adapting the oxide thickness by adjusting the diffusion process or the stack oxidation process influences R_{sh}, d_{Ox} and the emitter dark saturation current density j_{oe}. Therefore, a suitable combination of those processes must be chosen in order to maximize the efficiency of the final solar cell.

Second, the redistribution and activation of phosphorus in the stack oxidation process of the HiTSOx approach results in homogeneous doping over the wafer surface for R_{sh} = 128.7Ω/sq., with a low relative standard deviation of σ_{Rsh} = 1.9%, as shown in Fig. 4(b).

The impact of stacking the wafers in the thermal oxidation process on the emitter recombination is also investigated. For this, the emitter dark saturation current density j_{oe} is examined by quasi-steady-state photoconductance measurements (QSSPC) from symmetrical lifetime test structures. Free-standing and stacked samples are compared in order to evaluate whether or not j_{oe} is affected by stacking. The results obtained indicate that j_{oe} values for free-standing samples are similar to those for the stacked samples at comparable sheet resistance values, showing that the HiTSOx approach yields high-quality emitters and passivation with the thermal oxide grown within a stack. With the HiTSOx approach, j_{oe} is reduced to (32±1)fA/cm² at R_{sh} = (183±5)Ω/sq. [20], while a value of j_{oe} = (12±2)fA/cm² at R_{sh} = (389±10)Ω/sq. is obtained on textured surfaces after SiNx passivation and firing.

Implementation in the PERC process

The next step is the fabrication of PERC solar cells using the HiTSOx approach [21] as well as PERC solar cells in the ISE baseline [2] as a reference group. For the front-side metallization, a zero-busbar layout is used in both cases.

In this solar cell batch, the best solar cell for the reference sequence reaches η = 22.3%, closely followed by the HiTSOx approach with η = 22.2% (see Table 1). For both approaches, the median energy conversion efficiency is η = 22.2%. The HiTSOx approach shows a slightly increased short-circuit current j_{sc} and fill factor FF, but the main difference is the open-circuit voltage V_{oc}, which is around 3mV lower. Introducing a selective emitter to the HiTSOx approach results in a peak energy conversion efficiency of η = 22.4% and a slightly higher median energy conversion efficiency of η = 22.3%, compared to the reference sequence. This result shows that the HiTSOx approach enables similar and higher energy conversion efficiencies to be achieved, combined with significantly increased throughput potential, and thus reduced COO. It is expected that optimizing the diffusion and stack oxidation combination will lead to higher efficiencies in ongoing development at Fraunhofer ISE.

Additional high-throughput approaches

Wet chemistry

For wet-chemical processing, batch systems for alkaline texturing are currently used, in which up to six carriers with 100 wafers each can be

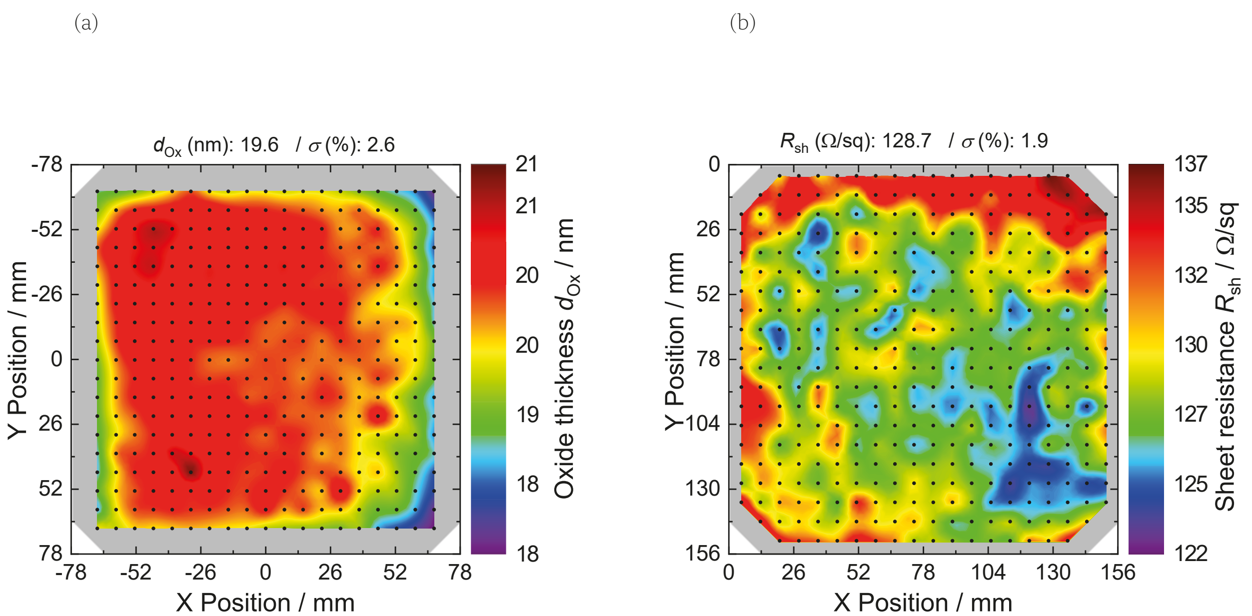

Figure 4. Spatially resolved measurements over the wafer surface of an M2-sized HiTSOx-processed wafer. (a) Thermal oxide thickness d_{Ox}, measured by ellipsometry in a 19×19 pattern on a saw-damage-etched wafer. (b) Sheet resistance R_{sh}, measured by four-point probing in a 20×20 pattern on a textured surface.

processed simultaneously. This equipment thus achieves throughputs of up to 12,000 wafers per hour. A further increase can be achieved by building systems for eight or ten carriers, but the system is not infinitely scalable. In addition to the actual texturing process, a bottleneck will always be the drying of the carriers, where the contact points between wafers and carriers are difficult to dry. This is where the inline process offers a decisive advantage: since no carrier is required here, both the rinsing and drying processes are much more efficient, which is reflected in lower water consumption.

A significant increase in efficiency and throughput can be obtained by combining the two processes, where wafers no longer travel horizontally but vertically through an inline system. In this case, 50–100 tracks can be realized instead of the usual five. Thus, at a belt speed of 3m/min, a throughput of 40,000 wafers per hour can be achieved. Such a concept, of course, raises new questions:

- How can vertical wafer transport proceed?
- How will vertically oriented wafers enter or leave a process bath?
- How do rinsing and drying processes run?

To answer these questions, an initial prototype for testing the transport mechanism was constructed at Fraunhofer ISE. The actual wafer transport takes place with the aid of profiled transport rollers; these have a recess for each wafer track, which serves as a guide for the vertical wafers. The wall of the process basin has slots which serve as a passage for the wafers. These slots, however, have the disadvantage that the process liquid escapes at high speed. For example, a flow rate of 10 litres/min was determined for a process bath with a height of 160mm; extrapolated to 50 inlet and 50 outlet slots, a pump capacity of 1,000 litres/min would therefore be required to maintain the level of the process bath.

The focus now is on developing a slot geometry that reduces the volume flow. A reduction of 20–30% has already been achieved with a geometry based on the Tesla valve. Further improvement of the geometry, however, has yielded a reduction of even up to 70%, which would bring the volume flow back within the range of regular pumps. Thus, the concept of vertical wafer transport could represent a further milestone in the quest to increase plant throughput.

Laser processing

Short laser pulses can be used to locally open the dielectric passivation layer in a very flexible and cost-efficient way [27]. Laser contact openings (LCOs) are created through laser ablation of the dielectric layer induced by a focused laser beam with a focal spot diameter of 20µm to 100µm [2]. For the rear-side openings of a PERC, infrared pulsed beam sources – solid state or fibre lasers – with pulse durations in the nanosecond regime are available with high average power. They are reliable and cost effective [28] and have become the standard tool for LCO.

Conventional machines for LCO offer a throughput of around 6,000 wafers per hour. Modern industrial lasers provide a pulse repetition rate of more than 4MHz, which would allow more than 20,000 standard LCO patterns to be created on an M12 area per hour, each consisting of more than 200,000 spots. Since average laser output power and pulse repetition rates have been steadily increasing [29], the throughput is somewhat limited by the speed of beam deflection, wafer detection and wafer handling.

On a scanning field of 210mm in diameter, conventional galvanometers deflect the beam on the wafer at a speed of up to 50ms^{-1}, which is not sufficient to be able to use full-power modern lasers in the case of sparse patterns such as LCO. Polygon scanners provide a beam deflection speed exceeding 1,000ms^{-1} along one dimension (fast axis), while along the other dimension (slow axis), the beam is guided by a galvanometer [30]. However, the use of this more complex beam guidance is only justified if the machine handles the wafers fast enough to translate this advantage into throughput.

To accurately align the laser openings with

> "It is expected that optimizing the diffusion and stack oxidation combination will lead to higher efficiencies."

	Process	J_{sc} [mA/cm²]	V_{oc} [mV]	*FF* [%]	η [%]
Median	Reference	40.3	679	81.0	22.2
	HiTSOx	40.5	676	81.2	22.2
	HiTSOx + SE	40.5	681	80.9	22.3
Best	Reference	40.4	679	81.2	22.3
	HiTSOx	40.5	676	81.2	22.2
	HiTSOx + SE	40.5	682	81.0	22.4

Table 1. *I–V* results for the HiTSOx approach without and with selective emitter (SE), and the reference sequence, with four to six wafers per process group [21].

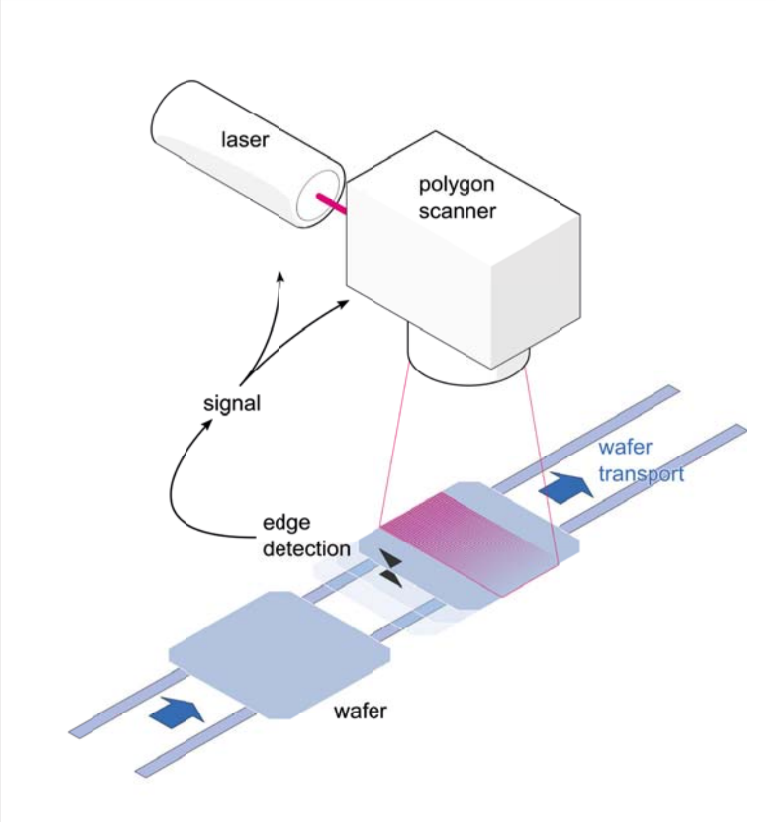

Figure 5. Integration of polygon scanners in an on-the-fly laser processing set-up as a high-throughput approach for inline LCO.

the workpiece, its location must be detected, and the laser pattern has to be placed accordingly. Detection of the wafer location can be realized at a separate station while processing another wafer in parallel, or, as in Fraunhofer ISE's approach, by using inline detection of the wafer's location on the belt (Fig. 5).

Since the wafer's location is measured at the time of arrival in the scanner's field of view, the need for a rigid, high-precision mechanical set-up to maintain the wafer position is eliminated. This approach promises a wafer delivery using a simple transport mechanism, such as a conveyor belt, but requires accurate measurement and precise control of the timings. For applications with comparatively low requirements in terms of positioning accuracy, such as rear-side LCO for PERC, this system design is suitable for delivering a throughput of more than 11,000 wafers per hour (M12).

Metallization approaches

Rotary printing

Today, flatbed screen printing is the predominant method for the front- and rear-side metallization of silicon solar cells with a market share of more than 98% [31]. However, the flatbed screen-printing process is inherently limited by the stop-and-go nature of the printing procedure. This aspect generally limits the possibility of substantially increasing the cycle time per wafer, despite the remarkable progress made in recent years. An attractive approach for overcoming this limitation is the application of continuous rather than sequential printing methods for solar cell metallization. Rotary screen printing [32] and flexographic printing [33] represent two particularly promising ways of carrying out the front- and rear-side metallization.

Within the framework of the funded Rock-Star research project (Contract No. 13N13512) [34], a project consortium of industry partners and research institutes has developed an innovative rotary printing platform machine which can perform the metallization of solar cells at a printing speed of up to 600mm/s (Fig. 6). Such a machine would enable a gross throughput of up to 8,000 wafers per hour on a single line within a virtual high-throughput backend line.

The application of rotary screen printing for the high-quality rear-side metallization of monofacial PERC solar cells has been successfully demonstrated [32,35]. PERC solar cells with a rotary screen-printed rear-side Al metallization have achieved a mean conversion efficiency similar to that for reference cells with a flatbed screen-printed metallization [34]. The feasibility of using rotary screen printing to apply the front-side metallization of PERC solar cells has been reported in several studies [32,34–36]. Typical H-pattern and busbarless front-side grids with a mean finger width down to $w_f \approx 45\mu m$ and below have been successfully printed using this technology [34]. A further reduction in printed finger width can be expected by optimizing the paste rheology and the properties of the rotary screens.

Flexographic printing is a widely used printing technology which is applicable to a wide range of applications in the field of graphic arts and technical printing [37]. With regard to solar cell metallization, flexography is primarily suited to the front-side metallization, as it enables the application of finely printed structures, even on particularly rough surfaces, such as textured silicon [38]. A particular benefit of this approach is the ability to print fine-line contacts with a reduced finger height compared with flatbed screen printing; this can help to effectively reduce the amount of silver (Ag) consumed in the front-side metallization.

The application of fine-line front-side contacts on typical 6" Cz silicon wafers down to a width of $w_f \approx 30\mu m$ has been successful using flexography [34]. Aluminium back surface field (Al BSF) solar cells with flexographic-printed busbarless front-side metallization have demonstrated a mean conversion efficiency of η = 19.0% [33]. Further research activities will primarily concentrate on optimizing materials, paste rheology and printing process parameters, with the aim of further reducing finger width, lateral finger resistance and silver consumption.

Dispensing

Over the last decade, Fraunhofer ISE has been working intensively on an industrial implementation of the parallel dispensing approach for PERC front-side metallization. Starting with a single-nozzle printing step in the early 2010s, the developers have managed to devise a parallel dispensing unit which allows the application of up to 200 parallel contact fingers with widths less than 20µm at an optical aspect ratio AR_o of greater than 0.7.

In a series of publications, Pospischil et al. [39–42] reported the enormous potential of dispensing technology by demonstrating the deposition of Ag fingers at speeds of up to 1,000mm/s. It was also shown that this printing technique is able to solve one of the main drawbacks of screen printing, namely the imprint of the individual wires of the mesh left behind on the printed structure [43] due to the rheological nature of the printing fluid, which is a highly filled suspension. These so-called *mesh marks* limit the conductivity of an Ag finger because of the locally reduced cross-sectional area [44]. Dispensing technology, on the other hand, offers a natural perfectly constant finger geometry across its length, resulting in an optimal usage of silver in regard to its conductivity. This advantage leads to a reduction in Ag lay-down of up to 20% compared with single-step screen printing [41]. Fig. 7 highlights the record finger having a finger width of only 17µm with a flawless finger geometry [41].

Contact firing approach

In an industrial solar cell production line, the contact firing process is carried out in a dual-lane conveyor belt furnace [45]. The typical approach for increasing the throughput is to increase the belt velocity v_{BELT} [46].

The standard firing process at Fraunhofer ISE is conducted at a v_{BELT} of 6m/min. Since the corresponding firing furnace is capable of belt velocities of up to 20m/min, faster firing processes were evaluated for monofacial PERC

"Dispensing technology offers a natural perfectly constant finger geometry across its length, resulting in an optimal usage of silver."

Figure 6. Rotary screen-printed front-side metallization of Cz silicon solar cells using the Rock-Star demonstrator machine at Fraunhofer ISE.

(a) (b)

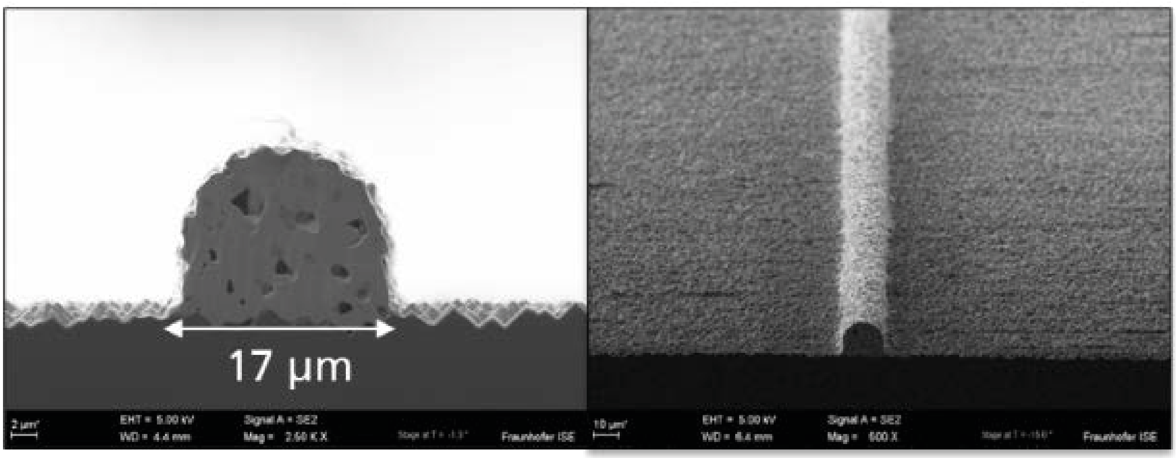

Figure 7. (a) Cross-sectional view of an Ag finger for PERC metallization applied using dispensing technology. (b) The homogeneity of the finger across its length is clearly visible [41].

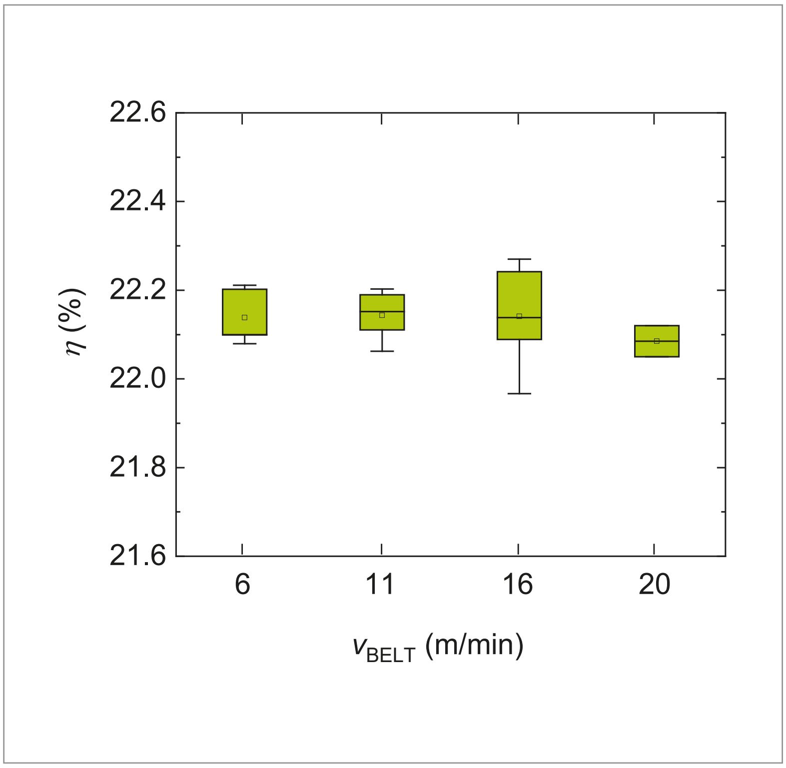

Figure 8. Results of the cell efficiency for different furnace belt velocities. Five cells are fired for each group.

cells. Compared with an industrial furnace, the Fraunhofer ISE furnace has a single lane, features only the firing process without a preceding drying process, and has an additional peak zone attached to the main peak zone. Despite these differences, this furnace is considered to be suitable for demonstrating the effect of higher velocities for industrial furnaces. To be more precise, the effect is demonstrated for higher velocities at a constant furnace length, resulting in shorter process times.

For v_{BELT} > 6m/min, the peak phase, including the peak temperature of the firing profile, is kept the same (as much as possible) with the help of thermocouple measurements in order to maintain similar conditions for the contact formation [46]. For this, the additional peak zone is used to prolong the cool-down ramp. In order to prolong the heat-up ramp, the burnout zones are (partially) used. Accordingly, the burnout phase of the firing profile inevitably shrinks at higher velocities [46]. Fig. 8 shows the resulting cell efficiencies.

On a positive note, the cell efficiency for all the evaluated faster firing processes for belt velocities of up to 20m/min can be kept at the same level as the standard process. Indeed, a shorter burnout phase does not seem to have any negative effects on cell performance. Considering a double-lane furnace and a wafer distance of 25mm on the belt, the technical throughput for an M2-sized wafer would yield 13,205 wafers per hour for v_{BELT} = 20m/min. Thus, the throughput increases by more than a factor of three when the belt velocity passes from 6 to 20m/min. Successful firing processes with this higher throughput can therefore be achieved at the cell level; however, as a next step, this favourable outcome will need to be verified at the module level. Since industrial furnaces do not usually have an additional peak zone, narrower peak zones for higher velocities should be evaluated as well.

“HiTSOx enables a 41% cost reduction to be realized for the thermal processes, while yielding homogeneous doping and uniform oxide growth within the wafer stack.”

Summary and conclusion

In the work reported in this paper, new approaches for increasing production tool throughput for PERC solar cells were investigated. First, the HiTSOx approach – a combination of adapted $POCl_3$ diffusion and stacked thermal oxidation – with a throughput of greater than 5,000 wafers per process and tube was presented. HiTSOx enables a 41% cost reduction to be realized for the thermal processes, while yielding homogeneous doping and uniform oxide growth within the wafer stack, as well as a high passivation quality with low emitter dark saturation current densities. Moreover, solar cell efficiencies similar to those obtained with state-of-the-art processing were reported, but at a significantly increased throughput.

New approaches under investigation at Fraunhofer ISE were also outlined. A wet-chemical processing approach with a vertical wafer transportation mechanism could represent a further breakthrough in increasing the plant throughput. For the laser processing in the PERC sequence, polygon scanning and inline position detection during the laser process allow increased throughputs. The metallization technologies outlined in this paper are rotary printing and flexographic printing for fine finger structures, both of which make high throughputs possible. In addition, dispensing shows enormous potential for high printing speeds and record finger widths. For contact formation, a high belt velocity increases the throughput while maintaining constant solar cell efficiency levels.

Acknowledgements

The authors would like to thank all their colleagues at the Fraunhofer ISE PV-TEC. This work was funded by the German Federal Ministry for Economic Affairs and Energy within the POLDI research project (under Contract No. 0324079), the NextTec research project (under Contract No. 03EE1001A) and the CUT-A PLUS research project (under Contract No. 0324282).

References

[1] Blakers, A.W. et al. 1989, "22.8% efficient silicon solar cell", *Appl. Phys. Lett.,* Vol. 55, No. 13, pp. 1363–1365.

[2] Preu, R. et al. 2020, "Passivated emitter and rear cell—Devices, technology, and modeling", *Appl. Phys. Rev.,* Vol. 7, No. 4, p. 41315.

[3] VDMA 2020, "International technology roadmap for photovoltaic (ITRPV): Results 2019", 11th edn (Apr.) [https://itrpv.vdma.org/en/].

[4] Min, B. et al. 2017, "A roadmap toward 24% efficient PERC solar cells in industrial mass production", *IEEE J. Photovolt.,* Vol. 7, No. 6, pp. 1541–1550.

[5] Werner, S. et al. 2017, "Structure and composition of phosphosilicate glass systems formed by $POCl_3$ diffusion", *Energy Procedia,* Vol. 124, pp. 455–463.

[6] Lohmüller née Werner, S. et al. 2018, "Analysis of phosphosilicate glass structures formed by atmospheric pressure and high throughput low pressure $POCl_3$ diffusion", *Proc. 2018 IEEE 7th WCPEC*, Waikoloa, Hawaii, USA, pp. 1530–1535.

[7] Cuevas, A. 1991, "A good recipe to make silicon solar cells", *Proc. 22nd IEEE PVSC*, Las Vegas, Nevada, USA, pp. 466–470.

[8] Basore, P.A. et al. 1994, "Simplified high-efficiency silicon cell processing", *Sol. Energy Mater. Sol. Cells,* Vol. 34, No. 1–4, pp. 91–100.

[9] Dullweber, T. et al. 2016, "Emitter saturation currents of 22 fA/cm^2 applied to industrial PERC cells approaching 22% conversion efficiency", *Proc. 32nd EU PVSEC*, Munich, Germany.

[10] Werner, S. et al. 2014, "Process optimization for the front side of p-type silicon solar cells", *Proc. 29th EU PVSEC*, Amsterdam, The Netherlands.

[11] Komatsu, Y. et al. 2009, "Innovative diffusion processes for improved efficiency on industrial solar cells by doping profile manipulation", *Proc. 24th EU PVSEC*, Hamburg, Germany, pp. 1–5.

[12] Komatsu, Y. et al. 2010, "Sophistication of doping profile manipulation – Emitter performance improvement without additional process step", *Proc. 25th EU PVSEC*, Valencia, Spain.

[13] Mühlbauer, M. et al. 2011, "Industrial low-pressure phosphorus diffusion for high performance and excellent uniformity", *Proc. 26th EU PVSEC*, Hamburg, Germany.

[14] Meßmer, M. et al. 2021, "High throughput solar cell processing by oxidation of wafer stacks", *Proc. 38th EU PVSEC*, Lisbon, Portugal.

[15] Lohmüller, E. et al. 2020, "Front side optimization on boron- and gallium-doped Cz-Si PERC solar cells exceeding 22% conversion efficiency", *Proc. 37th EU PVSEC* (virtual event).

[16] Lv, Y. et al. 2020, "Towards high-efficiency industrial p-type mono-like Si PERC solar cells", *Sol. Energy Mater. Sol. Cells*, Vol. 204, p. 110202.

[17] Mack, S. et al. 2009, "Impact of solar cell manufacturing processes on thermal oxide-passivated silicon surfaces", *Proc. 24th EU PVSEC*, Hamburg, Germany.

[18] Mack, S. et al. 2009, "Control and optimization of thermal oxidation processes for industrial solar cell fabrication", *Proc. 34th IEEE PVSC*, Philadelphia, Pennsylvania, USA, pp. 1024–1028.

[19] Mack, S. et al. 2011, "Silicon surface passivation by thin thermal oxide/PECVD layer stack systems", *IEEE J. Photovolt.,* Vol. 1, No. 2, pp. 135–145.

[20] Meßmer, M. et al. 2020, "High throughput low energy industrial emitter diffusion and oxidation", *Proc. 37th EU PVSEC* (virtual event), pp. 370–377.

[21] Meßmer, M. et al. 2021, "Industrial high throughput emitter formation and thermal oxidation for silicon solar cells by the high temperature stack oxidation approach", *physica status solidi (a)*.

[22] Nold, S. 2019, *Techno-ökonomische Bewertung neuer Produktionstechnologien entlang der Photovoltaik-Wertschöpfungskette: Modell zur Analyse der Total Cost of Ownership von Photovoltaik-Technologien.* Stuttgart: Fraunhofer Verlag.

[23] SEMI E35-0618, "Guide to calculate cost of ownership (COO) metrics for semiconductor manufacturing equipment".

[24] SEMI E10-0814E, "Specification for definition and measurement of equipment reliability, availability, and maintainability (RAM) and utilization".

[25] Deal, B.E. & Sklar, M. 1965, "Thermal oxidation of heavily doped silicon", *J. Electrochem. Soc.,* Vol. 112, No. 4, p. 430.

[26] Ho, C.P. 1978, "Thermal oxidation of heavily phosphorus-doped silicon", *J. Electrochem. Soc.*, Vol. 125, No. 4, p. 665.

[27] Preu, R. et al. 2000, "Laser ablation – A new low-cost approach for passivated rear contact formation in crystalline silicon solar cell technology", *Proc. 16th EU PVSEC,* Glasgow, Scotland, pp. 1181–1184.

[28] Westphäling, T. 2010, "Pulsed fiber lasers from ns to ms range and their applications", *Phys. Procedia,* Vol. 5, pp. 125–136.

[29] Zervas, M.N. & Codemard, C.A. 2014, "High power fiber lasers: A review", *IEEE J. Sel. Top. Quantum Electron.,* Vol. 20, No. 5, pp. 219–241.

[30] Streek, A. & Lee, M. 2017, "Ultrafast material processing with high-brightness fiber lasers", *Laser Technik J.*, Vol. 14, No. 4, pp. 22–25.

[31] VDMA 2021, "International technology roadmap for photovoltaic (ITRPV): 2020 results", 12th edn (Apr.) [https://itrpv.vdma.org/en/].

[32] Lorenz, A. et al. 2017, "High-throughput front and rear side metallization of silicon solar cells using rotary screen printing", *Energy Procedia*, Vol. 124, pp. 680–690.

[33] Lorenz, A. et al. 2016, "Flexographic printing – Towards an advanced front side metallization approach with high throughput and low silver consumption", *Sol. Energy Mater. Sol. Cells,* Vol. 157, pp. 550–557.

[34] Lorenz, A. et al. 2021, "The project 'Rock-Star':

The evolution of rotary printing for solar cell metallization", *Proc. 9th Worksh. Metalliz. Interconn. Cryst. Sil. Sol. Cells,* Genk, Belgium, p. 20008.
[35] Lorenz, A. 2017, "Evaluierung von Rotationsdruckverfahren für die Metallisierung von Silicium-Solarzellen", Dissertation, Institut für Mikrosystemtechnik und Informatik, Albert Ludwig University, Freiburg.
[36] Lorenz, A. et al. 2018, "Screen printed thick film metallization of silicon solar cells – Recent developments and future perspectives", *Proc. 35th EU PVSEC*, Brussels, Belgium, pp. 819–824.
[37] Flexographic Technical Association 2013, *Flexography: Principles and Practices 6.0,* 6th edn. Foundation of Flexographic Technical Association, Inc.
[38] Lorenz, A. et al. 2015, "Evaluation of flexographic printing technology for multi-busbar solar cells", *Energy Procedia,* Vol. 67, pp. 126–137.
[39] Pospischil, M. et al. 2013, "Development of a high-throughput fine line metallization process using CFD-simulation", *Proc. 39th IEEE PVSC*, Tampa, Florida, USA, pp. 2250–2253.
[40] Pospischil, M. et al. 2013, "Process development for a high-throughput fine line metallization approach based on dispensing technology", *Energy Procedia,* Vol. 43, pp. 111–116.
[41] Pospischil, M. et al. 2019, "Applications of parallel dispensing in PV metallization", *AIP Conf. Proc.,* p. 20005.
[42] Pospischil, M. 2017, *A Parallel Dispensing System for an Improved Front Surface Metallization of Silicon Solar Cells.* Fraunhofer Verlag.
[43] Tepner, S. et al. 2020, "Studying knotless screen patterns for fine line screen printing of Si-solar cells", *IEEE J. Photovolt.,* Vol. 10, No. 2, pp. 319–325.
[44] Tepner, S. et al. 2020, "Screen pattern simulation for an improved front-side Ag-electrode metallization of Si-solar cells", *Prog. Photovolt: Res. Appl.*, Vol. 28, No. 10, pp. 1054–1062.
[45] Xu, J., Zhang, J. & Kuang, K. 2018, *Conveyor Belt Furnace Thermal Processing.* Heidelberg: Springer.
[46] Ourinson, D. et al. 2019, "Evaluation of the burnout phase of the contact firing process for industrial PERC", *AIP Conf. Proc.*, p. 40015.

About the Authors

Marius Meßmer studied process engineering with a focus on energy technologies and energy conversion and management at the University of Applied Sciences Offenburg, Germany, and received his M.Sc. in 2019. For his master's thesis, he concentrated on selective emitter development and modelling. Since 2020 he has been working towards his Ph.D. in the field of high-throughput diffusion and oxidation processes at Fraunhofer ISE.

Andreas Wolf studied physics at the Technical University of Darmstadt, Germany, and the Royal Institute of Technology, Stockholm, Sweden. In 2007 he received his Ph.D. from the Leibniz University of Hannover, Germany, for his work on sintered porous silicon and layer transfer silicon solar cells that he carried out at the Institute for Solar Energy Research Hamelin, Germany. Since 2008 he has been with Fraunhofer ISE, where he currently heads the Thermal Processes Group in the Photovoltaics Division.

Martin Zimmer is head of the Wet Chemical Process Technology Group at Fraunhofer ISE. After finishing his studies in chemistry in Heidelberg, he received his Ph.D. from the Albert Ludwig University of Freiburg in cooperation with Fraunhofer ISE, where he investigated industrial texturization processes. His current research focuses on new wet-chemical production technologies in the context of Industry 4.0.

Fabian Meyer is head of the Laser System Development team at Fraunhofer ISE. He studied Physics at the Albert Ludwig University of Freiburg and at Imperial College London, and completed his Ph.D. at the University of Freiburg in 2020. His current work includes the development of innovative and adaptive laser machines for industrial and research applications.

Georg Hoppe studied physics at the University of Konstanz and at the Albert Ludwig University in Freiburg. After finishing his master's in 2015, he worked as an embedded software engineer. In 2017 he began work at Fraunhofer ISE in the field of high-throughput on-the-fly laser processing of silicon solar wafers as his Ph.D. project.

Andreas Lorenz is head of the Printing Technology Group at Fraunhofer ISE. After receiving his diploma degree in 2006, he worked for six years as a research engineer and junior product manager for a global machine manufacturer. In 2012 he joined

Fraunhofer ISE and worked on the development of rotary printing processes for solar cells. He received his Ph.D. in 2018, and since then has been a project leader responsible for several research projects in the field of solar cell metallization.

Sebastian Tepner studied electrical engineering and information technology at the university of Bremen, Germany. Since 2016, he has been working at Fraunhofer ISE in the Production Technology – Structuring and Metallization department. He is currently head of the Printing Process Modeling and Rheology team, which focuses on research on screen-printing process development and dispensing technology.

Daniel Ourinson was awarded his Ph.D. in the field of the contact firing process by the Albert Ludwig University of Freiburg, in cooperation with Fraunhofer ISE, where he continues to work on related topics.

Gernot Emanuel completed his diploma thesis at Fraunhofer ISE to complement his studies in electronics at Furtwangen University in 1999. Since then, he has been working in different areas in the Photovoltaics Production Technology division. From 2017 onwards, his research activities have been mainly in the field of laser processing technology.

Sebastian Nold is head of the Techno-economic and Ecological Analyses Team at Fraunhofer ISE. He studied industrial engineering at the Karlsruhe Institute of Technology (KIT), Germany, and at the University of Dunedin, New Zealand, earning his diploma in industrial engineering at the KIT in 2009. In 2018 he completed his doctoral thesis at the Albert Ludwig University of Freiburg on the techno-economic assessment of new silicon solar cell production technologies along the PV value chain. He has been working at Fraunhofer ISE since 2008 in the areas of cost modelling, technology assessment and techno-economic evaluation of new concepts in the production of silicon solar wafers, cells and modules as well as emerging PV technologies.

Baljeet Goraya is a project engineer within the Techno-economic and Ecological Analyses team at Fraunhofer ISE. He obtained his B.Eng. in mechanical engineering from MSRIT, India, in 2011, and studied renewable energy engineering and management at the Albert Ludwig University of Freiburg, where he received his M.Sc. in 2016. Since he joined Fraunhofer ISE in 2019, his work has focused on the techno-economic evaluation of established and emerging, next-generation solar PV technologies, as well as on evaluating production processes for PEM fuel cells.

Florian Clement heads the Production Technology – Structuring and Metallization department at Fraunhofer ISE. He studied physics at the Ludwig Maximilian University of Munich and the University of Freiburg, obtaining his diploma degree in 2005, and later receiving his Ph.D. in 2009 from the University of Freiburg. His research focuses on new structuring and metallization technologies for silicon solar cells, in particular printing technologies. He also co-founded HighLine Technology GmbH, a Fraunhofer ISE spin-off, in 2019.

Enquiries

Fraunhofer Institute for Solar Energy System (ISE)
Heidenhofstr. 2
79110 Freiburg, Germany

Tel: +49 761 4588-2287
Email: marius.messmer@ise.fraunhofer.de

TOPCon solar cells – Technology roadmap for 25.5%-efficiency industrial manufacturing

Xinxing Xu, Zhaowei Wang, Hongbo Tong & Hua Li, Longi Green Energy Technology Co., Ltd., Xi'an, Shaanxi, China

Abstract

This paper presents an analysis and the results of extensive simulations of the efficiency limits and roadmap to 25.5% of a tunnel oxide passivated contact (TOPCon) solar cell, on the basis of an efficiency level of 25.21% (designed area, identified by ISFH) achieved through three years of continuous technical optimization on a pilot line at Longi. It is demonstrated that the key points for reaching the target of 25.5% mainly rely on optimizing the boron selective emitter, the profile of the poly-Si layer (thickness, dopant concentration and its rate of descent), the bulk properties (minority-carrier lifetime > 20ms), the metal contact recombination and metallization, the texture morphology and the anti-reflection coating.

Introduction

The tunnel oxide passivated contact (TOPCon) cell concept is well known for yielding a high-efficiency crystalline silicon solar cell, and its development is now undergoing serious momentum. For the tunnel oxide passivated contact structure, a 1.5nm SiO_x layer is applied to the rear surface of an n-type silicon absorber, functioning as a high-quality chemical passivation layer, as well as having an electron tunnelling structure function. A heavily doped polysilicon (poly-Si) layer is employed over the ultrathin oxide layer as the effective carrier collection layer.

"For a TOPCon solar cell, the formation of the tunnelling oxide passivated contact is a critical process."

The TOPCon solar cell is one of the most promising next-generation industrial products, as it presents several advantages over the passivated emitter and rear (PERC) solar cell. First, the higher-efficiency potential of TOPCon compared with PERC has been demonstrated on a laboratory scale [1,2] as well as in a commercial manufacturing setting [3–5].

Second, the fabrication process for a TOPCon solar cell is compatible with mainstream production lines, with the addition of a few extra process steps – a tube diffusion system for the boron-doped emitter and a low-pressure chemical vapour deposition (LPCVD) or plasma-enhanced chemical vapour deposition (PECVD) for poly-Si fabrication. Meanwhile, no laser doping or opening is required in this production line (no boron selective emitter). The cost is also lower than that for heterojunction solar cells.

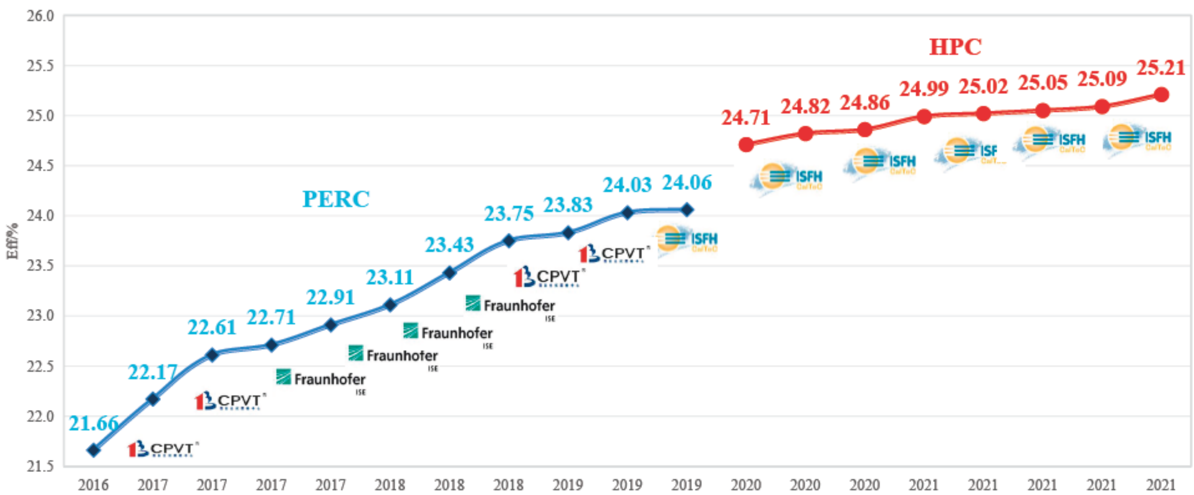

Figure 1. Recorded efficiencies of Longi R&D cells.

Third, based on n-type Czochralski (Cz) wafers, a TOPCon solar cell is not prone to suffering from light-induced degradation (LID) [6]. The temperature coefficient of a TOPCon solar cell is lower than that of mainstream products [7].

The tunnelling oxide passivated contact concept was first proposed by the Fraunhofer Institute in 2013 [8,9]. In just a few years, there have been dramatic developments in TOPCon solar cells owing to the efforts of a number of research institutions and industrial institutions. Fig. 1 presents the recorded efficiencies and pilot line production efficiencies of Longi R&D PERC and TOPCon solar cells. From the figure, it can be seen that the recorded efficiency has exceeded 25.21%, as identified by ISFH, which is about 1% higher than that of the mainstream PERC product; moreover, the power of a 72-half-cut-cell module has reached 570W.

For a TOPCon solar cell, the formation of the tunnelling oxide passivated contact is a critical process. An optimization of the doping profile of n^+ poly-Si can minimize the metal recombination and reduce the contact resistance. Similarly, a low doping concentration and a deep junction depth of the p^+ emitter on the front side is beneficial with regard to electrical properties. At the same time, it has been proved that the utilization of incident light dramatically improves through the use of light-trapping strategies, including texture morphology, metallization morphology and anti-reflection film [10,11]. It is strongly believed that the fabrication of TOPCon cells in mass production is the way forward to deal with grid parity, demonstrating several advantages ranging from lower production costs and capitalized costs to higher efficiencies. Besides, specific understanding of this structure encourages continuous progress at the industry level.

In this paper, the potential roadmap to another efficiency step-up to 25.5% will be summarized in relation to experience gained in mass production and associated theoretical development.

TOPCon solar cell development at Longi

Process flow for TOPCon solar cells fabricated at Longi

For the TOPCon solar cells, phosphorus-doped 1Ω·cm Czochralski-grown (170μm, <100>) Si wafers, sliced into 166×166mm pieces, are used. Fig. 2 shows a schematic of the TOPCon solar cell and the process sequence.

After cleaning and saw damage etching, the next step to be carried out is alkaline texturing (RENA Technologies process) in order to reduce the reflection to 10%. An optimized boron emitter is then formed as follows:

1. A BBr_3 source is used during the light-doping process, and a sheet resistance of 200Ω/sq. is obtained to reduce the surface recombination.

2. A laser is employed to remove the borosilicate glass (BSG) in the finger region.

3. The laser damage removal process is carried out.

4. To further reduce the contact resistance and metal recombination, a BBr_3 heavy-doping process is conducted, resulting in a sheet resistance of around 80Ω/sq.

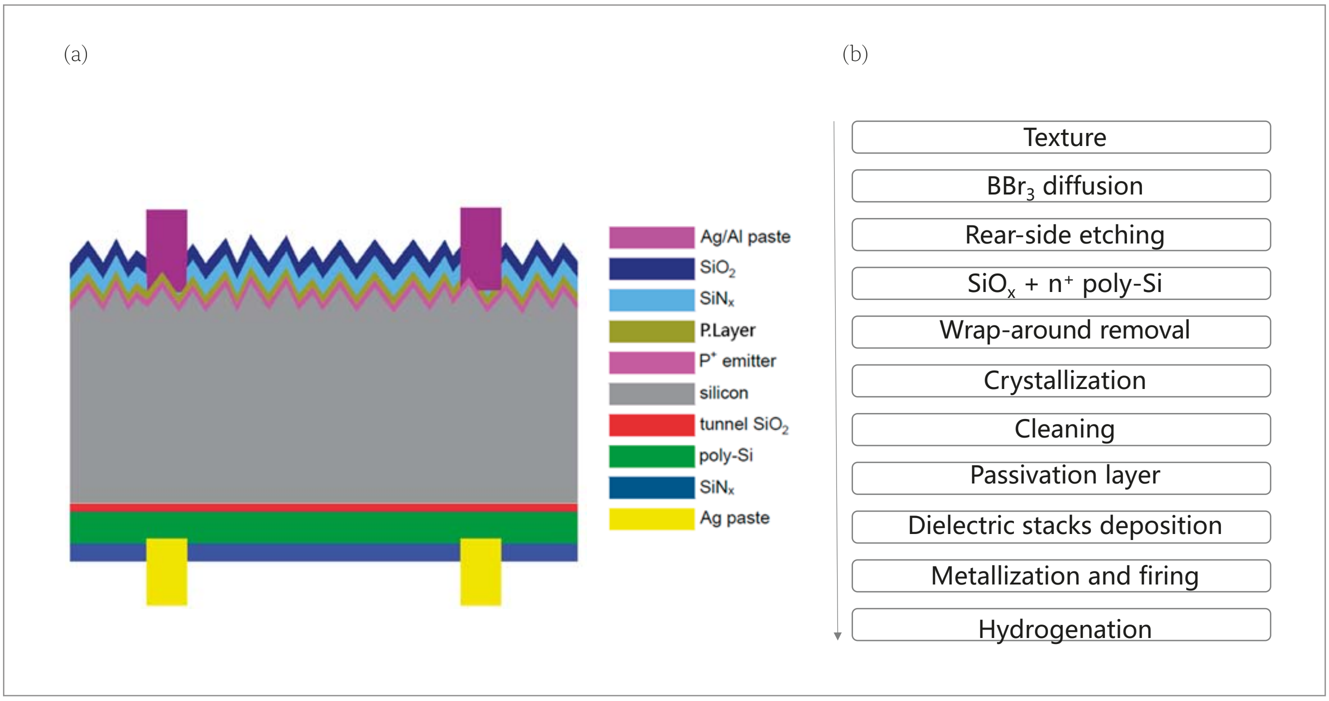

Figure 2. (a) Schematic of the TOPCon solar cell, and (b) the process sequence.

After the formation of the emitter, the BSG is removed and polished by means of a wet-chemical step on the rear side. Next, an ultrathin tunnel-SiO_x layer (~1.5nm) is formed by thermal oxidation, then in situ doped n^+ polysilicon (~130nm) is deposited by LPCVD. In the next step, the wrap-around of the poly-Si is removed, followed by crystallization in a tube furnace and the cleaning process.

After crystallization and cleaning, a 6nm passivation layer is deposited on the front side as the passivation layer, followed by the anti-reflection layer coating. On the rear side, a hydrogenated SiN_x layer is employed for further passivation by PECVD. At the metallization stage, silver/aluminium contacts are screen printed on the front side, and silver contacts on the rear, with subsequent firing in a belt furnace. After firing, a hydrogenation process is performed.

TOPCon technology development at Longi

Optimized doping profile

The properties of the emitter, including the doping density and the distribution of boron, significantly influence the optical and electrical properties of the solar cell [12]. For example, a heavily doped emitter can decrease the contact resistance; nevertheless, the solar cell suffers from recombination, as is the case for deeper doping profiles.

The optimized boron emitter is formed in several stages; the fabrication process of a boron emitter is shown in Fig. 3(a). The selective emitter structure could reduce the emitter saturation current density $J_{0,e}$; the average $J_{0,e}$ value of this type of structure is 9fA/cm^2. Meanwhile, 40µm-wide heavy doping can dramatically reduce the contact resistance to less than 1.5mΩ·cm^2, which is accompanied by a lower $J_{0,\text{metal}}$, less than 300fA/cm^2. Fig. 3(b) shows the electrochemical capacitance voltage (ECV) profile for light doping and heavy doping.

Optimized metallization scheme

Shading losses play an important role in efficiency losses. In order to reduce the efficiency loss resulting from the metallization shading, a new advanced metallization scheme was developed. The average width and height of the optimized metallization area was 23µm and 13µm, respectively, with an optimum finger width of 20µm.

Fig. 4 shows the geometry of the advanced fingers. The electrical properties of the TOPCon solar cell can be significantly improved by optimizing the metallization; for example, the efficiency can be increased by 0.2%. Table 1 lists the improvements in the electrical parameters, namely efficiency (η), open-circuit voltage (V_{oc}), short-circuit current (I_{sc}) and fill factor (FF). Apart from the gain in efficiency, the cost of the fingers can also decrease by 35%, which is very important for reaching grid parity.

Optimized silicon wafer

A series of experiments were carried out concerning the resistivity and lifetime of silicon wafers. Fig. 5 presents the experimental efficiency results as a function of resistivity and lifetime, revealing that an acceptable resistivity of ~1Ω·cm seems to be the most promising, whereas a higher or lower resistivity would be disadvantageous. The improvement in efficiency also comes with a longer lifetime of the silicon wafer (minority-carrier lifetime > 20ms). An optimization of the bulk properties confirmed a 0.2% improvement in efficiency.

Optimized cell efficiency

The optimized cells were sent to ISFH for third-party certification. The best performing cell fabricated according to the above-mentioned optimization strategies yielded an efficiency of 25.21% (designed area). The I–V curves and parameters are shown in Fig. 6, with V_{oc} = 721.6mV, I_{sc} = 10,117mA and FF = 83.9%.

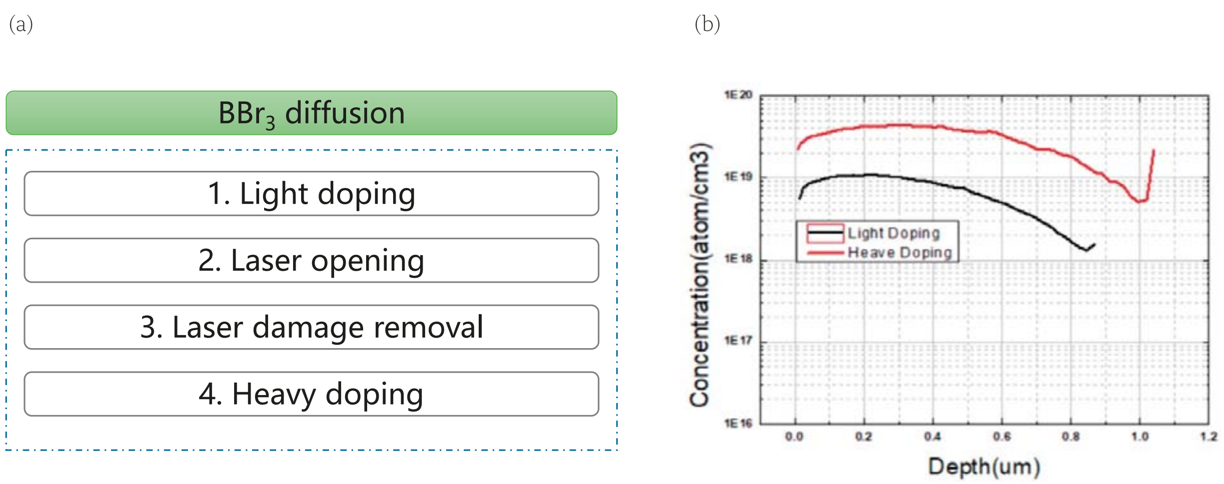

Figure 3. (a) Fabrication process for a boron selective emitter. (b) ECV profile for light doping and heavy doping.

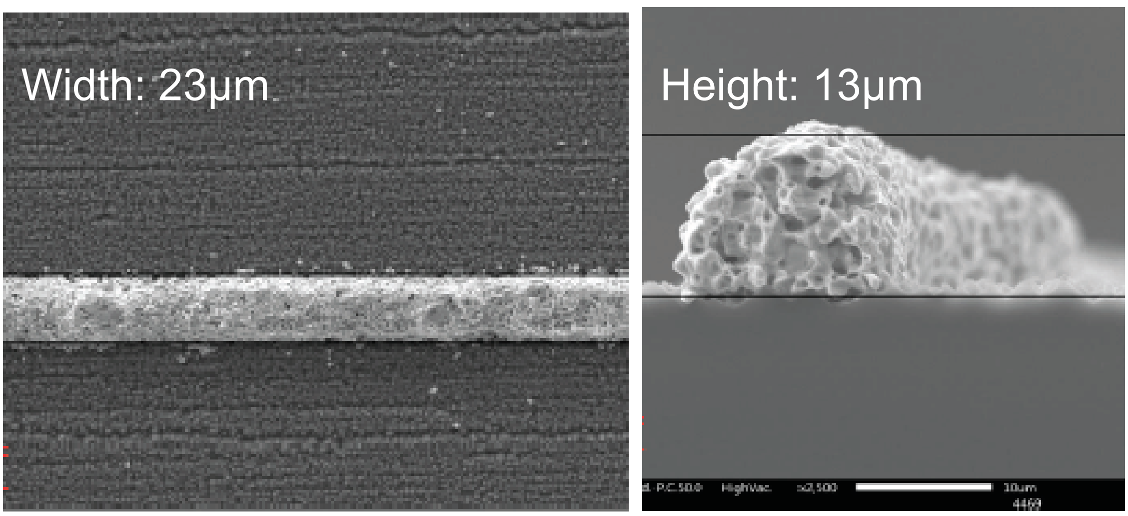

Figure 4. The resulting finger geometry for the advanced metallization scheme.

Advanced metallization	η [%]	V_{oc} [mV]	I_{sc} [mA]	FF [%]
Δ	0.2	2.3	41	0.12

Table 1. Improvements (Δ) in the electrical properties as a result of the advanced metallization scheme.

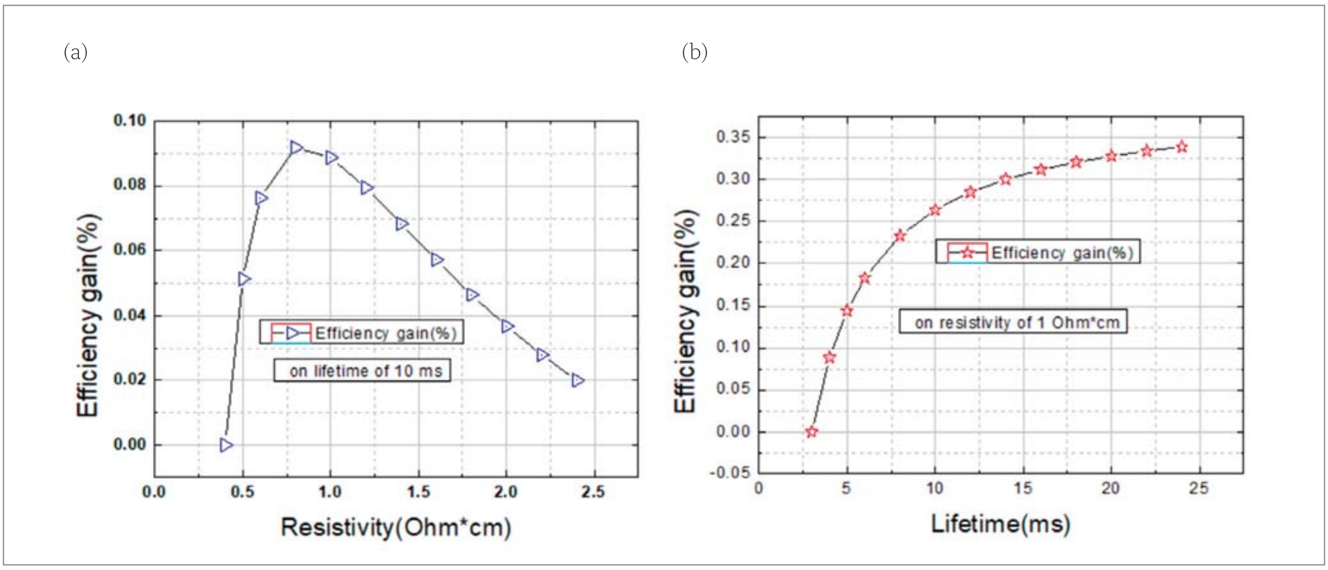

Figure 5. Experimental efficiency results as a function of (a) resistivity, and (b) lifetime.

Road map to 25.5%

Power loss analysis

A detailed loss analysis was carried out by means of a Quokka 3 simulation to understand the loss mechanisms and to identify options for improving cell performance [13]. The input parameters used in the simulation were based on experimental measurements taken from the 25.21% TOPCon solar cells.

Fig. 7 shows the power loss of the 25.21% TOPCon solar cell. The main losses include shading, front non-contacted recombination and front-surface transmission, equating to almost 67% of the total in the energy loss analysis. Nevertheless, the bulk properties (19.8%) and front contacted recombination (8.8%) should not be ignored for high-efficiency TOPCon solar cells.

The path to achieving 25.5%

Optimized light management

As an indirect semiconductor, crystalline silicon exhibits poor absorption. Optimized light management can effectively facilitate the usage of incident light. The pyramid structure was therefore optimized on the front surface to improve the light trapping.

Fig. 8(a) shows scanning electron microscopy (SEM) images of the optimized pyramid texture, while Fig. 8(b) gives the reflectance for the textured structure. From this result, it can be seen that the reflection

"The electrical properties of the TOPCon solar cell can be significantly improved by optimizing the metallization."

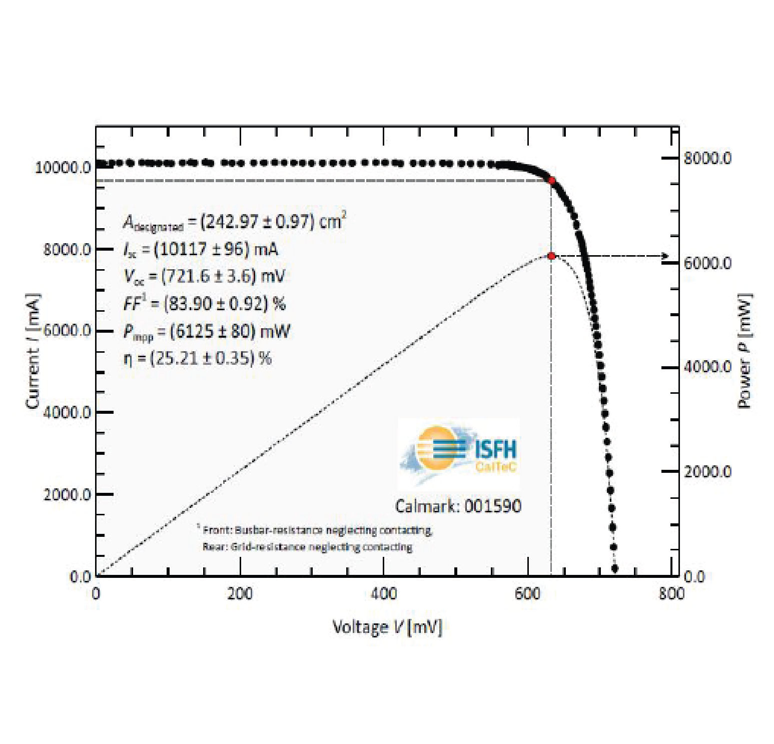

Figure 6. *I–V* curves for the best performing TOPCon solar cell.

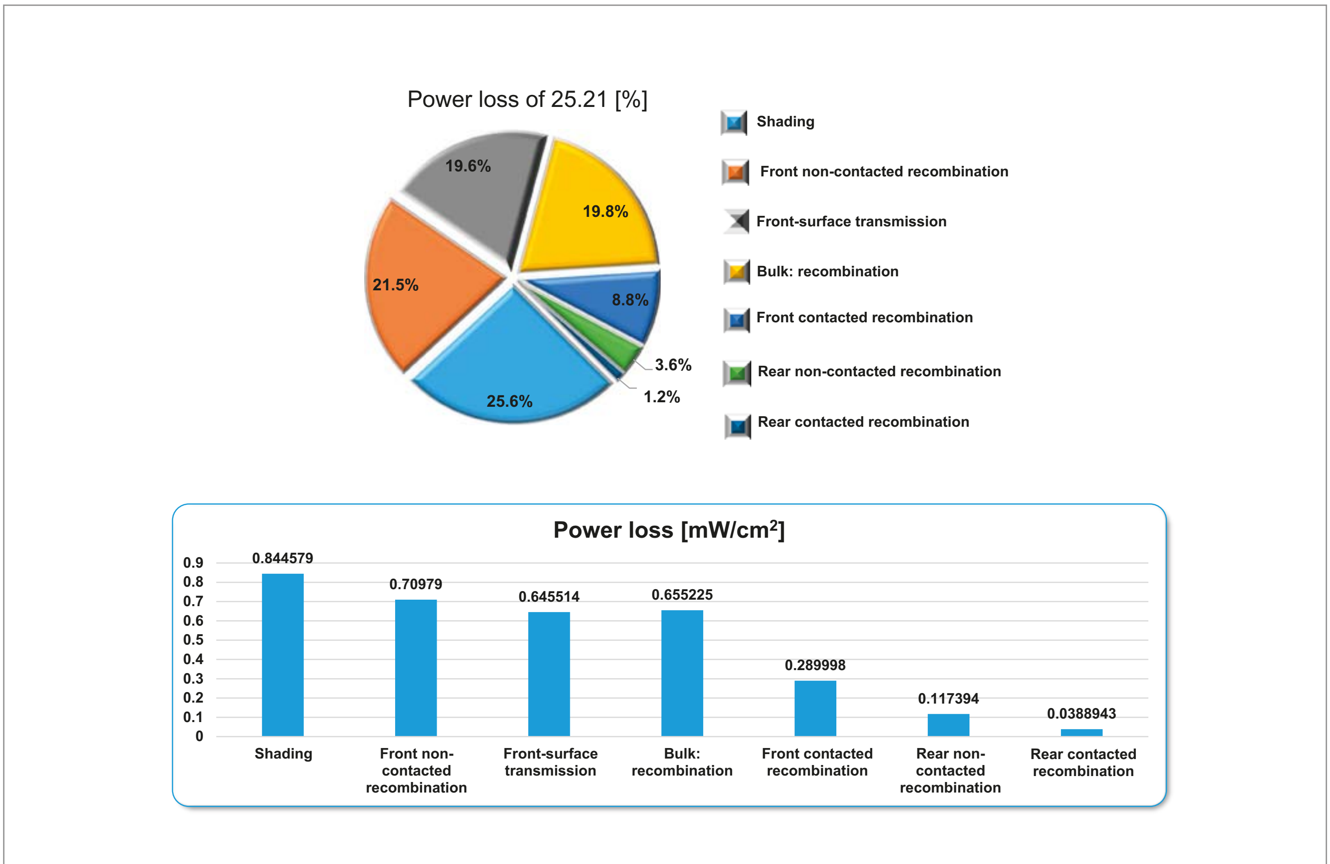

Figure 7. Simulation results for a power loss analysis of the 25.21% TOPCon solar cell.

"By optimizing the anti-reflection film through coating it with MgF_2, the transmission of incident light is higher than the baseline."

decreases throughout all wavelengths, indicating a more effective utilization of incident light. Apart from the morphology, coating films having a low refractive index further optimize the usage of sunlight, simultaneously resulting in excellent passivating properties on the front side. MgF_2 has the advantages of high thermal stability, low optical constant n, durability, and negligible absorption in the wavelength range of interest, thus making the material a good candidate for anti-reflection purposes [14]. By optimizing the anti-reflection film through coating it with MgF_2, the transmission of incident light is higher than the baseline, and a 0.2mA/cm^2 improvement in J_{sc} is realized.

Extra-fine metallization

A better doping profile of the emitter can reduce the recombination at the front side. To address the issue of decreased *FF* resulting from increased sheet resistance, an advanced metallization scheme B was developed.

Table 2 presents the parameters for different metallization schemes. To minimize the recombination of the emitter, the sheet resistance was increased from 200Ω/sq. to 300Ω/sq. A higher sheet resistance, however, can also lead to larger current transport losses towards the front side. Consequently, narrower fingers of width 18μm and smaller finger distances were used to mitigate the *FF* and I_{sc} losses. With the use of a narrower finger scheme, along with an appropriate emitter, a better carrier collection with reduced *FF* and I_{sc} losses can be obtained.

Optimized polysilicon

Parasitic absorption losses in the poly-Si on the rear side were considered one of the important optical losses. In order to reduce the optical loss resulting from the poly-Si, the thickness and the deposition conditions of the poly-Si should be optimized [15].

Table 3 presents the relevant parameters for two different poly-Si schemes, in which the phosphorus doping concentration is kept constant (higher than 7.0E+20cm^{-3}). When the poly-Si film thickness is reduced from 130nm in scheme A to 90nm in scheme B, the photogenerated current can increase by 0.15mA/cm^2. In addition, an optimization of the poly-Si fabrication process, for example reducing the polysilicon deposition temperature and pressure, can further decrease the parasitic absorption losses on the rear side.

Conclusions

After several years of development work on processes and techniques, TOPCon solar cells with an efficiency in 25.21% have been achieved. Simulations based on a characterization database have been carried out to demonstrate the main limits of current solar cells. The key points for obtaining a 25.5% efficiency relate to bulk properties, emitter optimization and optical loss minimization:

1. Bulk properties should initially be considered for creating high-efficiency TOPCon solar cells. For silicon wafers, an appropriate resistivity of ~1Ω and a longer lifetime (minority-carrier lifetime > 20ms) is necessary.

2. Optimization of the boron selective emitter can dramatically decrease the contact resistance, and also reduce the recombination loss at the front surface. It is necessary to maintain a balance between contact resistance and recombination.

"The key points for obtaining a 25.5% efficiency relate to bulk properties, emitter optimization and optical loss minimization."

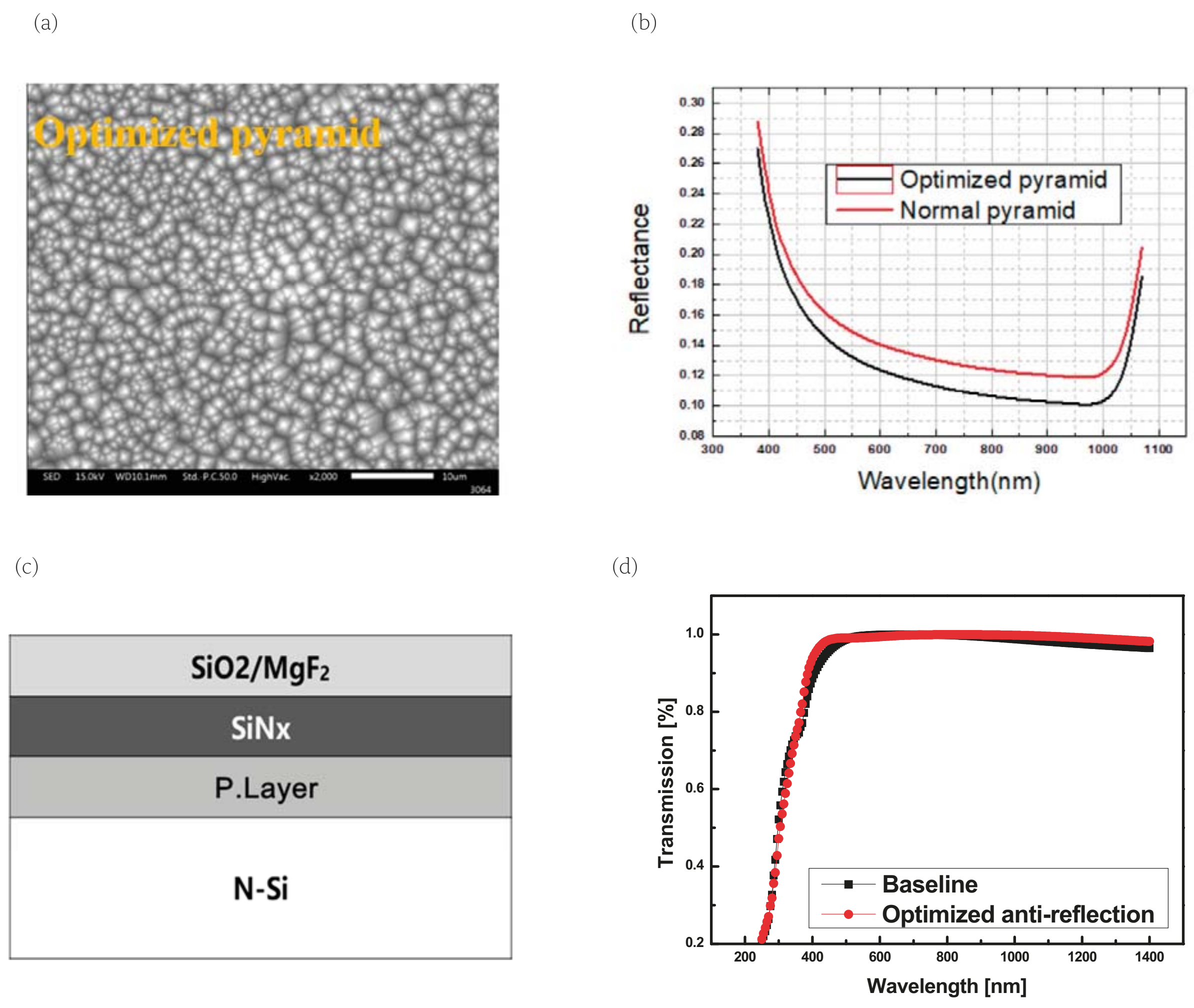

Figure 8. (a) Scanning electron microscopy (SEM) images of the optimized pyramid texture. (b) Reflectance for different texture structures. (c) Structure of the coating film on the front surface. (d) Transmission curves for different anti-reflection films.

Metallization	Efficiency [%]	Front side				Rear side	
		$R_{sheet, light doping}$ [Ω/sq.]	$J_{o,e}$ [fA/cm²]	$W_{fingers}$ [μm]	$D_{fingers}$ [mm]	$W_{fingers}$ [μm]	$D_{fingers}$ [mm]
Scheme A	25.2	200	9	23	1.3	30	1.1
Scheme B	25.5	300	7	18	0.9	30	0.8

Table 2. Parameters for the different metallization schemes.

Scheme	Efficiency [%]	Thickness [nm]	$R_{sheet,poly-Si}$ [Ω/sq.]	$J_{o,poly}$ [fA/cm²]	$J_{o,rear\ metal}$ [fA/cm²]
Poly-Si A	25.2	130	40	1.5	20
Poly-Si B	25.5	90	60	1.5	30

Table 3. Parameters for different poly-Si schemes.

3. Optical losses must be treated in respect of the front-surface morphology and anti-reflection films, as well as optimizing the metallization. An optimized pyramid structure, an MgF_2 coating film and extra-fine fingers should be employed in TOPCon solar cells.

References

[1] Chen, Y. et al. 2019, "Mass production of industrial tunnel oxide passivated contacts (i-TOPCon) silicon solar cells with average efficiency over 23% and modules over 345 W", *Prog. Photovolt: Res. Appl.,* Vol. 27, No. 10, pp. 827–834.
[2] Richter, A. et al. 2021, "Design rules for high-efficiency both-sides-contacted silicon solar cells with balanced charge carrier transport and recombination losses", *Nature Energy,* Vol. 6, No. 4, pp. 429–438.
[3] Richter, A. et al. 2017, "N-type Si solar cells with passivating electron contact: Identifying sources for efficiency limitations by wafer thickness and resistivity variation", *Sol. Energy Mater. Sol. Cells,* Vol. 173, pp. 96–105.
[4] Green, M. et al. 2021, "Solar cell efficiency tables (version 57)", *Prog. Photovolt: Res. Appl.,* Vol. 29, No. 1, pp. 3–15.
[5] Haase, F. et al. 2018, "Laser contact openings for local poly-Si-metal contacts enabling 26.1%-efficient POLO-IBC solar cells", *Sol. Energy Mater. Sol. Cells,* Vol. 186, pp. 184–193.
[6] Chen, D. et al. 2017, "Evidence of an identical firing-activated carrier-induced defect in monocrystalline and multicrystalline silicon", *Sol. Energy Mater. Sol. Cells,* Vol. 172, pp. 293–300.
[7] Kafle, B. et al. 2021, "TOPCon – Technology options for cost efficient industrial manufacturing", *Sol. Energy Mater. Sol. Cells,* Vol. 227, 111100.
[8] Moldovan, A. et al. 2015, "Tunnel oxide passivated carrier-selective contacts based on ultra-thin SiO_2 layers grown by photo-oxidation or wet-chemical oxidation in ozonized water", *Proc. 42nd IEEE PVSC,* New Orleans, Louisiana, USA, pp. 1–6.
[9] Feldmann, F. et al. 2014, "Passivated rear contacts for high-efficiency n-type Si solar cells providing high interface passivation quality and excellent transport characteristics", *Sol. Energy Mater. Sol. Cells,* Vol. 120, pp. 270–274.
[10] Saive, R. 2021, "Light trapping in thin silicon solar cells: A review on fundamentals and technologies", *Prog. Photovolt: Res. Appl.,* Vol. 29, No. 10, pp. 1125–1137.
[11] Fonash, S. 2014, *Introduction to Light Trapping in Solar Cell and Photo-detector Devices.* London, San Diego, Waltham, Oxford: Academic Press, Elsevier.
[12] Schiele, Y. et al. 2013, "Study on boron emitter formation by BBr_3 diffusion for n-type Si solar cell applications", *Proc. 28th EU PVSEC,* Paris, France, pp. 1242–1247.
[13] Fell, A. et al. 2017, "The concept of skins for silicon solar cell modeling", *Sol. Energy Mater. Sol. Cells,* Vol. 173, pp. 128–133.
[14] Rezaei, N. et al. 2019, "Optical optimization of a multi-layer wideband anti-reflection coating using porous MgF_2 for sub-micron-thick CIGS solar cells", *Solar Energy,* Vol. 177, pp. 59–67.
[15] Min, B. et al. 2018, "Increasing the photo-generated current in solar cells with passivating contacts by reducing the poly-Si deposition temperature", *AIP Conf. Proc.,* Vol. 1999, No. 1, 040015.

About the Authors

Xinxing Xu graduated with a Bachelor of Science degree in applied physics from Southeast University of Nanjing, China. He works at Longi as a director engineer, and was responsible for improvements in TOPCon cell efficiency. He has over 11 years' experience in the PV industry.

Enquiries

Xinxing Xu
Longi Green Energy Technology Co., Ltd.
Block B, No.8989 Shangji Road
Xi'an Economic and Technological Development
Shaanxi 710018, China

Email: xuxx@longi.com
Website: www.longi.com/en/

Future industrial solar PV technologies: Record cell efficiency announcements versus industrial reality

Radovan Kopecek & Joris Libal, International Solar Energy Research Center ISC Konstanz, Germany

Abstract

Record cell efficiency announcements have a history that is as old as the PV industry. Whereas up until around 2015 such announcements were mostly published by PV institutes processing small solar cells 2×2cm² in area, during the last five years industrial cell and module manufacturers have begun to publish record cell and module efficiency announcements more and more frequently for so-called *large-area industrial devices*. These efficiency announcements are somewhat heterogeneous in terms of device structures (not always corresponding to the commonly used nomenclature) as well as in terms of measurement conditions. The values range from the recently published 26.3% efficiency for a silicon heterojunction technology (HJT) solar cell from LONGi, with measured fill factor (*FF*) close to the theoretical limit (exceeding 86%), to 21.1% for actual, currently available, modules in mass production from Trina Solar. Accordingly, this paper discusses what is actually behind these announcements and how an evolutionary industry sector such as PV is becoming, it seems, decidedly revolutionary with large jumps in efficiency. In reality, these announcements give the wrong impression: the PV industry still needs to be conservative, as PV modules must be low cost and long-term stable at the same time. This is why the transfer of innovations to mass production will now (and also in the future) always require a certain amount of time, and PV technology development will continue to proceed in an evolutionary way through a step-by-step introduction of innovative concepts.

Introduction

By 2020, solar PV – with its bifacial passivated emitter and rear cell (PERC) technologies – had been crowned the new king of the energy markets [1], sporting extremely low offers in tenders in the Middle East and North African (MENA) states, such as Saudi Arabia, drawing prices as low as 1USct/kWh [2] in 2021. As PERC is currently on the verge of reaching its efficiency limits, the question now is: what is next? And which cell technology will take the thrown as the new 'emperor'? Moreover, is there going to be a rapid shift from p-type Si-based PERC to n-type Si cell technologies, as was the case about five years ago when the PV industry switched very quickly from Al-BSF to PERC? As shown in Fig. 1, PV-Tech Research [3], as well as a significant part of the PV community, believes so.

> "Record cell efficiency announcements are now being published at a steadily increasing frequency."

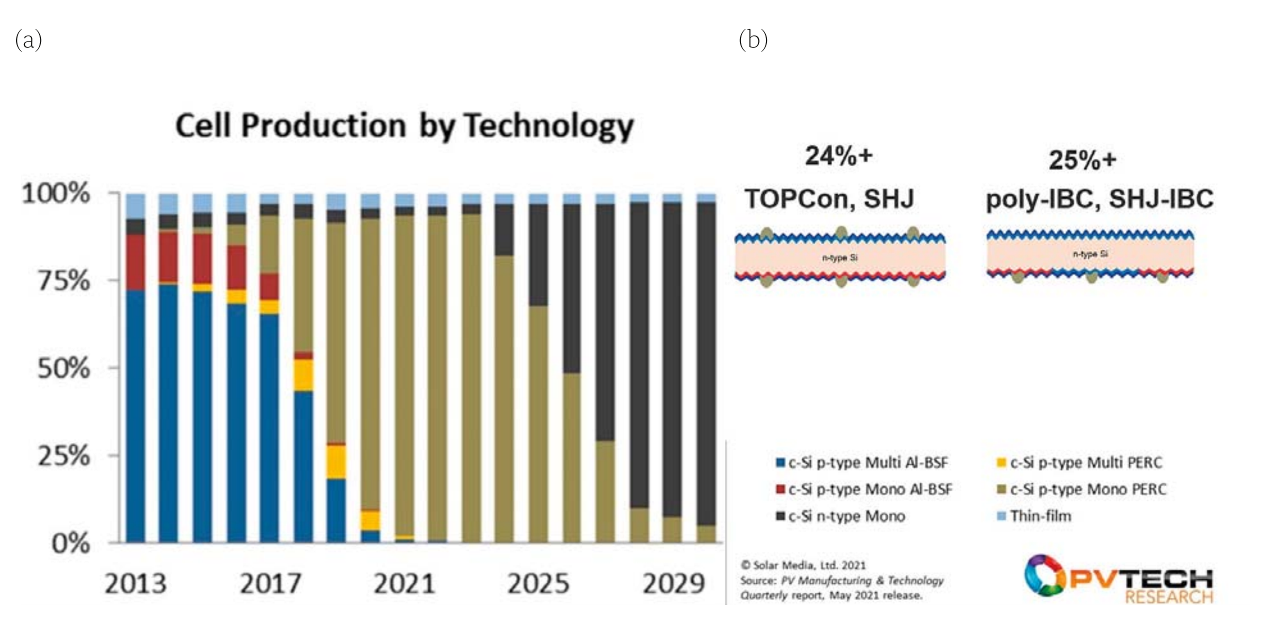

Figure 1. (a) Historical data showing the switch from Al-BSF technology (blue and red bars) to PERC (light brown bars) and forecast of a switch to n-type technology (grey bars) in coming years [3]. (b) Schematic cross sections for TOPCon, HJT and poly-IBC, HJT-IBC.

But what will be the next mainstream technology? Silicon heterojunction technology (HJT)? Tunnel oxide passivated contact (TOPCon)? A combination of both in an interdigitated back contact (IBC) structure? Tandem cells? The race is on and the record cell efficiency announcements are now being published at a steadily increasing frequency. PERC record efficiencies at the cell and module levels are announced by Tier 1 manufacturers with the aim of supporting the claim that this technology still has the potential for significant efficiency increases. The various announcements regarding n-type Si cell technology, on the other hand, are intended to show which of the different options will be the most promising one to choose in the future.

Solar cell improvements in industry

In a very clear and simple representation, Fig. 2(a) depicts a linear yearly growth of cell efficiency in the industry of about 0.6%$_{abs}$, as reported by Martin Hermle [4]. The switch from Al-BSF to PERC was set in motion in 2016, when Al-BSF technology reached its efficiency limit; this was mainly the result of the limited surface passivation of the rear side by the homogeneous Al-BSF, as shown in the cross section in Fig. 2(b).

With a dielectric stack (AlO_x/SiN_x) below the Al paste and Al-BSF point contacts, a better rear-side passivation can be realized, leading to an average open-circuit voltage (V_{oc}) of 680mV and a maximum of 690mV. Now, to go beyond 700mV, passivating contacts with poly-Si in TOPCon must be used. To surpass 720mV, passivating contacts need to be used on both polarities, or a-Si layers in HJT technology have to be employed. Then, in the next step, in order to overcome the Auger limit or even the Shockley–Queisser limit, tandem structures are necessary. Accordingly, this linear curve is based on first-order incremental improvements of the voltage by a better passivation with advanced cell structures.

> "The efforts of various players to promote their respective roadmaps has led in the past to an increasing number of 'industrial' record cell and module efficiency announcements."

A comparison can be made of these technologies with the various mobile networks and their speeds: 3G (Al-BSF at 665mV) is nowadays virtually obsolete, and the working horse is currently 4G (PERC at 685mV), with 5G (passivating contacts at 700mV) already in place. For most applications (e.g. ground-mounted utility-scale PV systems), however, 4G is still sufficient and the – up until now – more expensive 5G is only required for certain applications. Nevertheless, in a few years' time 5G will be the norm for all applications, and we will even be preparing the ground for 6G (tandem).

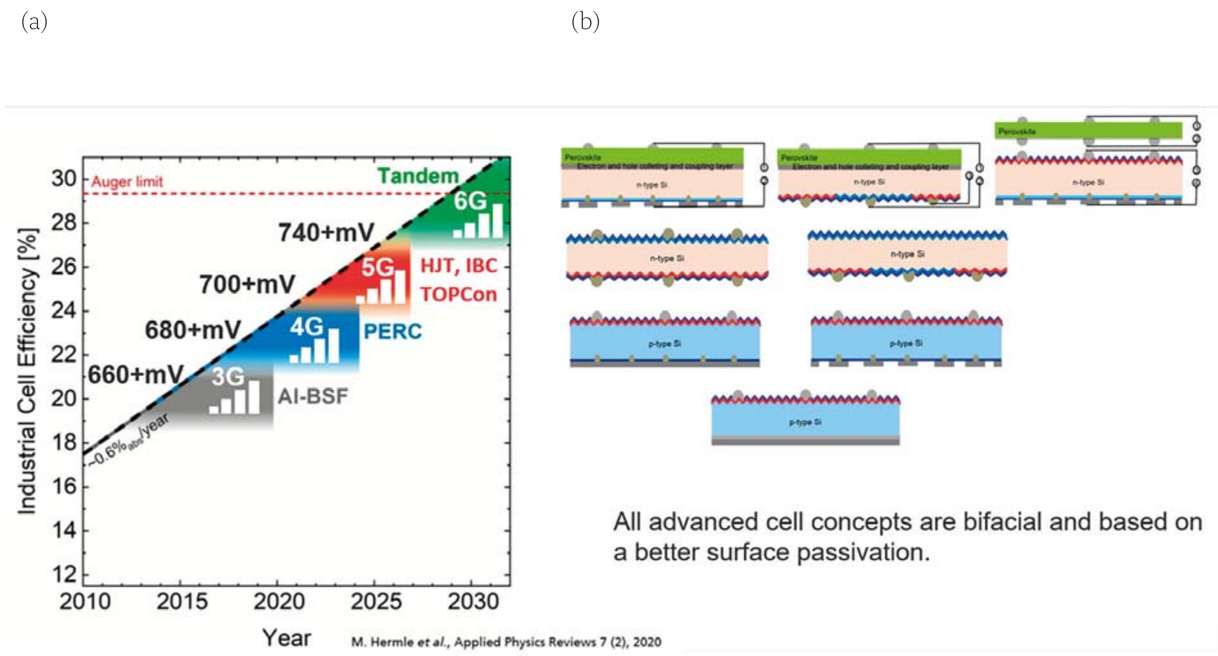

Figure 2. (a) Efficiency (open-circuit voltage) improvements and limits of c-Si technologies in the past, along with future predictions, with an analogy to the 3G–6G mobile networks (graph adapted from Hermle et al. [4]). (b) Schematic cross sections for Al-BSF, mono and bifacial PERC, TOPCon, HJT, IBC and two-, three- and four-terminal tandem configurations.

Considering the various technologies that have been implemented during the last few decades in the PV industry, and which have achieved a mainstream market share, one can reasonably conclude that the PV industry has always followed an evolutionary technology roadmap. On the other hand, the efforts of various players to promote their respective roadmaps (some evolutionary, others rather disruptive) has led in the past to an increasing number of 'industrial' record cell and module efficiency announcements, mostly from Tier 1 manufacturers.

In the following sections, an attempt will be made to further dissect the practices and peculiarities related to the various record efficiency announcements.

"The active area module efficiency is not relevant in the appraisal of the benefits of high module efficiency in terms of savings for area-related balance of system cost."

High-efficiency cell announcements

Most of the time, high-efficiency announcements reveal nothing more than the practical limit of each technology, as depicted in the graph in Fig. 2(a). However, more often than not there is a gap in efficiency of at least 1%$_{abs}$ between what is possible – using additional process steps or non-industrial process steps as well as specific, R&D-like measurement conditions – and what can be implemented in mass production in a cost-effective way. Consequently, there are several elements of such announcements that tend to cause a certain amount of confusion with the public (investors, CEOs, scientists and other stakeholders):

- The nomenclature used for the cell concepts is different from that for the cells actually being announced. For example, the 24.06% PERC cell announced from LONGi in 2019 already had a selective poly-Si on the front side in order to deliver 694mV, while the 25.4% TOPCon from JinkoSolar in 2021 most likely also has poly-Si passivating contacts not only on the rear side but also on the front, leading to a V_{oc} of 720mV.

- Sometimes, even when the announcement of an 'industrial solar cell' makes the headlines, laboratory-type processes, such as double anti-reflective coating (ARC) including MgF_2 deposition by thermal evaporation, have been used in the fabrication of such cells. Many of these processes have been known for decades and used in R&D in order to demonstrate the potential of certain materials or cell concepts; however, they are just too complex and too expensive to be implemented for mass production.

- Even though a reported efficiency has been measured by an independent calibration laboratory or certification body, the *I–V* measurement will have been performed under conditions that – until recently – have only been used in the field of R&D:
  - o Active area efficiency is measured instead of aperture area efficiency (at the cell level as well as at the module level).
  - o Cell efficiency measurements are taken with multiwire contacting, and efficiency values reported without taking into account the shading by the metal grid (or at least by the busbars).
  - o Contacting methods are used that result in the metal grid series resistance (front or rear side, or both sides) to be neglected, leading to measured fill factors (*FF*s) that are very close to the pseudo-fill factor (i.e. theoretical limit of *FF* for zero series resistance and infinite shunt resistance).
  - o Such 'R&D-like' efficiency measurement conditions are not suited to properly characterizing industrial solar cells, as they are not representative for the efficiency that can be reached at the module level: at the module level, the shading of the metal grid(s) as well as their series resistance will contribute to reducing the module efficiency, thus increasing the cell-to-module power loss.

- In the case of the reported efficiency values being based on in-house measurements, there is the risk of an overly optimistic calibration, leading to an overestimation of the efficiency.

Very often, in the related press releases, the above-listed peculiarities associated with efficiency measurements are only stated in the fine print and require careful reading in order to allow a correct appraisal of the reported efficiency value.

One recent example of misleading efficiency reporting is the 23.03% record module efficiency, which was – as reported by Trina [5] – an 'aperture efficiency'. While the standard module efficiency is the *total area* efficiency, which is the electrical power output (P_{mpp} at standard test conditions – STC) divided by the irradiance on the total area divided by the total area of the module (module length multiplied by the module width), the *aperture area* module efficiency excludes the area occupied by bussing ribbons and junction boxes, as well as the mandatory gaps between the outer solar cells and the edge of the laminate in addition to the frame. In consequence, the aperture area efficiency reaches higher values (approaching the cell efficiency) than the total area module efficiency. Accordingly, the active area module efficiency is not relevant in the appraisal of the benefits of high module efficiency in terms of savings for area-related balance of system cost.

A fairly recent example of the R&D-like measurement conditions mentioned above is the surprisingly high *FF*s measured at certain calibration laboratories. If one reads the fine print, for instance, inserted below the *I–V* curve measured at ISFH CalTec shown in Fig. 3 [6], the reasons for the extremely high *FF* (close to the theoretical limit) and the high short-circuit current measured on LONGi's 26.3%-efficient HJT record cell become apparent: while the current benefits from back reflection of light by the gold-coated chuck, the *FF* is enhanced as a result of a large fraction of the total series resistance of the cell being neglected. In the case of an industrial cell line, however, pins are used to contact the busbars on the front and rear sides of the cells, thereby mimicking the way the cells are interconnected by ribbons within the PV module and without providing any back reflection of light into the rear of the cell.

Table 1 summarizes the record announcements versus reported average efficiencies in production (including a potential overestimation by in-house measurements) and available module efficiencies

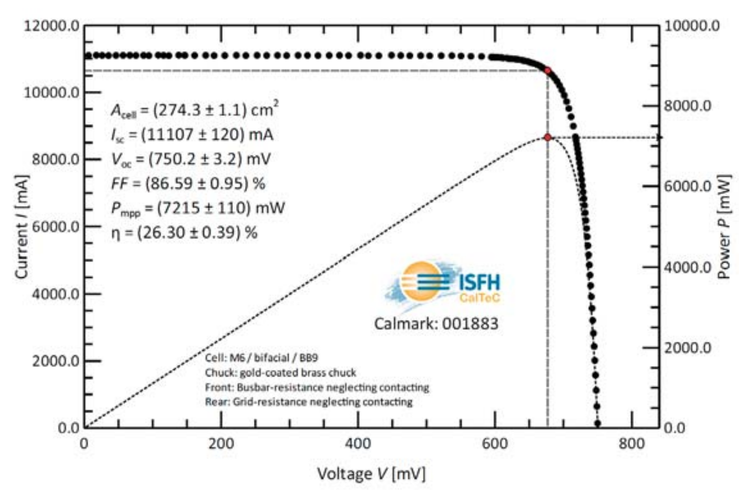

Figure 3. Calibrated *I–V* measurement at ISFH of the 26.3% highest efficiency HJT cell from LONGi [6].

on the market, as well as the potential voltage and efficiency of the various technologies.

The PV market is witnessing a fade-out of *Al-BSF (3G)*, as it is also monofacial. The average cell efficiencies in production reach up to 20%, with a V_{oc} of around 665mV. A few years back, one of the record efficiencies announced was 20.29% [9], but the module efficiencies on the market are well below 20%.

The king of the energy markets, *bifacial PERC (4G)*, yields average solar cell efficiencies of around 23% in production. PERC module efficiencies on the market are mostly below 21%, but can reach up to 21.1% (e.g Trina [9]). For the 24.06% record PERC cell efficiency already achieved by LONGi in 2019 [10], a selective poly-Si was used on the front; the cell also has other features that have not yet been implemented in industrial production, and which will require in any case additional process steps coming in at a higher cost.

PERC-based technologies – such as TOPCon and PERC-based IBC – benefit from reduced cost as a result of the technological progress in PERC technology as well as the economy of scale for equipment and material thanks to PERC mass production. The major challenge, as in almost all n-type technologies, is to reduce the Ag consumption for the metal contacts, which is currently a very important R&D topic.

TOPCon (5G) cells reach in production an average efficiency of about 23.5%, whereas a record cell efficiency of 25.4% [11] has been recently demonstrated by JinkoSolar. In this case, neither the exact process flow and cell architecture nor the single *I–V* parameters (I_{sc}, V_{oc}, *FF*) have been published by Jinko. However, considering that a very high V_{oc} is required in order to reach an efficiency above 25%, it can be assumed that – in addition to other non-industrial features –a selective poly-Si(B) was most likely used, which is more complex than the current industrial TOPCon process and not yet ready for industrial mass production. Depending on the current silver price, the COO (cost of ownership) for a standard TOPCon cell is currently about 15–30% higher than that for PERC (e.g. [17]. But, the higher efficiency, higher bifaciality, lower degradation and lower temperature coefficient for P_{mpp} make these modules already attractive not only for rooftop applications but also for ground-mounted utility-scale solar, as well as for hot regions and on systems with high ground albedo too.

PERC-based IBC (5G) (Jolywood, SPIC, Trina, ValoeCell), with a 25.04% efficiency demonstrated by Trina [12], is commercially produced at average efficiencies of around 24%, having a potential of 25%. At the moment, such cells are mostly suited to rooftop PV applications. With the ongoing reduction of Ag metallization, the bifacial version could also be used on a utility scale in the future.

In the case of *low-cost HJT (5G)* (REC, Meyer Burger, Maxwell), an efficiency of 25.26% was demonstrated by Maxwell [13], whereas *complex HJT (5G)* (Panasonic, Kaneka, LONGi) has reached record efficiencies of 26.3%, as very recently shown by LONGi [17]. *Complex IBC (5G)* devices are produced by SunPower and LG. At the laboratory level, an efficiency of 26.1% has been demonstrated by ISFH on a poly-Si on oxide (POLO) structure [15], and 26.6% by Kaneka using an HJT-IBC structure [16].

Non-industrial cell processes and R&D-type measurements used for 'industrial' record efficiency announcements

Table 2 summarizes a list of ways to modify an industrial solar cell process, or how to measure differently from the standard technique, in order to achieve significantly higher cell efficiencies, but at the expense of industrial feasibility and cost effectiveness.

Summary and outlook

In summary, there are many record cell announcements making the news – even

Technology	Equipment	Record cell efficiency announcements [%]	Reported average cell efficiency in production [%]	Available module efficiency [%]	V_{oc} potential in production [mV]	Efficiency potential in production [%]
Al-BSF	Standard	20.29 [8]	19.5–20.0	<20%	670	20.5
PERC	Standard PERC based	24.06 [10]	22.5–23.5	20.2–21.1 [9]	685	23.5
TOPCon		25.40 [11]	23.0–24.5	21.4 [9]	725	24.5
Low-cost IBC		25.04 [12]	23.5–24.5	21.3 [9]	725	24.5
Low-cost HJT	Thin-film based	25.26 [13]	23.5–24.5	21.9 [9]	735	25.0
Complex HJT	Thin-film and electronic industry based	26.3 [14]	24.5–25.0	21.7 [9]	740	25.5
Complex IBC	Thin-film and electronic industry based	26.1 [15] 26.6 [16]	25.0–25.5	22.0–22.8 [9]	740	26.0

Table 1. High-efficiency announcements (red column) versus the available module efficiency reality (green column) of all relevant c-Si technologies on the PV market (adapted from PV-Tech [6]).

from industrial cell manufacturers – that demonstrate the capabilities of the respective R&D divisions when using their laboratories and advanced pilot lines but which do not allow an apple-to-apple comparison with the respective technologies currently (or close to being) up and running in industry. Accordingly, it is difficult to deduce from such announcements when (and if ever), and at what production cost, the related technologies will be implemented with similar efficiencies in industrial production.

'Trick', 'uncertainty' or gain that cannot be transferred to the module	Absolute efficiency gain [%] compared to mainstream industrial process sequence	Comments
WAFERS		
Use of hand-picked premium material (FZ-Si or very good Cz-Si)	Up to 0.5%	It is possible to use p-type wafers with >5ms (and n-type >10ms) lifetimes, but these are not yet available as commercial material (i.e. they are significantly more expensive).
Pre-gettering or extra hydrogenation of material	Up to 0.5%	Pre-treatment (takes place before the actual cell process) of the as-cut wafers that consists of performing, for example, a $POCl_3$-diffusion with subsequent wet-chemical removal of the P-doped layer containing gettered impurities from the bulk of the wafers.
Use of small-area wafers	Up to 1%	Overcoming inhomogeneities in non-standard processes and/or wafer material quality, reduction of series resistance losses (shorter finger length).
SOLAR CELL PROCESSES		
Very good, laboratory-type cleaning (e.g. RCA)	Up to 0.5%	Extensive (and expensive) cleaning methods not used in the PV industry can be used prior to critical high-temperature processes.
Advanced texture (masking + etching)	Up to 0.5%	Very good and complex texture can be applied to the surface with, for example, masking and wet-chemical treatment.
Long diffusions	Up to 0.3%	Long diffusions not used in production can lead to, for example, better selectivity of the emitter.
High-quality, thick thermal SiO_2 layers for surface passivation or as masking steps	Dependent on cell architecture	Thick thermal SiO_2 layers allow more flexibility regarding the cell architecture when used as a masking layer, and provide perfect surface passivation. Process cost, however, is too high for industrial PV manufacturing (duration and pre-cleaning).
Light blue ARC	Up to 0.4%	The ARC can be adapted to the sun simulator, for example with an increased minimum amount of reflection in UV (in a wavelength range where glass and encapsulants are strongly absorbant, i.e. advantage is lost at the module level).
Double ARC	Up to 0.4%	For example, using laboratory processes, such as thermal evaporation of MgF_2.
No edge isolation	Up to 0.4%	Omitting the edge isolation results in cells that feature a higher efficiency but which cannot be used in commercial modules.
Additional printing steps	Up to 0.4%	Additional printing steps and the use of more metal paste for improving the finger aspect ratio can result in an extremely high *FF*.
Plating, evaporated contacts or other nonstandard techniques	Up to 1%	Alternative complex metallization methods can lead to a boost in all cell *I–V* parameters.
MEASUREMENTS		
'Active area efficiency'	Up to 1%	Calculated efficiency with no grid (fingers and busbars) shading on the front.
'Implied efficiency'	Up to 1.5%	Calculated efficiency with the assumption of no voltage losses and no series resistance losses after metallization (using implied voltage and pseudo-*FF*).
Erroneous in-house measurements	Up to 1.5%	Using incorrect calibration can have an impact on measurement accuracy.
Zero-busbar measurement (*I–V* at STC obtained using GridTouch contacting method)	Up to 0.7%	Only the fingers are printed, reducing the shadowing and V_{oc} losses from absent busbars. Gain compared to five-BB scheme can be up to 0.7%, but even assuming a multiwire interconnection at the module level, only a part of the efficiency gain can be transferred to the module.
Non-standard contacting of cells that neglects series resistance	0.5% to 1.5%	Even measurements within CalLabs can differ, mainly because of the contacting scheme used.

Table 2. Overview of non-industrial process steps and R&D-type efficiency measurements that can be used in order to fabricate record cells (updated version of the list included in the PV-Tech blog [7].

> "There are many record cell announcements which do not allow an apple-to-apple comparison with the respective technologies currently up and running in industry."

That said, record cell efficiencies allow a glimpse of what the mid-term future might bring. Ultimately, if one has the scope for determining for a given cell technology the highest cell efficiency currently available in commercial production, the most practical and reliable way is to look for the respective module with the highest P_{mpp} at STC (for a given module area) that is commercially available, and – taking account of the total cell area as well as a realistic cell-to-module P_{mpp} ratio – to ascertain the related cell efficiencies.

The c-Si PV industry has always had, and will have in the future, an evolutionary development, with year-on-year increases in efficiency of 0.3–0.6%$_{abs}$. This will still be the case in the next ten years, until the practical efficiency limit of 26–27% is reached. What will happen after that is still unclear. The success of tandem solar cell devices will very much depend on the successful development of perovskites and corresponding tandem architectures with regard to stability, reverse behaviour, etc.

The average efficiencies of industrial PERC solar cells will remain between 22.5% and 23.5%, whereas the average efficiencies of industrial n-type devices will be well above 24% in one to two years, and surpass 25% in three to five years. Available PERC modules will yield efficiencies of around 21%, whereas n-type module efficiencies will exceed 22% from 2022 onwards, and most likely 23% from 2025 onwards. What will happen after c-Si hits its practical efficiency limit of 26–27% remains uncertain.

References

[1] PV-Tech 2020 [https://www.pv-tech.org/iea-solar-the-new-king-of-power-will-break-records-for-decades-to-come/].
[2] S&P Global 2021 [https://www.spglobal.com/platts/en/market-insights/latest-news/electric-power/042621-saudi-arabia-solar-target-raised-after-seven-projects-added-including-record-low-cost].

[3] Solar Media 2021, PV Manufacturing and Technology Quarterly Report, May.
[4] Hermle, M. et al. 2020, *Appl. Phys. Rev.,* Vol, 7, No. 2.
[5] Trina Solar 2021 [https://www.trinasolar.com/de/resources/newsroom/thu-07012021-1124].
[6] PV-Tech 2021 [https://www.pv-tech.org/future-industrial-solar-pv-technologies-champion-cell-announcements-versus-industrial-reality/].
[7] PV-Tech 2019 [https://www.pv-tech.org/future-industrial-pv-technologies-champion-cell-announcements-verses-indust/].
[8] Kim, K.H. et al. 2017, "Record high efficiency of screen-printed silicon aluminum back surface field solar cell: 20.29%", *Jap. J. Appl. Phys.,* Vol. 56, No. 8S2, 08MB25.
[9] Clean Energy Reviews 2021 [https://www.cleanenergyreviews.info/blog/most-efficient-solar-panels].
[10] PV-Tech 2019 [https://www.pv-tech.org/longi-solar-has-bifacial-mono-perc-solar-cell-world-record-verified-at-24-0/].
[11] JinkoSolar 2021 [https://ir.jinkosolar.com/news-releases/news-release-details/jinkosolars-high-efficiency-n-type-monocrystalline-silicon-solar].
[12] PV-Tech 2018 [https://www.pv-tech.org/trina-solar-takes-n-type-mono-ibc-cell-to-record-25-04-conversion-efficienc/].
[13] TaiyangNews 2021 [http://taiyangnews.info/technology/25-26-HJT-solar-cell-efficiency-for-huasun-energy/].
[14] TaiyangNews 2021 [http://taiyangnews.info/technology/26-30-efficiency-for-longis-hjt-solar-cell/].
[15] Hollemann, C. et al. 2020, "Separating the two polarities of the POLO contacts of an 26.1%-efficient IBC solar cell", *Sci. Rep.,* Vol. 10, p. 658 [https://www.nature.com/articles/s41598-019-57310-0].
[16] ZME Science 2017 [https://www.zmescience.com/ecology/renewable-energy-ecology/solar-cell-close-ideal-limit/].
[17] Kafle, B. et al. 2020, "TopCon – Technology options for cost efficient industrial manufacturing", *Proc. 37th EU PVSEC* (virtual event), pp. 242.

About the Authors

Dr. Radovan Kopecek obtained his Diploma in physics at the University of Stuttgart in 1998, and received his M.S. from Portland State University, Oregon, USA, in 1995. In 2002 he finalized his Ph.D. dissertation in Konstanz, and was a group leader at the University of Konstanz until the end of 2006. One of the founders of ISC Konstanz, Dr. Kopecek has been working at the Institute as a full-time manager and researcher since 2007, and is currently the head of the Advanced Solar Cells Department. Since 2016 he has been on the board of directors of EUREC.

Dr. Joris Libal works at ISC Konstanz as an R&D project manager, responsible for technology transfer and cost calculations in the areas of high-efficiency n-type solar cells and innovative module technology, as well as for ISC's activities in the field of energy yield simulations. He received his Diploma in physics from the University of Tübingen and his Ph.D. in the field of n-type crystalline silicon solar cells from the University of Konstanz. He has been involved in R&D along the entire value chain of crystalline silicon PV, having held various positions at the University of Konstanz and the University of Milano-Bicocca, and, before joining the ISC in 2012, he was an R&D manager at the Italian PV module manufacturer Silfab SpA.

Enquiries

Radovan Kopecek
ISC Konstanz
Rudolf-Diesel Straße 15
78467 Konstanz, Germany

Tel: +49 (0) 7531 / 36 183 - 22
Email: radovan.kopecek@isc-konstanz.de
Website: www.isc-konstanz.de

Technology requirements for Ni/Cu plating metallization in commercial PV

Yuan-Chih Chang[1], Sisi Wang[1], Rong Deng[1], Xiaoli Li[2], Beibei Zhu[3], Shaoyuan Li[4] & Jingjia Ji[1]

[1]School of Photovoltaic and Renewable Engineering, University of New South Wales, Sydney, Australia; [2]Shenzhen Institute of Advanced Technology, Chinese Academy of Sciences, China; [3]School of Materials Science and Engineering, Southeast University, China; [4]Faculty of Metallurgical and Energy Engineering, Kunming University of Science and Technology, China

Abstract

Until now, Ni/Cu-plated contacts have not been widely favoured in the PV industry despite them being more cost-effective than screen-printed Ag/Al contacts, and the possibility of their further enhancing the cell efficiency in many concepts. One of the main challenges is that moving from one mature technology to another requires putting a great deal of intense effort in equipment and process development. Several fabrication aspects need to be considered in order to ensure the quality of Ni/Cu-plated contacts: 1) generation of contact patterns; 2) plated contact growth; and 3) post-processing for reliable cell and module performance. This paper reviews those associated fabrication technologies for the mass production of Ni/Cu-plated contacts. The technologies currently in use in the PV industry for plated contacts, as well as the developing technologies having high scaling-up potential, will be reviewed. In addition, the future requirements for plating metallization will be discussed.

Introduction

The PV market has been steadily growing during the last few decades. The continuous advancements in PV technology have made solar energy become more efficient and affordable. Since 2019, the price of electricity from large-scale PV power plants without any government subsidies has already been cheaper than from coal-fired power plants [1]. Although the record lab cell efficiencies are approaching theoretical limits, the mass production of such high-efficiency solar cells needs to consider more concepts, particularly in manufacturing reliability and overall cost. This generally leads to a delay in efficiency improvements which is reflected on conventional solar cells. Currently, passivated emitter and rear cell (PERC) devices are the industry-dominating technology, with a market share of over 80%, while tunnel oxide passivated contact (TOPCon) and silicon heterojunction (SHJ) solar cells are usually considered promising candidates for the next-generation high-efficiency solar cells [2,3].

In addition, screen-printing metallization by Ag/Al and Al paste is the mainstream process used in the PV industry for forming metal contacts, mainly because of its simplicity and high throughput [4]. However, there are several concerns around screen-printing technology remaining the major metallization method. First, the evolution of thinner and larger silicon wafers greatly increases the mechanical impact of screen-printing paste on the cell precursors, thereby leading to greater risks of wafer bowing and breakage. Second, TOPCon and SHJ solar cells typically rely on an ultrathin oxide or an a-Si layer to achieve excellent passivation, and therefore high efficiency [5]. The firing process in screen-printing metallization, however, has a high risk of damaging their selective passivation function. Finally, and most importantly, the high silver consumption could become a major disadvantage, limiting the future development of PV [6]. By 2020, the PV industry had already used more than 10% of the global silver supply, mainly for contact formation. In contrast, PERC solar cells mainly use Ag just for the front contacts, while TOPCon and SHJ solar cells need Ag for both the front and the rear contacts – approximately double the Ag consumption [7–9]. As global PV is expected to dramatically increase from ~135GW in 2020 to ~70TW in 2050, there will not be enough Ag for solar PV usage [9–12]. In the pursuit of higher efficiencies and cheaper solar energy, it is necessary to seek out other possible alternatives to metallization.

Among the various metallization technologies, Ni/Cu plating should be seriously contemplated, as it could fundamentally meet the previously mentioned challenges while having scaling-up potential [13–15]. From the early 1990s, plating was used in BP Solar's buried contact (BC) solar cells, and those plated contacted solar cells showed less degradation than screen-printed solar cells after 20 years' use [16–19]. This result implied that solar cells with plated contacts could be sufficiently durable. In the period 2009–2013, Suntech's Pluto technology adopted plating metallization and came up with the world's first p-type commercial solar cell having an efficiency of more than 20% [20–22]. SunPower also used plating in interdigitated back contact (IBC) solar cells, achieving an efficiency above 20% in

"In the pursuit of higher efficiencies and cheaper solar energy, it is necessary to seek out other possible alternatives to metallization."

solar panels integration [4,23].

In recent years, there has been more and more research looking into the potential of plating metallization in solar cells with passivated contacts and other structure/material devices [24,25]. Despite the consistent reports of challenges in adhesion and reliability, the highest efficiency of commercial solar cells now created by SunDrive use plated contacts without any Ag involved [26]. In fact, for several years the ITRPV has highlighted the potential of plated contacts, yet there has been no notable growth in this particular market [2,3]. The reason for this is, perhaps, because starting up a newly built production line demands a certain amount of effort and financial investment in order to make its resulting product quality, reliability and process throughput superior to that of the existing technology [27]. However, the current equipment and process development for plated contacts do not yet seem to be fully ready for this – either lacking in reliability or generating too much waste in associated processing (i.e. use of a full-area seed layer in lithography patterning approach). This paper presents a review of the existing and emerging technologies that need to be optimized in advance for a cost-effective realization of Ni/Cu-plated contacts in PV.

In general, the formation of Ni/Cu-plated contacts on well-passivated samples entails the following steps:

1. Generation of the contact patterns via opening the surface dielectrics
2. Ni plating
3. Cu plating

The application of Ni sinter used to be the standard process between steps 2 and 3 for forming nickel-silicide as the ohmic contact and Cu^{+} diffusion barrier. In recent years, however, there has been an increasing trend to skip this step, or to shift it to the end of the fabrication process [13,14,27]. Here, PERC cell precursors are selected as the main topic of discussion in the plating metallization process, as they are expected to continue to dominate the market in the next 10 years [2]. However, some of the fabrication processes might not be well suited to other emerging cell structures with passivation contacts, in which case alternative strategies will be discussed.

Generation of plated contact patterns

Prior to plating, metal contact patterns need to be developed on the well-passivated surface. Among the various methods for creating contact openings, laser scribing might be the fastest and simplest

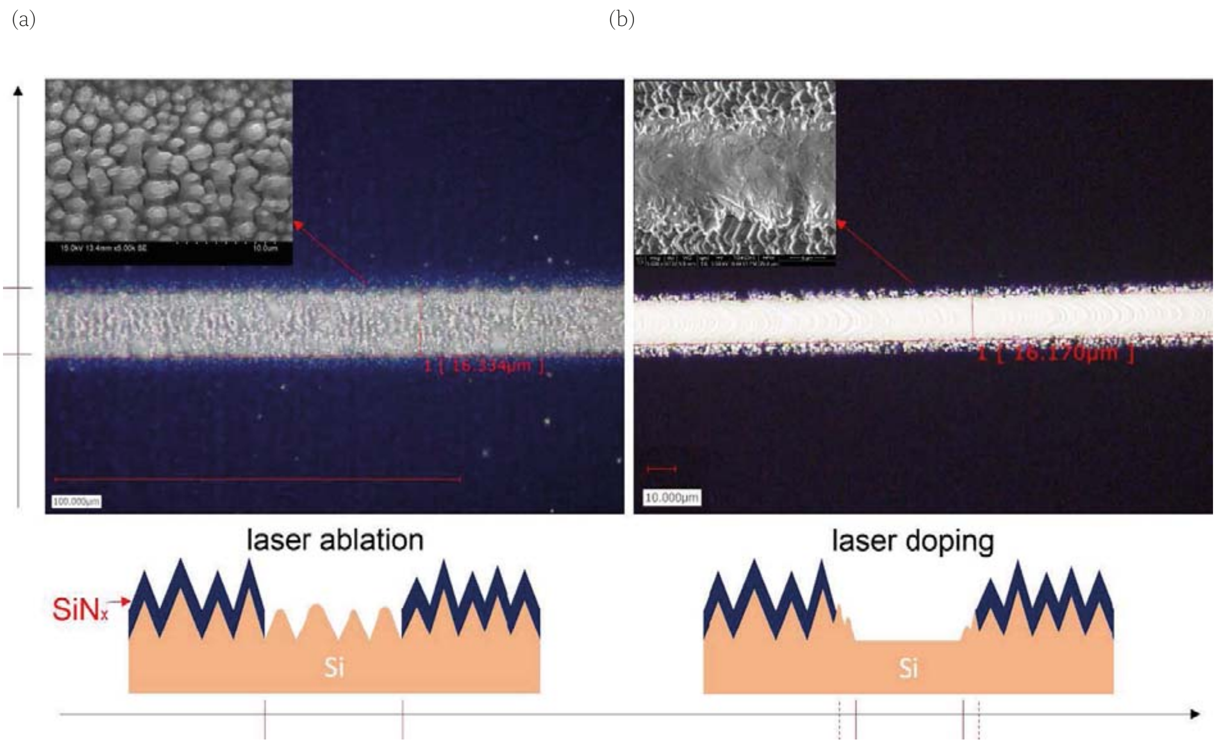

Figure 1. A representative cross-section schematic, and the microscope and SEM images for (a) laser ablation and (b) laser doping. The laser ablation was performed by a ps-UV laser, and laser conditions were chosen with the aim of only removing surface dielectrics; however, a slight morphology change in the underlying Si pyramids is often unavoidable. The laser doping was performed by a CW-green laser; because the laser used has a Gaussian disturbed power density, the edges of the opening are usually not very well defined, since the laser power in this region melts only the surface dielectric and not the underlying Si.

one; indeed, the high throughput might be its most attractive feature to manufacturers. Moreover, in recent years, the laser-doped selective emitter (LDSE) has steadily become a standard on the PV production line, which suggests a lower initial investment and smoother technology transfer when laser scribing is used for contact patterning.

There are several opening approaches that could be performed by laser scribing. Possibly the most straightforward one is *laser ablation*, which makes use of laser irradiation to remove only the surface dielectrics and leave most of the underlying microstructure unchanged. Fig. 1(a) shows a representative cross-section schematic, and the microscope and scanning electron microscope (SEM) images for laser ablation on a SiN_x-coated textured surface.

The surface dielectrics that need to be removed consist of typically a ~70–80nm SiN_x, a ~100–110nm SiO_2, a ~70nm-SiN_x/~6–15nm-SiO_2 stack layer, a ~50–60nm-SiN_x/~10nm-AlO_x or other similar combination stack layers [4,28,29]. Those materials and thicknesses are normally chosen taking into consideration the anti-reflection coating (ARC) and passivation purposes. To achieve such opening patterns, the focus of the laser beam should be on the interface between the surface dielectrics and the silicon. Laser irradiation is mostly absorbed by the surface silicon and eventually converts into heat. Depending on the characteristics of the laser used (wavelength, operation types, etc.), this heat can result in melting or vaporization of the silicon [29–31]. The former case leads to a transfer of heat, thereby decomposing the dielectrics, while the latter case results in thermal stress, causing the dielectrics to lift off. For a textured surface, laser ablation has been reported to enhance the contact adhesion because of the increase in Si/metal interface area [32,33].

A laser can also be used to both remove the surface dielectrics and selectively dope the underlying Si. This approach is called *laser doping (LD)*, which is based on the LDSE technology developed at UNSW in 2007. It involves four steps:

1. Melting of Si
2. Removal of dielectric layers
3. Diffusion of dopants
4. Recrystallization of molten Si

The entire laser doping process takes place in less than one microsecond [30]. In this process, the laser energy needs to be high enough to melt the surface Si but not so high as to ablate/vaporize the Si substrate.

The dopant can be present in the form of a chemical liquid or a solid deposited film. When the molten Si rises to a sufficiently high temperature to decompose the surface dielectrics, the 'doping' process begins – both dopant and decomposed dielectrics will then rapidly diffuse into the molten region. Upon recrystallization, the front of the melt moves back towards the surface, then the molten region undergoes epitaxial growth. A representative cross-section schematic, and the microscope and SEM images for laser doping on a SiN_x-coated textured surface are shown in Fig. 1(b). The laser doping approach can effectively create contact openings for the subsequent plating process and is beneficial for selective emitters (SEs) in terms of contact performance (contact resistance, J_o, etc.) [30,31].

The laser-ablation and laser-doping approaches have both been widely reported in many studies as contact opening methods for plating metallization in PERC and TOPCon solar cells [29,32–38]. Although the resulting efficiencies might not yet be superior to those of current industrial cells, it should be noted that there are usually a few processing parameters that have not been fully explored and optimized for cells with plated contacts in those trials. Furthermore, the use of different laser conditions (e.g. laser power, scanning speed, etc.) could significantly influence the plating metallization results, and hence the cell performance [39–42]. Detailed investigations in laser conditions particularly for plated contacts therefore need to be conducted before introducing plating metallization into the production line.

Laser structuring might not be ideal, however, for SHJ solar cells [43]. First, in SHJ solar cells, the metal contact is formed on a transparent conductive oxide (TCO), such as indium tin oxide (ITO). This TCO can act as a Cu^+ diffusion barrier, thereby relaxing the stress in Ni plating, but direct Cu plating on TCO has poor adhesion. Moreover, the areas between the fingers must be isolated to avoid parasitic plating, as TCO is conductive. Finally, the doped a-Si layer plays an essential role in SHJ solar cell passivation, but it is unlikely that the TCO can be completely removed by laser scribing without affecting this underlying layer. Consequently, a different contact patterning approach is necessary for SHJ solar cells.

In general, the contact patterning in SHJ solar cells typically involves a lithography process (mask deposition and removal, etc.), despite the variety of processing routes that have been reported [43–53]. In most approaches, a thin seed layer is first deposited on the TCO by physical vapour deposition (PVD). Then a series of mask layer stacks, which could consist of photosensitive organic material,

> "The laser energy needs to be high enough to melt the surface Si but not so high as to ablate/vaporize the Si substrate."

resin solution, hotmelt ink or even dielectric/metal layers, are formed on top of the seed layer by screen-printing, spraying, inkjet printing or plasma-enhanced chemical vapour deposition (PECVD). Depending on the mask technique used, the contact patterns would later be developed by photobiography, inkjet or laser structuring. After plating, the mask and unwanted metal are removed by wet-chemical etching.

The overall process flow is clearly more complex than that for PERC and TOPCon cells where laser scribing is applicable: Fig. 2 shows a typical process flow comparison of laser scribing and the lithography patterning approach for Ni/Cu-plating metallization. Most importantly, the need for a full-area seed layer on the TCO to improve contact adhesion could be the most unappealing part of those approaches, because it means there is a large amount of material waste (>95%) and extra cost involved [9,52]. The latter consequence leads to the metallization costs for SHJ cells becoming even greater than for PERC cells, thus resulting in SHJ cells being less competitive in the PV market [9,49]. The insufficient adhesion of direct plating on TCO contacts, however, might also relate to inappropriate plating approaches (e.g. vertical plating), which will be discussed in the next section.

Growth of plated contacts

There are several different plating methods available for contact formation in solar cells. According to the way the plating circuit is connected, the contact can be formed by electroplating, light-induced plating (LIP) or bias-assisted LIP. A detail review of the working principles related to those plating circuits can be found in the literature [14], but here, more about the plating technologies will be reviewed, namely plating layout, equipment design and applications.

Vertical continuous plating (VCP) is currently the mainstream technology used in mass production plating, for example in printed circuit board (PCB) manufacturing. Nowadays, most conventional PV plating equipment also adopts this design layout [27,52]. Basically, metal clips are used to hold the cell precursors by the edges, which are then immersed in the plating bath and removed when the desired thickness has been deposited. Fig. 3 shows a schematic of the vertical plating approach.

Different techniques have been developed (pulse plating, high-throw DC plating, etc.) to improve the plating results and processing reliability [54]. The major advantages of the vertical plating approach are its simple processing, low floor space requirement and reduced fume emissions. Empirically, the vertical plating works well in

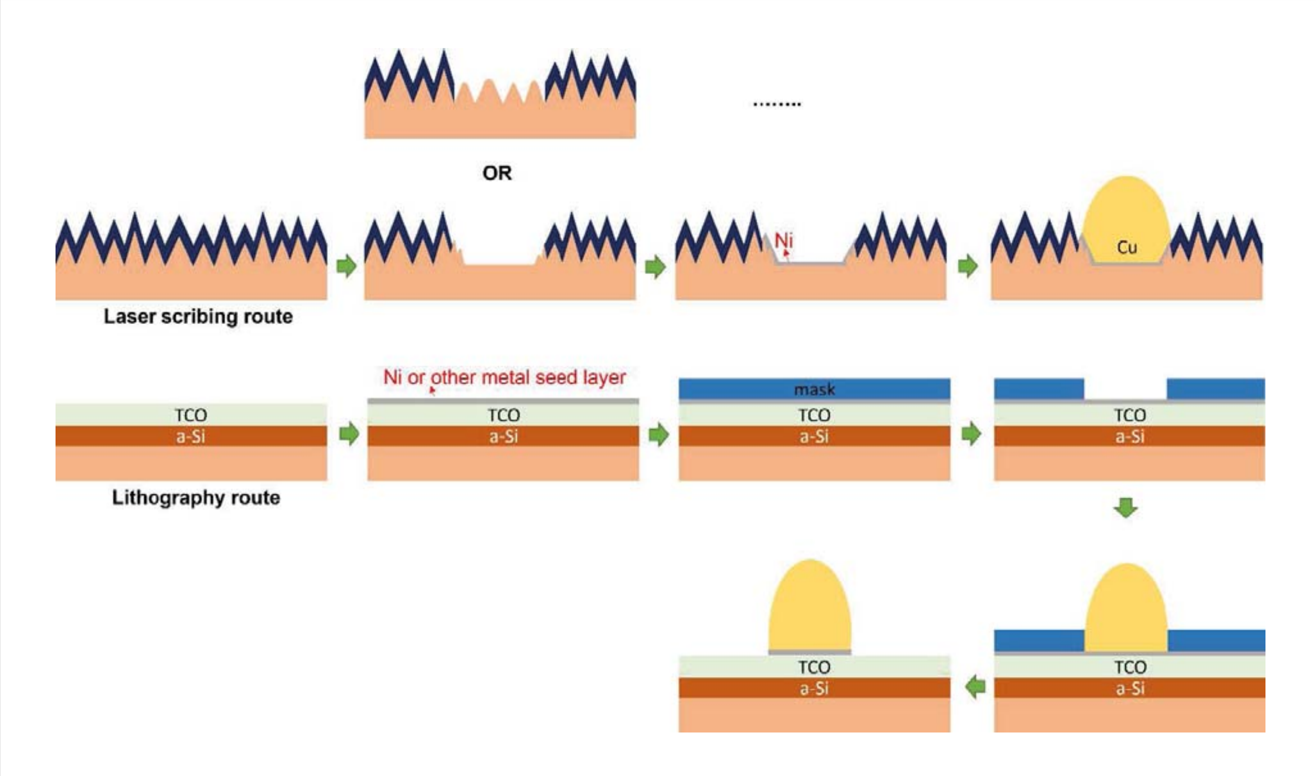

Figure 2. Comparison of the typical process flows for two contact patterning approaches. The top process flow uses laser scribing, by either laser ablation or laser doping, while the bottom one uses lithography to develop the contact patterns. Although various lithography approaches have been reported for SHJ cells, they generally need (1) full-area metal seed layer deposition and (2) residue removal after Cu plating, both of which increase process complexity and incur additional material waste.

solar plating when a thin metal seed layer is pre-deposited on the cell precursors [55,56]. However, to accommodate the growing need for high aspect ratios and complex surfaces (black-silicon, etc.), horizontal plating might be the best option.

Furthermore, the use of metal clips for sample holding and acting as a cathode has caused many problems in PV plating. First, holding the point contacts increases the mechanical impact on the cell precursors. Nowadays, PV manufacturers continue to push Si wafers to thinner and larger sizes at a rapid rate [2]; this makes the issues of microcracks worse and even leads to wafer breakages in the plating process. Second, in the direct plating case (plating without the use of a metal seed layer), the inhomogeneous current distribution between the metallic clips and the semiconductor/TCO surface can decrease the plating uniformity, especially in cell precursors requiring bifacial plated contacts [52]. This is because the area having a low chemical potential (i.e. low resistance) tends to be more easily plated, thereby resulting in *directional plating* – from the area close to the metal clips towards to area away from the metal clips [57,58]. The finished plated contacts are therefore usually too thick at the edges and more prone to peeling away. Moreover, uneven plating extends the plating processing time, and cell precursors need to be soaked in the plating bath for longer, which leads to the risk of surface dielectrics being over-etched. In consequence, there is an emerging interest in horizontal plating, despite the increased complexity associated with operation, maintenance and equipment development.

Horizontal plating line was first introduced to PCB manufacturing in the late 1980s and is generally only used when the vertical plating approach is not practical or is unable to satisfy the technical requirements (high aspect ratio, complex multilayer structures, etc.) [59]. In the case of solar cells, the basic operation concept involves immersing only the surface to be plated in the plating solution, and the opposite side directly contacts the cathode. A schematic of the horizontal plating approach is presented in Fig. 4.

The full back contact characteristics greatly promote the plating uniformity, thereby making plating without a metal seed layer both viable and reliable, which is beneficial with regard to material cost and manufacturing complexity [27,42,60,61]. However, careful selection of the contact patterning concepts is also important in such direct plating cases. For example, the surface conditions (surface morphology, doping density, etc.) of the contact opening area are modified, and as a result may not be very uniform in terms of electrochemical potential after laser scribing. Regardless of whether this occurs, even though

“To accommodate the growing need for high aspect ratios and complex surfaces, horizontal plating might be the best option.”

the desired plating approach is used, the plating quality is still limited by poor laser scribing [37,39,42,62,63].

Furthermore, because of the use of a larger tank in horizontal plating, the requirements of plating solution agitation and replacement are usually greater (to reduce the temperature gradient, to balance the high evaporation rate, etc.). In some designs, swiping or rotation of the cell precursors is even utilized; however, with those treatments there are also difficulties in maintaining the precursor at the same level during plating, and therefore undesirable rear-side wetting or floating of the precursors cannot be completely avoided [27]. Nevertheless, in conjunction with an appropriate contact patterning approach, several successful direct plating results using a horizontal plating line have been reported for TOPCon and SHJ cells [25,52,60,61,64]. This supports the potential of plated contacts for meeting the criteria of not only achieving higher efficiencies but also reducing costs.

So far, the reported horizontal plating approaches generally treat one side of the cell precursor at a time. As bifacial designs become more and more popular, the single-side plating characteristic will certainly become a concern: the processing time for plating is doubled, as well as there being the additional risk of breakage through samples flipping over [27,65]. To address such concerns, equipment development for simultaneous bifacial plating via the horizontal plating approach was recently revealed by UNSW [65]. This inline design utilizes a 'dripping' supply of plating solution, as well as a discontinuous plating bath, to allow LIP and electroplating to be performed simultaneously. Despite the reported best efficiency results not yet reaching the levels of current industrial PERC cells, a satisfactory contact performance demonstrates its feasibility and potential.

In summary, the horizontal plating approach is more suited to solar cell plating, as it allows viable direct plating, but further investigation to satisfy the requirements of both reliability and high throughput, perhaps through simultaneous bifacial plating, is needed in order to meet the rapidly growing market share of bifacial solar cells.

Other associated considerations

Apart from the standard contact formation procedure, other aspects need to be seriously considered, such as efficiency gain, modules and interconnection. Despite Ni/Cu-plated contacts often being acknowledged for their potential for efficiency enhancement on account of their reduced shading and low contact resistance, further improvements through appropriate methods are always desirable. For example, by integrating UNSW hydrogenation technology in between the Ni sintering and the Cu-plating steps, up to ~0.6% increase in efficiency has been recently reported for bifacial PERC cells with plated contacts [37,42,66]. Other possible techniques capable of provide similar benefits could be explored.

Module reliability might be the most important concern for PV metallization in the transfer from screen printing to plating. PV modules normally provide a 25-year performance warrantee (80% nameplate power after 25 years' usage, which equates to <0.5% degradation rate per year) and

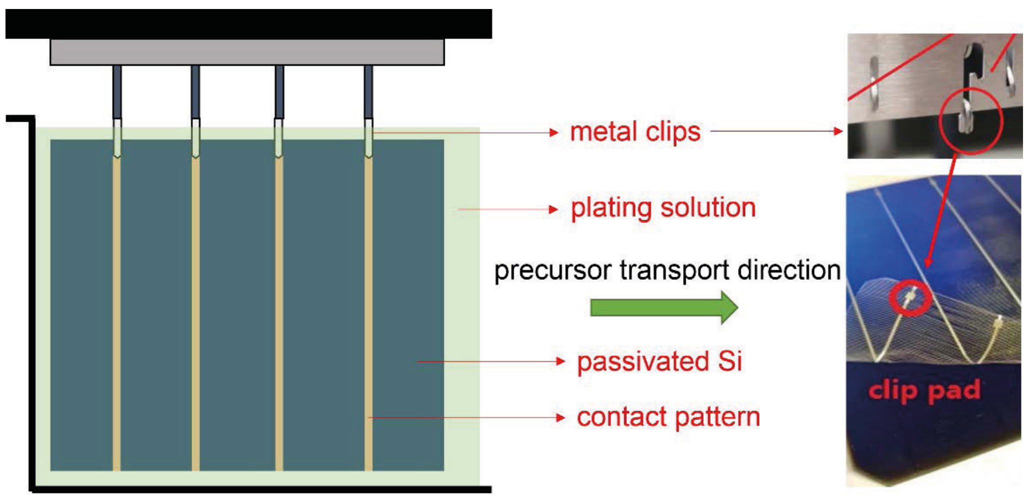

Figure 3. Schematic of a vertical plating line used for solar cell plating. The right shows a zoomed-in image of the metal clips, as well as the potential undesired peel-off that can occur at the cell edges due to non-uniform plating.

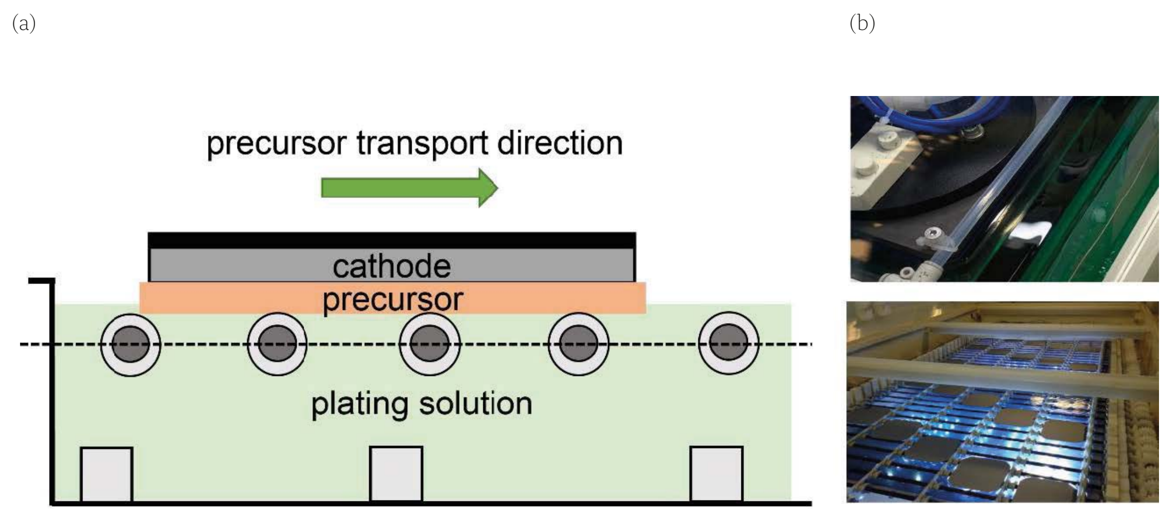

Figure 4. (a) Schematic of the horizontal plating line used in solar cell plating. (b) Photographic examples of cell precursors in the plating process.

"Module reliability might be the most important concern for PV metallization in the transfer from screen printing to plating."

other associated safe operation guarantees [67]. To reach such a standard, enormous efforts have been made on developments in solar cell design and fabrication, as well as advancements in module and interconnection technologies.

More challenges are expected when Ni/Cu-plating metallization is introduced into the production line, as material and fabrication methods are different [27,68]. For example, standard soldering is not well suited to plated contacts because of the concerns about stress. Approaches such as SmartWire, ribbon gluing and wire interconnection are emerging to address such issues, and even further improve module performance. New concerns, however, are also becoming apparent: for example, the additional usage of scarce metals (such as bismuth) in SmartWire technology may limit the supply chain [9]. Moreover, issues such as the large quantity of hazard waste produced by plating and reliable characterization technologies for inline plating of samples and finished products should also be carefully considered and standardized [9,27,68].

Conclusions

In 2021 the global PV generating capacity achieved the terawatt (TW) level and is estimated to reach ~70TW by 2050, which means that a production capacity of ~3TW will be required per year by the PV industry. Despite the price of large-scale PV power plants already being cheaper than that of coal-fired power plants, there are concerns around further development possibly being limited by the scarce metal usage, particularly Ag, in metallization. To significantly reduce, or even eliminate, the necessary use of Ag, shifting the currently dominated screen-printing technology to plating metallization could be a promising solution. However, to introduce new technology into large-scale manufacturing, new challenges arise and need to be overcome first before that technology can stand alone in the market. In this paper, several technologies have been reviewed that need to be comprehensively investigated and developed for the large-scale manufacturing of Ni/Cu-plated contacts in PV.

With regard to the requirement for contact pattern generation, the laser scribing approach is expected to be the most suitable because of its simple and rapid processing capability. Laser scribing can be carried out by either laser ablation or laser doping, and has been successfully implemented on PERC and TOPCon solar cells. While the former would promote better adhesion on a textured surface in view of the larger Si/metal interface, the latter could enhance cell performance by using selective emitters. It has to be emphasized that in either approach, the laser scribing conditions need to be chosen carefully, as the resulting surface conditions (morphology, doping, etc.) can significantly influence the plated contact formation. However, in the case of SHJ solar cells, the lithography process would be preferable owing to its unique layer structure. Different processing routes have been reported and have delivered satisfactory results, but the common use of a PVD seed layer could create additional financial concerns, and therefore warrants further investigation.

Currently, vertical continuous plating is the mainstream method used in PV manufacturing. Although such a layout offers the convenience of bifacial plating by a relatively low space requirement, it generally results in poor plating uniformity when a metal seed layer is not used. Consequently, there is an emerging trend of using the horizontal plating approach to resolve such issues and achieve a better aspect ratio. Several successful direct plating results for almost all types of cell structure have been reported by using the horizontal plating approach, and some are already in pilot line development. However, most existing (and under development) horizontal plating equipment only plate a single side at a time, which could be a concern, as the market share of bifacial cells is expected to grow rapidly in the next decade. It might be worthwhile, therefore, to look into a specific horizontal plating design layout that allows both sides of the cell precursors to be plated simultaneously.

Besides the technologies directly related to contact formation, there are other issues that should also be seriously considered. These include techniques for further cell efficiency enhancement, module and interconnection reliability, waste hazard processing and standard characterization development. In conclusion, it is never simple to move from one mature technology to another, especially when there is a need for complex process integration. A comprehensive investigation of each necessary concept is necessary. In order to encourage a wide adoption of Ni/Cu-plated contacts in commercial PV, developments in technology and equipment (e.g. reliability, throughput and cost-effectiveness) will first have to reach a certain level.

"In order to encourage a wide adoption of Ni/Cu-plated contacts in commercial PV, developments in technology and equipment will first have to reach a certain level."

Acknowledgements

This work was supported by the Australian Government through the Australian Renewable Energy Agency (ARENA) through RND2017/004. The Australian Government, through ARENA, supports Australian R&D in solar PV and solar thermal technologies to make solar energy become cost competitive with other energy sources. The inclusion of any views, information or advice expressed herein is the responsibility of the authors and is not necessarily endorsed by the Australian Government. The kind support from Yu-Shiang Tuan and Te-Hung Hsu throughout the writing process is also gratefully acknowledged.

References

[1] International Renewable Energy Agency 2020, "Renewable Power Generation Costs in 2019" [https://www.irena.org/-/media/Files/IRENA/Agency/Publication/2020/Jun/IRENA_Power_Generation_Costs_2019.pdf].

[2] VDMA 2021, "International technology roadmap for photovoltaic (ITRPV): 2020 Results", 12th edn (Apr.) [https://itrpv.vdma.org/en/].

[3] VDMA 2020, "International technology roadmap for photovoltaic (ITRPV): Results 2019 including maturity report 2020", 11th edn (Oct.) [https://itrpv.vdma.org/en/].

[4] Neuhaus, D.H. & Münzer, A. 2007, "Industrial silicon wafer solar cells", *Adv. in OptoElec.*, Vol. 2007. doi: 10.1155/2007/24521.

[5] Allen, T.G. et al. 2019, "Passivating contacts for crystalline silicon solar cells", *Nature Energy,* Vol. 4, No. 11, pp. 914–928. doi: 10.1038/s41560-019-0463-6.

[6] Tao, M. et al. 2020, "Review – Research needs for photovoltaics in the 21st century", *ECS J. Solid State Sci. Technol.*, Vol. 9, No. 12, p. 125010. doi: 10.1149/2162-8777/ABD377.

[7] Garside, M. 2020, "Global silver demand in 2019 by end use", *Silver Inst.* [https://www.statista.com/statistics/253345/global-silver-demand-by-purpose/.

[8] The Silver Institute 2021, "Silver supply & demand" [https://www.silverinstitute.org/silver-supply-demand/].

[9] Zhang, Y. et al. 2021, "Design considerations for multi-terawatt scale manufacturing of existing and future photovoltaic technologies: Challenges and opportunities related to silver, indium and bismuth consumption", *Energy Environ. Sci.,* Vol. 14, doi: 10.1039/D1EE01814K.

[10] Breyer, C. et al. 2018, "Solar photovoltaics demand for the global energy transition in the power sector", *Prog. Photovolt: Res. Appl.,* Vol. 26, No. 8, pp. 505–523. doi: 10.1002/PIP.2950.

[11] Verlinden, P.J. 2020, "Future challenges for photovoltaic manufacturing at the terawatt level", *J. Renew. Sustain. Energy,* Vol. 12, No. 5, p. 053505. doi: 10.1063/5.0020380.

[12] Haegel, N.M. et al. 2019, "Terawatt-scale photovoltaics: Transform global energy", *Science*, Vol. 364, No. 6443, pp. 836–838. doi: 10.1126/SCIENCE.AAW1845.

[13] Rehman, A. ur & Lee, S.H. 2014, "Review of the potential of the Ni/Cu plating technique for crystalline silicon solar cells", *Materials*, Vol. 7, No. 2, pp. 1318–1341. doi: 10.3390/ma7021318.

[14] Lennon, A., Yao, Y. & Wenham, S. 2013, "Evolution of metal plating for silicon solar cell metallisation", *Prog. Photovolt: Res. Appl.,* Vol. 21, No. 7, pp. 1454–1468. doi: 10.1002/pip.2221.

[15] Rahman, A. ur & Lee, S.H. 2015, "Crystalline silicon solar cells with nickel/copper contacts", in *Solar Cells – New Approaches and Reviews*, Kosyachenko, L.A., Ed., London: InTech. doi: 10.5772/59008.

[16] Alonso-Abella, M. et al. 2014, "Toledo PV plant 1 MWp – 20 years of operation", *Proc. 29th EU PVSEC*,

Amsterdam, The Netherlands, pp. 2728–2733. doi: 10.4229/EUPVSEC20142014-5BV.1.44.
[17] Nampalli, N. et al. 2014, “Outdoor testing of field-aged BP Saturn modules with nickel-copper plated contacts”, *Proc. 6th WCPEC*, Kyoto, Japan, pp. 1091–1092.
[18] Wenham, S.R., Honsberg, C.B. & Green, M.A. 1994, “Buried contact silicon solar cells”, *Sol. Energy Mater. Sol. Cells,* Vol. 34, No. 1–4, pp. 101–110. doi: 10.1016/0927-0248(94)90029-9.
[19] Bruton, T. et al. 2003, “Towards 20% efficient silicon solar cells manufactured at 60 MWp per annum”, *Proc. 3rd WCPEC*, Osaka, Japan, pp. 899–902 [https://ieeexplore.ieee.org/document/1305428].
[20] Wang, Z. et al. 2012, “Advanced PERC and PERL production cells with 20.3% record efficiency for standard commercial p-type silicon wafers”, *Prog. Photovolt: Res. Appl.,* Vol. 20, No. 3, pp. 260–268. doi: 10.1002/PIP.2178.
[21] Shi, Z., Wenham, S. & Ji, J. 2009, “Mass production of the innovative PLUTO solar cell technology”, *Proc. 34th IEEE PVSC*, Philadelphia, Pennsylvania, USA pp. 001922–001926. doi: 10.1109/PVSC.2009.5411566.
[22] Sugianto, A. et al. 2012, “Over 20%-efficient laser-doped passivated rear contact solar cells on industrial-sized commercial grade p-type CZ wafers”, *Proc. 27th EU PVSEC*, Frankfurt, Germany, pp. 700–705.
[23] Mulligan, W.P. et al. 2003, “Solar cell and method of manufacture”, US Patent US7897867B1 [https://patents.google.com/patent/US7897867B1/en].
[24] Hatt, T. et al. 2021, “Electroplated copper metal contacts on perovskite solar cells”, *Solar RRL,* Vol. 5, No. 9, p. 2100381. doi: 10.1002/solr.202100381.
[25] Kluska, S. et al. 2020, “Plating for passivated-contact solar cells”, *Photovoltaics International*, Vol. 44 [https://www.pv-tech.org/technical-papers/plating-for-passivated-contact-solar-cells/].
[26] PV Magazine 2021, “Australian start-up sets 25.54% efficiency record for silicon cell” [https://www.pv-magazine.com/2021/09/10/australian-startup-sets-25-54-efficiency-record-for-silicon-cell/].
[27] Lennon, A., Colwell, J. & Rodbell, K.P. 2019, “Challenges facing copper-plated metallisation for silicon photovoltaics: Insights from integrated circuit technology development”, *Prog. Photovolt: Res. Appl.,* Vol. 27, No. 1, pp. 67–97. doi: 10.1002/pip.3062.
[28] Chang, Y.C. et al. 2019, “Large-area nanosphere gratings for light trapping and reduced surface losses in thin solar cells”, *IEEE J. Photovolt.*, Vol. 9, No. 4, pp. 1012–1019. doi: 10.1109/JPHOTOV.2019.2918183.
[29] Geisler, C. 2015, *Characterization of Laser Doped Silicon and Overcoming Adhesion Challenges of Solar Cells with Nickel-Copper Plated Contacts.* Stuttgart: Fraunhofer Verlag.
[30] Tjahjono, B.S. 2010, “Laser doped selective emitter solar cells”, Ph.D. thesis, School of Photovoltaic and Renewable Energy Engineering, University of New South Wales, Sydney, Australia.
[31] Sugianto, A. 2011, “Development of commercial high-efficiency solar cells incorporating selective emitters and rear passivated contacts”, Ph.D. thesis, School of Photovoltaic and Renewable Energy Engineering, University of New South Wales, Sydney, Australia.
[32] Karpour, A. & Wenham, S.R. 2010, “The importance of surface roughness in the adhesion of electroless-plated metal in inkjet printed grooves”, *Proc. 35th IEEE PVSC*, Honolulu, Hawaii, USA, pp. 1410–1413. doi: 10.1109/PVSC.2010.5614406.
[33] Rehman, A. ur et al. 2016, “Ni/Cu/Ag plated contacts: A study of resistivity and contact adhesion for crystalline-Si solar cells”, *Electron. Mater. Lett.*, Vol. 12, No. 4, pp. 439–444. doi: 10.1007/s13391-016-4003-2.
[34] Grübel, S.B. et al. 2019, “Plated Ni/Cu/Ag for TOPCon solar cell metallization”, *Proc. 36th EU PVSEC*, Marseille, France [https://www.ise.fraunhofer.de/content/dam/ise/de/documents/publications/conference-paper/36-eupvsec-2019/Gruebel_2BO23.pdf].
[35] Lee, E. et al. 2011, “Improved LDSE processing for the avoidance of overplating yielding 19.2% efficiency on commercial grade crystalline Si solar cell”, *Sol. Energy Mater. Sol. Cells,* Vol. 95, No. 12, pp. 3592–3595. doi: 10.1016/j.solmat.2011.07.030.
[36] Büchler, A. et al. 2016, “Optimizing adhesion of laser structured plated Ni-Cu contacts with insights from micro characterization”, *Energy Procedia,* Vol. 92, pp. 913–918. doi: 10.1016/j.egypro.2016.07.101.
[37] Wang, S. et al. 2019, “Advanced passivation of laser-doped and grooved solar cells”, *Sol. Energy Mater. Sol. Cells,* Vol. 193, pp. 403–410, 2019, doi: 10.1016/j.solmat.2019.01.025.
[38] Wang, S. et al. 2016, “Selective emitter solar cell through simultaneous laser doping and grooving of silicon followed by self-aligned metal plating”, *Sol. Energy Mater. Sol. Cells,* Vol. 169, pp. 151–158. doi: 10.1016/j.solmat.2017.05.018.
[39] Molpeceres, C. et al. 2012, “Influence of wavelength on laser doping and laser-fired contact processes for c-Si solar cells”, *Proc. SPIE SOLAR ENERGY + TECHNOLOGY (Laser Mater. Process. Solar Energy)*, Vol. 8473, p. 847308, San Diego, California, USA. doi: 10.1117/12.929456.
[40] Moussi, M.S.A. et al. 2019, “532 nm laser treated selective emitter profiles study with SIMS and ECV technics”, *Proc. 36th EU PVSEC*, Marseille, France, pp. 483–485. doi: 10.1017/CBO9781107415324.004.
[41] Cimiotti, G. et al. 2015, “Design rules for solar cells with plated metallization”, *Energy Procedia*, Vol. 67, pp. 84–92. doi: 10.1016/j.egypro.2015.03.291.
[42] Chang, Y.-C. et al. 2022, “Investigation of laser doping and plating process for cost-effective PV metallization”, *Sol. Energy Mater. Sol. Cells*, Vol. 235, p. 111445. doi: 10.1016/J.SOLMAT.2021.111445.
[43] Aguilar, A. et al. 2016, “Development of Cu plating for silicon heterojunction solar cells”, *Proc. 43rd IEEE PVSC*, Portland, Oregon, USA, pp. 1972–1975. doi: 10.1109/PVSC.2016.7749972.
[44] Khanna, A. et al. 2015, “Screen-printed masking of transparent conductive oxide layers for copper plating of silicon heterojunction cells”, *Appl. Surf. Sci.,* Vol. 349, pp. 880–886. doi: 10.1016/J.

APSUSC.2015.05.085.
[45] Munoz, D. et al. 2013, "Strategies of cost reduction and high performance on a-Si:H/c-Si heterojunction solar cells: 21% efficiency on monolike substrate", *Proc. 39th IEEE PVSC*, Tampa, Florida, USA, pp. 3071–3073. doi: 10.1109/PVSC.2013.6745109.
[46] Yu, J. et al. 2016, "Tungsten doped indium oxide film: Ready for bifacial copper metallization of silicon heterojunction solar cell", *Sol. Energy Mater. Sol. Cells,* Vol. 144, pp. 359–363. doi: 10.1016/j.solmat.2015.09.033.
[47] Heng, J.B. et al. 2015, ">23% high-efficiency tunnel oxide junction bifacial solar cell with electroplated Cu gridlines", *IEEE J. Photovolt.*, Vol. 5, No. 1, pp. 82–86. doi: 10.1109/JPHOTOV.2014.2360565.
[48] Leu, S. et al. 2014, "Metallization schemes dedicated to SmartWire Connection Technology for heterojunction solar cells", *Proc. 29th EU PVSEC*, Amsterdam, The Netherlands, pp. 1333–1336.
[49] Li, Z. et al. 2014, "Patterning for plated heterojunction cells", *Energy Procedia*, Vol. 67, pp. 76–83. doi: 10.1016/j.egypro.2015.03.290.
[50] Adachi, D. Hernández, J.L. & Yamamoto, K. 2015, "Impact of carrier recombination on fill factor for large area heterojunction crystalline silicon solar cell with 25.1% efficiency", *Appl. Phys. Lett.,* Vol. 107, No. 23, p. 233506. doi: 10.1063/1.4937224.
[51] Geissbuhler, J. et al. 2014, "Silicon heterojunction solar cells with copper-plated grid electrodes: Status and comparison with silver thick-film techniques", *IEEE J. Photovolt.*, Vol. 4, No. 4, pp. 1055–1062. doi: 10.1109/JPHOTOV.2014.2321663.
[52] Hatt, T. 2019, "Establishing the 'native oxide barrier layer for selective electroplated' metallization for bifacial silicon heterojunction solar cells", *AIP Conf Proc.,* Vol. 2147, No. 1, 040005. doi: 10.1063/1.5123832.
[53] Glatthaar, M. et al. 2021, "Stable copper plated metallization on SHJ solar cells & investigation of selective Al/AlO_x laser patterning", *Proc. 38th EU PVSEC*, Lisbon, Portugal, pp. 2–5.
[54] Products Finishing 2015, "Vertical acid copper plating for PCB manufacturing" [https://www.pfonline.com/articles/whats-new-in-vertical-acid-copper-plating-for-pcb-manufacturing].
[55] Jianming, Fu et al. 2011, "Solar cell with metal grid fabricated by electroplating", Patent US-20110277825-A1.
[56] Despeisse, M. et al. 2017, "Copper plating process for bifacial heterojunction solar cells", *Proc. 33rd EU PVSEC*, Amsterdam, The Netherlands, pp. 753–756.
[57] MicroChemicals, "Basics of microstructuring: Electro-plating" [https://www.microchemicals.com/].
[58] Rose, I. & Whittington, C. 2014, *Nickel Plating Handbook*. Brussels: Nickel Institute. doi: 10.1002/9783527813964.ch12.
[59] Huang, A. 2004, "Milestones in horizontal plating: A brief look at the history of the technology reveals Asia as the willing innovator" [https://www.thefreelibrary.com/_/print/PrintArticle.aspx?id=113600873].
[60] Gensowski, K. et al. 2019, "Direct contact plating-Inline plating solution for ZEBRA IBC by local contacting", *AIP Conf. Proc.,* Vol. 2156, No. 1, p. 20007. doi: 10.1063/1.5125876.
[61] Grubel, B. et al. 2021, "Direct contact electroplating sequence without initial seed layer for bifacial TOPCon solar cell metallization", *IEEE J. Photovolt.,* Vol. 11, No. 3, pp. 584–590. doi: 10.1109/JPHOTOV.2021.3051636.
[62] Chang, Y.-C. et al. 2020, "The effect of different laser wavelengths on bifacial plated laser doped selective emitter solar cells", *Proc. 37th EU PVSEC* (virtual event), pp. 383–387.
[63] Wang, S. 2018, "Laser technology in the fabrication of high efficiency solar cells", Ph.D. thesis, School of Photovoltaic and Renewable Energy Engineering, University of New South Wales, Sydney, Australia.
[64] Hatt, T. et al. 2019, "Native oxide barrier layer for selective electroplated metallization of silicon heterojunction solar cells", *Solar RRL*, Vol. 3, No. 6. doi: 10.1002/solr.201900006.
[65] Chang, Y.-C. et al. 2021, "Equipment development for simultaneously bifacial plating metallization in bifacial solar cells", *Proc. 38th EU PVSEC*, Lisbon, Portugal.
[66] Hallam, B.J. et al. 2015, "Advanced hydrogenation of dislocation clusters and boron-oxygen defects in silicon solar cells", *Energy Procedia,* Vol. 77, pp. 799–809. doi: 10.1016/j.egypro.2015.07.113.
[67] Jordan, D.C. et al. 2016, "Compendium of photovoltaic degradation rates", *Prog. Photovolt: Res. Appl.,* Vol. 24, No. 7, pp. 978–989. doi: 10.1002/PIP.2744.
[68] Faes, A. et al. 2018, "Metallization and interconnection for high-efficiency bifacial silicon heterojunction solar cells and modules", *Photovoltaics International*, Vol. 41, p. 65.

About the Authors

Dr. Yuan-Chih Chang completed her Ph.D. at UNSW with a focus on light-trapping in thin crystalline silicon PV through nanophotonics. She is currently a postdoctoral researcher at UNSW, working in particular on developing simultaneous bifacial plating technology. Her research interest lies in advancing PV technology at an economical cost. She has also worked on in-house IBC baseline development for nanophotonic light trapping and industrial black silicon texturing projects.

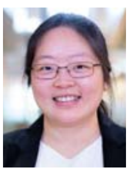

Dr. Sisi Wang received her Ph.D. from UNSW for her work on laser processes for the fabrication of high-efficiency solar cells. She focused on the development of a self-aligned laser doping process that simultaneously grooves the silicon, and laser-based implementations for advanced hydrogenation technology. She is

currently a postdoctoral fellow at UNSW, where she is working on light-induced plating, laser-doping and advanced hydrogenation, and in particular on developing simultaneous bifacial plating technology.

Dr. Rong Deng is a postdoctoral research fellow in the School of Photovoltaic and Renewable Energy Engineering at UNSW. She completed her Bachelor of Engineering (Honours Class I) in 2018, and her Ph.D. on end-of-life recycling of silicon PV modules, with a thesis title "Towards a circular economy", at UNSW in 2021. Her research interests include end-of-life management of PV modules, PV sustainability, techno-economic assessment and life-cycle assessment of silicon PV technologies and solar cell plating.

Xiaoli Li received his Master of Engineering Science in photovoltaics and solar energy and environmental engineering from UNSW in 2014. From 2015 to 2020 he worked at Yunnan Minzu University as a management department deputy section chief. In late 2020 he joined Shenzhen Institute of Advanced Technology as an assistant dean. His research focuses on solar PV energy, carbon neutrality and environmental policy.

Dr. Beibei Zhu received her Ph.D. in materials science and engineering from UNSW in 2015. From 2016 to 2017 she worked at Nanyang Technological University (NTU) in Singapore as a postdoctoral researcher, and then joined Southeast University as a lecturer in early 2018. The focus of her research is the synthesis and characterization of thermoelectric functional materials.

Prof. Shaoyuan Li is a member of the faculty of Metallurgical and Energy Engineering at Kunming University of Science and Technology (KUST). He received his bachelor's in material physics from Yanshan University in 2009, and his Ph.D. from KUST in 2014. He was a visiting professor at UNSW from 2019 to 2020. His current research interests are metallurgical-grade silicon purification, high-efficiency solar cells, PV waste recycling and energy storage.

Associate Prof. Jingjia Ji is an expert in solar cell R&D and in developing tools for manufacturing. Before his current role at UNSW, he was the head of the R&D line at Suntech Power for many years, enabling Suntech to be the first to implement laser doping and plating in large-scale manufacturing, which led to world-record commercial cells.

Enquiries

Yuan-Chih Chang
School of Photovoltaic and Renewable Engineering
University of New South Wales
Sydney, NSW 2052, Australia

Tel: +61 403 692 006
Email: y.chang@unsw.edu.au

The sun is rising on conductive adhesives

Daniel Tune[1], Torsten Rössler[2], Gernot Oreski[3], Carolyn Carriere[4], Christina Kaiser[2], Tudor Timofte[1], Nils Klasen[2,5], Julian Weber[2], Bengt Jäckel[6], Stephan Großer[6], Matthias Pander[6], Marko Turek[6], Marco Galiazzo[7], Ignacia Devoto[1,8], Thomas Fischer[9], Ingo Ullmann[1], Dominik Rudolph[1] & Andreas Halm[1]

[1]International Solar Energy Research Center ISC Konstanz, Germany; [2]Fraunhofer Institute for Solar Energy Systems ISE, Freiburg, Germany; [3]Polymer Competence Center Leoben PCCL, Leoben, Austria; [4]French Alternative Energies and Atomic Energy Commission CEA, France: [5]Institute for Applied Materials – Materials and Biomechanics IAM-WMB, Karlsruhe Institute of Technology KIT, Germany; [6]Fraunhofer Center for Silicon Photovoltaics CSP, Halle (Saale), Germany; [7]Applied Materials, Inc., Santa Clara, California, USA; [8]Faculty of Natural Sciences II, Martin Luther University, Halle-Wittenberg, Germany; [9]teamtechnik GmbH, Freiberg, Germany

Abstract

Although electrically conductive adhesives (ECAs) have been around in the PV industry for several years in panels based on conductive backsheets as well as in the so-called *shingled* or *tiled* modules, several evolving trends and new technologies are currently converging to bring ECAs firmly into the mainstream spotlight. These include the ongoing move to thinner wafers and larger cell formats, as well as the inevitable increase in market penetration of high-efficiency concepts based on heterojunction (HJT) and silicon–thin-film tandem cell architectures. With mature product offerings now available from several of the leading industrial PV equipment and tool manufacturers, and latest-generation ECAs available from suppliers, this article aims to provide important background information on ECAs, as well as give a brief overview of some of the challenges and cutting-edge developments in ECA-related PV applications.

Introduction

ECAs in PV have two primary uses: 1) as a replacement for solder in traditional soldered applications (e.g. ribbon stringing), and 2) in other applications in which traditional solder would either not be viable (e.g. shingling) or not produce a satisfactory outcome (e.g. temperature-sensitive cell concepts). Compared to solder, the material properties of ECAs – such as their electrical conductivity, elastic modulus and thixotropy – can be very finely tuned, often over very wide ranges. The complex nature of ECA composites means that there are many more levers that experts can pull in order to craft the perfect product for a particular use, and major ECA manufacturers have been known to work closely with module producers to create tailored solutions.

A decade ago, ECAs had a reputation for being inferior to solder in regard to long-term reliability, with problems such as embrittlement, water ingress and corrosion playing major roles in this. However, recent years have seen big improvements in these and other characteristics, so much so that ECAs can now not only stand their ground against solder but also in some ways offer superior performance. Finally, despite the relatively high cost of some ECAs due to high silver content, ECAs also have the desirable characteristic of being free of toxic lead, which is particularly important for manufacturers in many regions because of ongoing developments in their respective regulatory environments.

“For the shingle interconnection method, ECAs are a key technology, as they form mechanically flexible joints that can absorb mechanical stress.”

History

The history of the use of ECAs in microelectronics packaging goes back to the 1950s and has been summarized by Nicolics & Mündlein [1]. Over the past decades, ECAs have found widespread application in bonding silicon chips to lead frames and in the attachment of passive chips in automotive electronics, RFID tags or LED fabrication [2,3]. Other applications have been addressed in order to avoid hazardous lead in electronic devices, so that ECAs are used as promising lead-free materials for flip-chip and surface-mount attachment of devices to circuit boards [4]. A particular class of ECA, namely anisotropic conductive tape, is used for manufacturing LCDs [5].

In PV module integration the first publications on using ECAs go back to 2001 [6,7]. During the time of serious silicon supply shortage up until the mid to late 2000s, a wafer thickness reduction from around 300µm to below 180µm was forecast that would improve effective silicon usage. Driven by these concerns, ECAs gained much interest for the interconnection of very thin solar cells, in which lower thermomechanical stress after interconnection decreases cell bending and increases the fracture strength compared to soldered cells [8].

One of the first major applications of ECAs in PV modules was the integration of metal wrap-through solar cells in the conductive backsheet approach [9]. In parallel, ECAs have been used to integrate HJT solar cells in modules [10–12]. ECAs prove to be a soft and reliable method for interconnection at temperatures below 200°C. The absence of hazardous

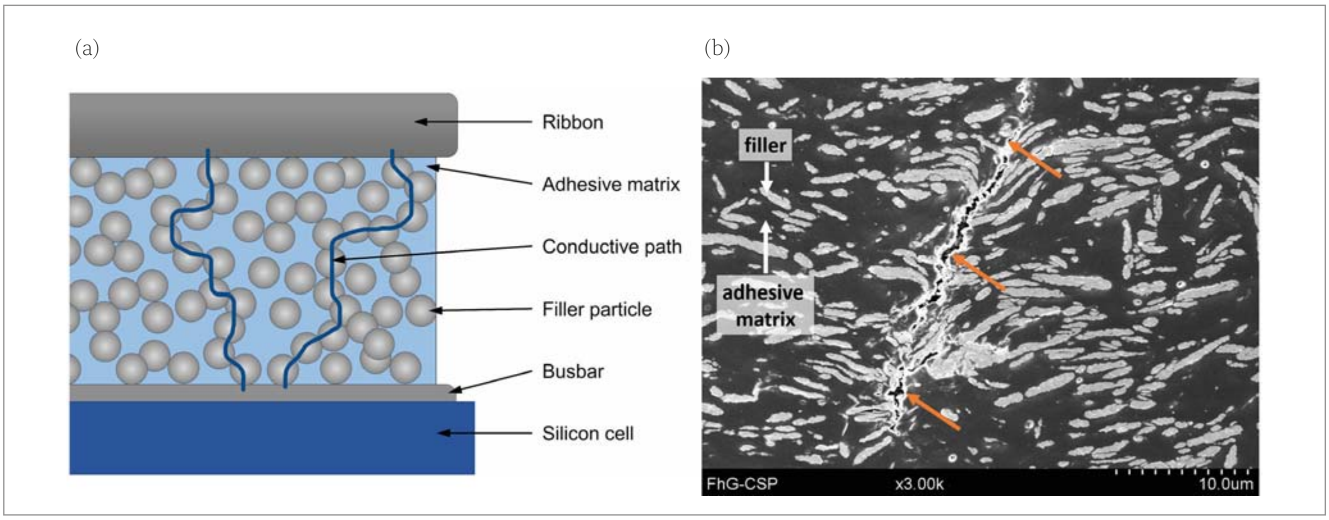

Figure 1. (a) Percolation through ECA bonds. (b) Cross-sectional SEM image showing the microstructure of ECA, with a cohesive crack marked by orange arrows.

lead is an important advantage of HJT cell and module technology. In recent years, German equipment manufacturer teamtechnik commercialized a stringer to process ECAs on an industrial scale, which ENEL in Italy and Hevel in Russia introduced into their production lines [13,14]. Since then, other leading tool makers – such as Applied Materials, Mondragon and others – have introduced their own advanced ECA stringers, and high-value advances in the technology continue to be made.

Other applications of ECAs that were introduced in the late 2000s include the connection of bus conductors of monolithic thin-film or organic solar panels, as well as shingling or ribbon interconnection of flexible thin-film solar cells [15,16]. Eventually, the shingle interconnection of crystalline solar cells gained a lot of attention in the mid-2010s when, for example, SunPower/Maxeon started to commercialize the 'Performance Series' [17]. Since then, other module manufacturers, especially in Asia, included similar products in their portfolios. For the shingle interconnection method, ECAs are a key technology, as they form mechanically flexible joints that can absorb mechanical stress.

Composition, function and characterization

ECAs are composites of conductive particles (a.k.a. *filler*) in a non-conductive adhesive matrix, wherein the conductive particles provide the required electrical conductivity, and the adhesive matrix holds the particles together and supplies the bonding strength. The adhesive is generally a heat-cured epoxy, acrylate or silicone; however, in principle any adhesive can be used, with the caveat that it must be chemically and thermomechanically compatible with the other solar cell and module materials as well as with the conductive filler.

ECAs used in PV are usually delivered as frozen, two-component mixtures of the adhesive base and a curing agent, which are thawed shortly before use and should be used completely within a period of several hours. Alternatively, they can be delivered as two separate components, which are easier to store since they do not require freezing, but dedicated on-site mixing equipment is required in this case to prepare the material for use. ECAs can be deposited at specific positions or in desired layouts on the target substrate via several means, including screen or stencil printing and pressure-time or jet dispensing, although, in practice, only screen or stencil printing are currently widely used in high-throughput production.

Unlike in bulk conductors such as solder, conduction in ECAs occurs via percolation (see Fig. 1(a)). In other words, charge is conducted between adjacent particles, and conductive pathways, consisting of chains of particles, bridge the separation between the bonded surfaces. A critical parameter in such systems is the percolation threshold, which depends on the volume concentration of particles, their shape and their three-dimensional arrangement. Below the percolation threshold, and for a given particle shape and size distribution, ECAs exhibit a relatively high resistivity which depends on the particle concentration. When the particle concentration is increased to the percolation threshold, the resistivity rapidly decreases by several orders of magnitude, and any further increases in particle concentration have little further effect on the resistivity, but can increase the ampacity. The higher the filler content, the lower the adhesion force, since the filler occupies a greater proportion of the bond interface area, displacing the adhesive.

"The primary challenge in ECA development is to create a system with the lowest possible percolation threshold providing good electrical properties while maximizing the adhesion strength."

The primary challenge in ECA development is therefore to create a system with the lowest possible percolation threshold providing good electrical properties while maximizing the adhesion strength. For a given filler and filler concentration, the adhesive strength and other important characteristics of the cured material – such as the elastic modulus and glass transition temperature – can be improved by tuning the molecular weight(s) of the component polymer(s) and their branching ratio(s), dispersity and side chain functional groups, as well as through the addition of plasticizers and additives, and by the amount and type of curing agent. Likewise, the characteristics of the uncured material – such as the rheology, pot-life and appropriate temperature profile for curing – can be similarly adjusted.

Conductive filler particles in ECAs can be spheres, granules, rods, flakes or fibres, and may be solid or hollow. Shapes with high aspect ratios – such as rods and fibres – have a greater potential to form conductive pathways and thus yield the lowest percolation thresholds, but are also more likely to form aggregates. In contrast, higher surface area spheres tend to produce the most homogeneous composite, but require a higher concentration to reach the percolation threshold. Flakes provide an excellent balance of high aspect ratio and high surface area for interacting with the adhesive, but can also be costlier to produce, whereas granules tend to be the cheapest shape to produce.

In practice, the distributions of filler particle sizes and shapes are often closely guarded trade secrets of the manufacturers. ECA filler particles must not only be highly conductive but also be chemically compatible with the components of the adhesive matrix (both uncured and cured) and resistant to corrosion. For these reasons, silver is often used as the filler because of its relative inertness and high conductivity; however, as with much of the rest of the PV manufacturing industry, the high cost of silver, coupled with the high exposure to commodity price risk, is a strong driver in the search for alternative materials and/or material solutions. Market-available examples of such alternatives include the use of hollow silver spheres, which exhibit the same percolation threshold concentration as solid spheres but with potentially very large reductions in silver mass, as well as the use of other cheaper metals, such as copper, with a silver coating to inhibit corrosion. As the annual consumption of ECAs for PV applications increases over the next few years, we can expect to see further advances and new technology developments to meet market demands for product features and cost reductions.

ECAs can be either *isotropically conducting* (ICAs), where the material conducts equally well in all directions, or *anisotropically conducting* (ACAs), where the material conductivity is much higher in one direction than in the other. In the cured state, ICAs are generally two to three orders of magnitude more resistive than ACAs ($10^{-2}\Omega$cm vs. $10^{-4}\Omega$cm). ACAs as used in PV applications are more conductive in the *z* direction than laterally (i.e. between the ribbon and the cell in ribbon-stringed concepts, or between the two cells in shingled concepts); however, this only occurs after curing under *z*-axis compression. This means that, in addition to the ECA amount and curing temperature profile, the applied force during curing is another process lever that can be tweaked to optimize module product performance.

An understanding of the current transport for reliable and efficient ECA interconnections requires knowledge of the underlying microstructure. The microstructure can be revealed using several techniques – such as X-ray analysis, optical or electron microscopy (e.g. after the preparation of cross sections at random or specific positions) – down to (for example) the nanometre scale at defects sites.

On the one hand, the microstructure allows for the development of ECAs, a control of optimized conductive filler contents, filler shapes or filler dispersion in the polymer matrix with an impact on the resistance of the contact or thermal conductivity. The filler network microstructure and surface chemistry play important roles in the development of the conduction path. Since ECA contacts exhibit a thickness in the micron range, a microstructure analysis of contact cross sections allows a realistic insight into the actual contact geometry and ECA distribution, providing an assessment of the real contact area which is influencing the adhesion and therefore the peel force. Different production processes or material combinations can thus be quantitatively compared by microstructure analysis.

On the other hand, the impact of accelerated ageing specifically on the ECA contact can be made clearly visible in the microstructure and assigned to distinct failure mechanisms. Cross-sectional images reveal cohesive or adhesive cracks (see Fig. 1(b)), delamination, bubbles, ECA squeeze-out or structural changes (i.e. by galvanic corrosion). Furthermore, precise information about the microstructure can be used to support simulations to predict stresses and reliability.

The electrical properties of ECA-bonded joints can be sensitively probed by analysis of the contact resistance, which has a direct effect on the series resistance of modules created with ECA interconnections. Changes to the ECA bulk, or to the ECA–metallization or ECA–ribbon interface, can manifest as increases in the contact resistance long before any discernible visual changes, making contact resistance analysis a powerful tool in the improvement and optimization of ECAs and ECA bonding processes.

In interfaces between metals and crystalline or semicrystalline semiconductors, the transmission line method (TLM) (Fig. 2(a,b)) has traditionally been used to measure the contact resistance, and has a strong foundation in physical models of such systems. However, the interface between solar cell metallization and the adhesive–filler composites of which ECAs are composed is substantially different to the interfaces in those systems. Although

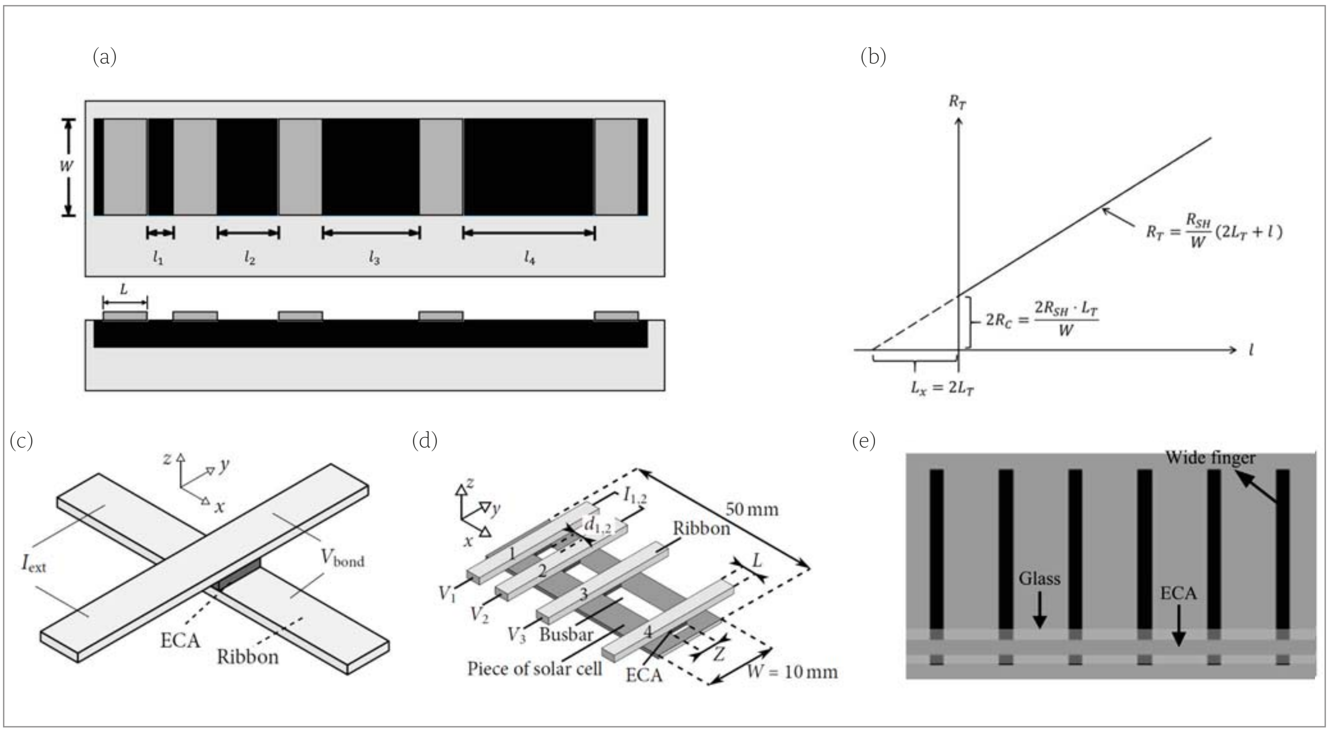

Figure 2. (a) Traditional TLM test structure [18]. (b) TLM plot for parameter extraction [18]. (c) Stacked Greek cross test structure [19]. (d) Ribbon–busbar test structure [19]. (e) Wide-finger test structure [20].

TLM can be (and has been) used to usefully track changes in the contact resistance of ECA-bonded joints through, for example, accelerated ageing tests, the objective relevance and true comparability of any values thus obtained remain unconfirmed. The actual contact area also influences the electrical performance of the contact; even though such changes can be quantitatively measured by the degradation of the contact resistance, there will be always a dependence on the contact size. For this reason, TLM can also be used to extrapolate the specific contact resistivity between adhesive and adherend, which does not depend on the size of the contact. Nevertheless, inconsistencies have been observed in the literature-reported values of contact resistivities in devices, depending on their dimensions (from nanometre in microelectronics up to centimetre scale in PV devices). The addition of ECAs as a means of contacting increases the complexity of the system and therefore also the extrapolation of the contact resistivity. Thus, efforts are currently under way to adapt the TLM methodology for ECA-based contacts (Fig. 2(c–e)) in order to extrapolate the contact resistivity of this type of joint.

Whatever characterization tools or methods are used to assess the material and interfacial properties of ECA-bonded joints, and thus improve the material characteristics and/or processing conditions, there is no substitute for extensive bill of materials (BOM) screening to avoid unanticipated chemical interactions with additives or components of the encapsulant or backsheet, as well as thermomechanical incompatibilities with the module stack. Fig. 3 shows the results of such a BOM study comparing different combinations of ECA, encapsulant and backsheet in a shingled module configuration. Stark differences in the long-term reliability of the different combinations are clearly evident.

Applications

As already mentioned, one of the earliest uses of ECAs in PV was in premium modules based on conductive backsheets. However, as the properties of ECAs have been tuned towards PV applications, the range of uses of ECAs in PV has not only grown to include high-efficiency, high-reliability concepts, such as shingling and ribbon interconnection of HJT cells, but is now beginning to encompass more mainstream and budget concepts, such as passivated emitter and rear cell (PERC)- and polycrystalline-based modules.

"There is no substitute for extensive bill of materials (BOM) screening to avoid unanticipated chemical interactions with additives or components of the encapsulant or backsheet."

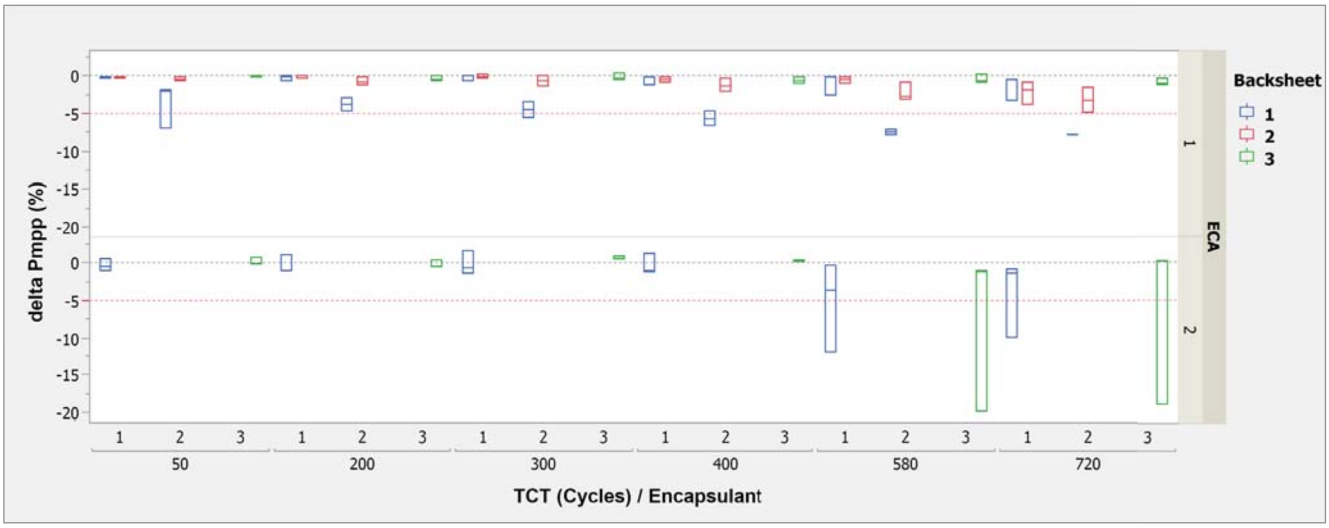

Figure 3. Comparison of different shingled mini-module BOM combinations of two ECAs, three backsheets and three encapsulants, showing stark differences in the degradation of module performance as a function of the number of thermal cycles. The grey dotted line indicates the initial power level, while the red dotted line represents the –5% pass/fail criterion as defined in IEC 61215.

Conductive backsheet

With respect to module integration, the interconnection of rear-contacted solar cells poses challenges, since classical stringing is not applicable. Excessive cell bowing after single-sided ribbon attachment can hinder automatic handling; tabber-stringers need to be specially adapted.

The conductive backsheet (CBS) approach is a dedicated interconnection technology for back-contact solar cells (mainly IBC or MWT). The Dutch company Eurotron and the ECN/TNO research centre have pioneered this alternative interconnection technology. By taking advantage of the fact that all contacts are located on the rear side, cells are interconnected by methods based on printed circuit board technology. An ECA (or solder paste) is deposited by screen/stencil printing or dispensing on either the solar cell metallization or the CBS to form local contacts between the two components during lamination. The circuit for current flow itself is a thin, patterned copper layer that is mostly laminated onto a classic PV backsheet. An insulation layer between the cells and the copper layer prevents short circuits, and, because all cell–cell interconnections are underneath the solar cells, no shading losses occur. Because the conductors are as wide as the solar cell, the thickness can typically be limited to 35μm for copper layers. Fig. 4 shows a cross-sectional image of the resulting module sandwich.

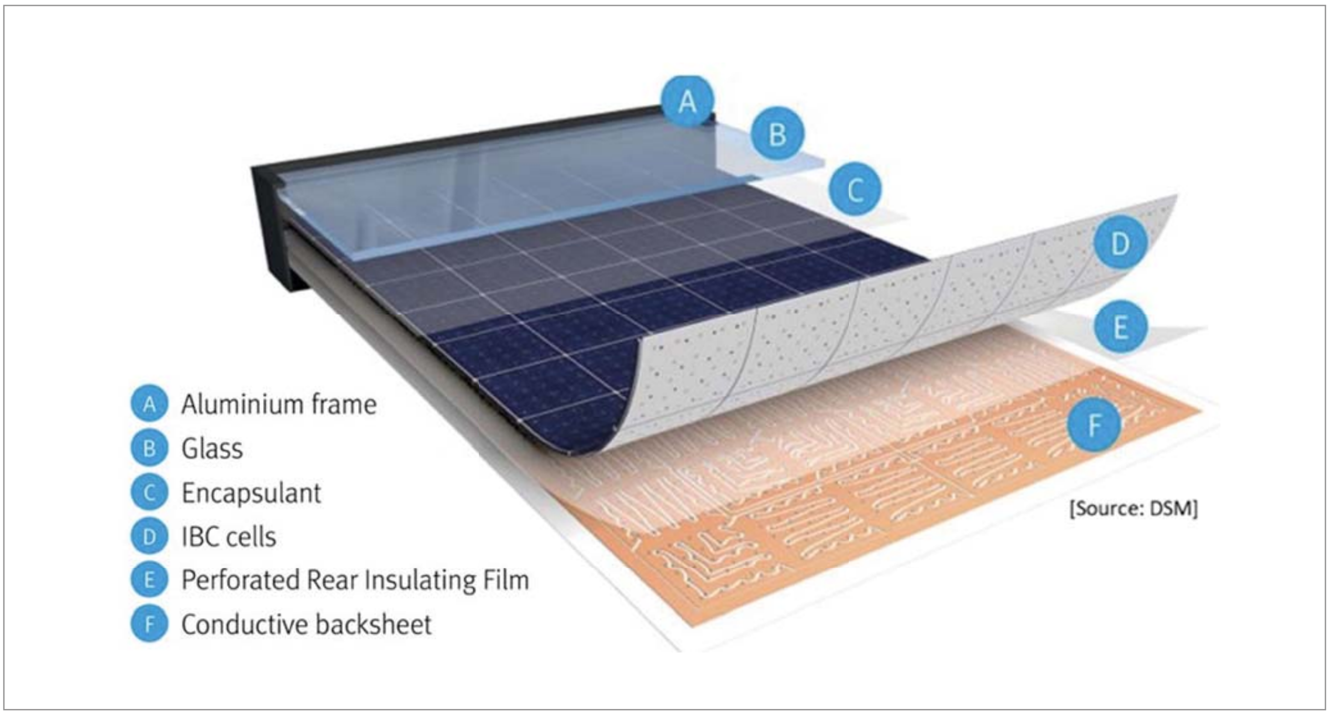

Figure 4. General structure of a CBS laminate [21]. The module is assembled from the rear to the front: first the backsheet, then encapsulant/isolation, ECA, cells, encapsulant and glass. Electrical contact between the cells and the backsheet circuit is then made by curing the ECA during lamination.

The advantages of this approach to module fabrication include low resistive power losses and a low-stress module manufacture (pick-and-place step to lay up the cells, contact formation during lamination). The full copper rear side additionally provides excellent heat dissipation characteristics that can lower the normal module operating temperature. The flexibility of the design of the circuit pattern makes CBS suitable for full, half or other cell-fraction formats and will enable the integration of active circuit elements in future applications.

CBS technology depends on small, highly conductive local contacts that need to bridge the distance introduced by the thickness of the rear insulator (typically 200µm). Hence, ECA enables this technology to work not only because of its versatile processing and high conductivity but also because of its good elasticity. The fact that ECA cures during lamination helps to overcome the bowing issues, since contact between cells and backsheet is made during lamination, and thus the laminate compensates the thermomechanical stress between the components, especially the rigid front glass plane. Additionally, the elasticity of the cured ECA mitigates residual stresses and thermomechanical stresses in the laminate that lead to joint fatigue, making CBS modules very robust against thermal expansion/contraction.

Ribbon contact / busbar replacement

The use of ECAs as solder replacement is a very attractive route in dedicated PV cell interconnections such as: HJT cells, which require processing at lower temperatures; back-contacted cells, which demand a better control of cell warpage after interconnection than in the case of two-side-contacted cells; and thin solar cells (<160µm) with a reduced thermomechanical stress budget. The

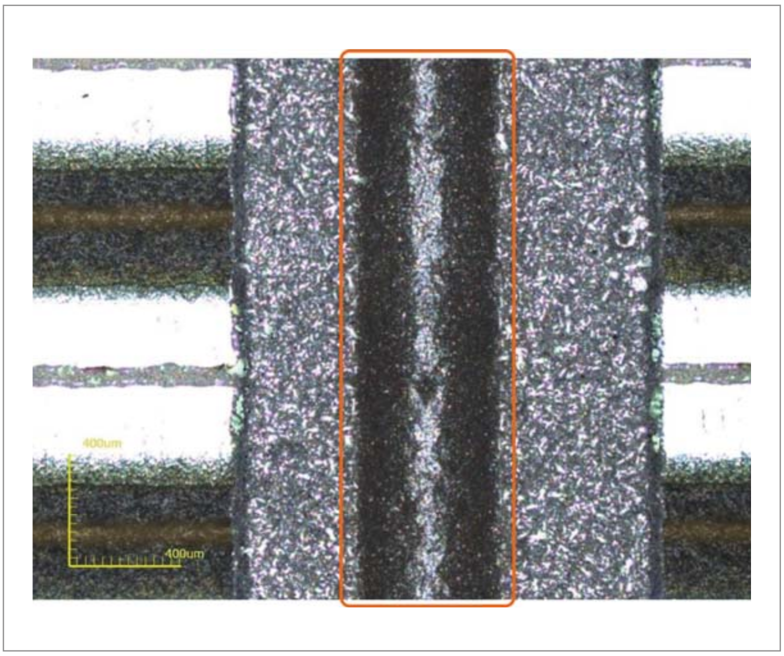

Figure 5. Light microscopy image of an IBC cell section with screen-printed ECA (dark bar within orange line perimeter) cured on a 1.5mm-wide busbar.

mechanical properties of the cured ECAs as well as their processing requirements, including curing temperatures in the range 100–170°C and curing times of usually several seconds (but up to 1–2 min for lamination-cured ECAs), address the above-mentioned process constraints.

As a case study, the interconnection of back-contacted cells ('ZEBRA' IBC cells developed at ISC Konstanz) with silver-coated copper ribbons and two commercially available, PV-specific ECAs with different polymer matrices (acrylic and epoxy) was compared to traditionally soldered reference cells [22]. Fig. 5 shows an example of the ECA line on one of the busbars. After curing of the ECA according to manufacturer specifications, the 180° ribbon peel forces obtained were around 1.15Nmm^{-1} for the ECA-bonded ribbons and 1.5Nmm^{-1} for the soldered ribbons; the cell warpage of the M2-sized cells after manual laboratory stringing was in the range 9–14mm for the ECA-bonded cells and 10–11mm for the soldered cells. By using industrial stringing units (teamtechnik TT2100 for soldering and TT1600ECA for ECA bonding), the high bowing values could be reduced by approximately 35%. This was achieved by several means, including improving the spatial homogeneity of the heat distribution over the cell, avoiding temperature overshooting, controlling the cool-down and the pressing of down-holders of the stringer during all processing steps up to and including the cool-down step.

At least double the duration of IEC standard reliability tests (IEC61215-2) could be easily sustained using glass–backsheet mini-modules (each with two half-cell strings) and EVA as encapsulation. Such modules passed 2,000h of damp heat testing (DHT, 85°C at 85% relative humidity) and 400 cycles of thermal cycling testing (TCT, −40°C to 85°C in a cycle time of 6h) with no delamination, discoloration or loss of P_{mpp} greater than 5%$_{rel}$ (tests showed a maximum 2.6%$_{rel}$ loss), confirming the compatibility with other module components and the predicted excellent long-term operation.

In the same study, voids were also observed in cross sections of the ECA joints, as shown in Fig. 6, and is a known issue for both soldering [23] and adhesive interconnections [24]. According to current test results, this aspect is not classified as critical; nevertheless, minimizing or avoiding these cavities would increase the performance (lower electrical resistance, higher adhesion force) and reliability of the joint. Overall, the mechanical properties of the cured ECA matrix must be able to withstand light deformations caused by thermomechanical stress, mechanical loads and common dynamic mechanical loads, such as vibrations from the surroundings.

"The use of ECAs as solder replacement is a very attractive route in dedicated PV cell interconnections such as HJT cells."

Positive technical, processing and reliability aspects cannot alone drive a technology to mass production if the cost structure is incompatible with common market pricing per Wp. Considering current ECA material costs and rapid reductions in the adhesive quantity per interconnection, it is certainly possible to at least achieve cost parity with soldering processes while still retaining the range of benefits of ECAs. In particular, ECA-bonded joints provide a lead-free interconnection and an expected easier and more convenient recycling of PV components from ECA-bonded joints compared to soldered joints in PV panels. This means a move in the right direction with respect to the environmental friendliness of PV panels.

Despite the sometimes-perceived status of ECAs in PV as being 'under development', industrial tools have long ago moved on, with the first high-throughput ECA stringer presented to the market by teamtechnik in 2014. Since then, many trials have been performed at the company to get a deeper understanding of the ECA application in terms of applying, curing and handling, and other tool manufacturers have since launched their own versions on the market. From 2018 onwards, there have been teamtechnik TT1600ECA stringers in industrial production 24/7, and, for the near future, a continuing trend towards increased market share is assumed.

However, manufacturers of such tools have had to overcome several challenges specific to ECA

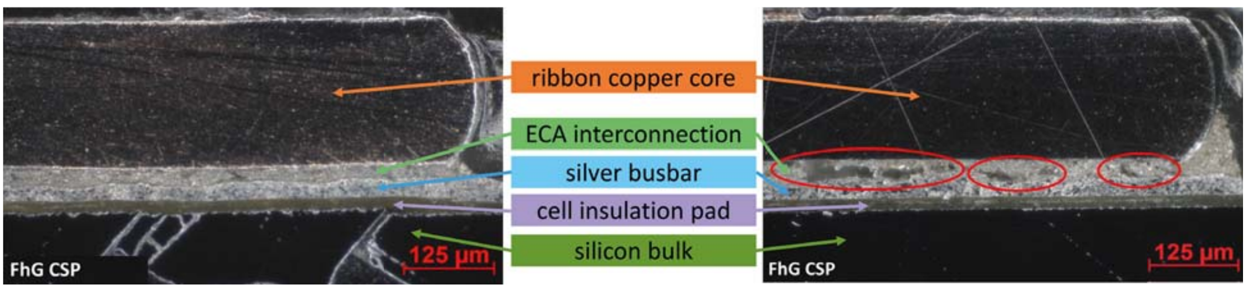

Figure 6. Cross section of an IBC 'ZEBRA' cell, with ribbon and ECA joints showing good interconnection (left), and bad interconnection (right) with voids (marked by red ellipses).

"The ECA stringing process is of interest for a number of cell types, including HJT, IBC, tandems and thinner PERC cells."

stringing, including the requirement for high positioning tolerance of the ribbon onto the ECA print. Examples of ECA ribbon stringers such as the TT1600ECA offer the key advantages of low-stress and lead-free connections, as well as the absence of flux vapours in the machine, resulting in lower cleaning and maintenance burdens, and customers report a high level of machine availability and process stability. The high throughput of such machines, coupled with opportunities to reduce and minimize silver consumption by coordinated layouts of busbars and ECA printing, can significantly lower the cost of ownership. The use of structured ribbons – such as the light-capturing ribbon LCR™ – is also possible without any reduction in throughput. In short, the ECA stringing process is of interest for a number of cell types, including HJT, IBC, tandems and thinner PERC cells.

Ribbon-contact reliability

Only a relatively simple production equipment update is needed to achieve lead-free products. The replacement of lead-containing solder by ECA is an alternative, and standard solar cells with H-grids can be used. A direct comparison was performed, using the same solar cell type and only the solder was replaced by ECA and another ribbon (tin-free).

The long-term reliability of a product directly correlates to the quality measures used to control the manufacturing processes. In a detailed study, the curing process of the ECA was examined using standard PERC cells. Two different ECAs were investigated with different curing temperatures,

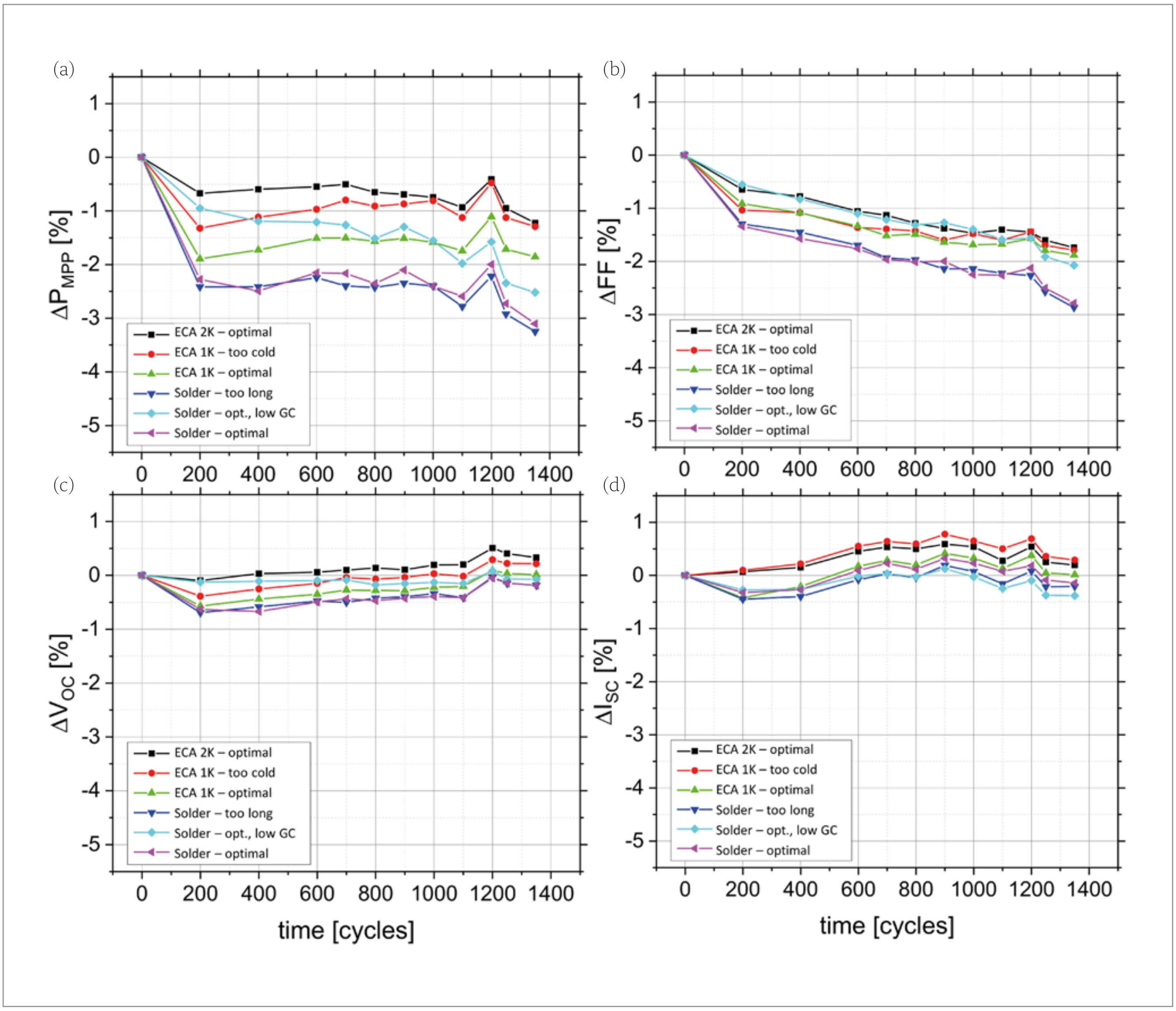

Figure 7. Trend charts of modules with 60 full cells during extended thermal cycling in accordance with IEC 61215-2 MQT 11, with different electrical contacting consisting of either two- (2K) or one-component (1K) ECAs with different process temperatures and, for comparison, soldered contacts also with process variations. (a) P_{mpp} under standard test conditions (STC), where the initial decrease is mainly attributed to LID/CID effects. (b) Fill factor, where a constant trend is visible for all modules. (c-d) V_{oc} and I_{sc}, which both remain relatively constant, indicating that the PERC cells did not internally degrade.

and these were compared with the standard soldering process. Full-size, 60-cell modules were manufactured with the same BOM, and the extended TCT results are shown in Fig. 7. Besides TCT, extended DHT (more than 2,000h) and humidity–freeze testing (HFT, more than 100 cycles) were performed. The performance of the modules fabricated using ECA was similar to that for the soldered references, with the main degradation being cell related.

After the first 200 cycles, a loss in power of 0.5–2.5% was observed, mainly attributed to the fact that the modules were not light soaked prior to the test. As a current (near I_{mpp}) is applied to the modules during the heating phase (–40°C to 85°C per IEC 61215-2), this acted as the initial light stress to induce the light-induced degradation (LID) effect per current-induced degradation (CID). Over the period of more than 1,000 cycles of TCT, no decrease in I_{sc} or V_{oc} was observed, leading to the conclusion that the PERC cell itself was very stable. During the test, a small but constant loss in fill factor (*FF*) can be observed, indicating some increase in series resistance. However, all modules show the same trend/slope, endorsing the statement in the introduction to this paper that ECAs can have at least similar reliability and durability to standard lead solder contacts.

Electroluminescence (EL) images confirm the stability of the ECA contacts on such PERC cells, with little visible change within the testing period. In a parallel long-term testing sequence, shingled modules using 1/6-cut cells were also investigated. Generally, the EL images appeared similar to the ones shown later in Fig. 8 but with the addition of other types of visible defects, such as greyish areas that appear in most cells, but underlie a sort of reversible process. A combined microstructure analysis, electrical performance (flash testing) and imaging techniques (EL and magnetic field analysis) is currently under way to more precisely understand the root cause.

Heterojunction cells

Silicon heterojunction solar cells offer the possibility of obtaining energy conversion efficiencies greater than 25% by reducing recombination effects at the metal contacts. This is achieved by displacing the metal contacts from the silicon surface by the deposition of hydrogenated amorphous silicon layers on the surface of the silicon absorber [25]. One challenge of this hydrogenated amorphous silicon layer is its sensitivity to temperatures above 220°C [26]. To overcome this issue, metallization is mostly implemented by low-temperature screen-printed silver pastes which are thermally treated at temperatures around 200°C. In comparison to the standard Ag firing pastes, these low-temperature pastes provide a lower adhesion to the wafer surface [27]. This, and the different microstructure of the metallization, complicates standard interconnection by soldering [28].

> "ECAs can have at least similar reliability and durability to standard lead solder contacts."

To overcome the challenges of soldering HJT solar cells, the interconnection of ribbons via ECA is one of the main alternatives. In addition to their lead-free nature, the biggest advantages of ECAs for interconnecting HJT solar cells are their low curing temperatures, the fast and easy application via screen printing, the sufficient adhesion (even to busbar-less cells), and the possibility of using structured ribbons. The industrial implementation of this interconnection method has already been achieved, and modules with HJT solar cells interconnected by ECAs can be found on the PV market.

One of the main challenges for ECA interconnections, however, is the high cost of some ECAs, with several of the widely used ones having filler content of up to 80% [29]. Nevertheless, there are different approaches to overcoming this problem, such as drastically reducing the amount of ECA used by variation of the application patterns, as described in more detail below. For example, a continuous ECA line between solar cell and ribbon can be replaced by a dotted line, thereby reducing the ECA amount significantly without losses in module performance [30]. There are also different kinds of ECAs on the market where the silver particle content is reduced, as in the anisotropic conductive adhesives, or is replaced by other metals, such as copper.

With growing demand and further research, the cost of ECAs can be expected to decline over time. In addition, the overall silver consumption in a glued module can be reduced in several ways. One option is the adjustment of the metallization pattern: for example, by using double fingers instead of the full busbars, by going from five busbar configurations to six or more, and combining those approaches with an adjustment of the finger patterns. Another possibility is to use pure copper ribbons instead of silver-coated ribbons [31]. Overall, it can be said that ribbon interconnection with ECAs is an ideal approach for HJT modules, and the problem of higher costs is currently being tackled in R&D by different approaches.

In particular, the reduction of silver consumption in PV is one of the most relevant topics because of environmental impact and economic reasons, with the PV industry being one of the main worldwide silver consumers, representing about 10% of global demand. Anticipating a continuous solar industry expansion, technological breakthroughs are necessary in order to reduce the silver consumption and avoid silver shortage issues.

An initial optimization has to be implemented at the cell design level. Increasing the number of ribbons or wires on the cell layout allows a decrease in the quantity of silver employed in

> "One of the main challenges for ECA interconnections is the high cost of some ECAs."

cell metallization. However, when using ECA interconnection technology, this solution may imply an increase in the amount of ECA itself and the number of ribbons; hence, an optimal trade-off needs to be found. A second optimization solution is to reduce the silver consumption during the interconnection process at the module level. Indeed, several paths could be considered:

- Reduce the silver content in ECA.
- Reduce ECA consumption.
- Implement ribbons/wires without a silver coating.

All of these solutions should be implemented while maintaining the same module performances and reliability.

Within the framework of the Horizon 2020 GOPV project [32], CEA-INES investigated the reduction of the amount of ECA in HJT cells. The reliability after TCT400 (IEC 61215) of samples with different ECA pad designs, allowing ECA reductions of 40, 45, 55 and 65%, was compared to the reference – a sample with full ECA lines deposited. Results of the tests showed that samples with a significant decrease in ECA consumption of 40–45% could withstand up to twice the TCT norm, with a relative P_{mpp} loss of –2.0% and a ΔFF of –0.5%, vs. initial levels, which are similar to the losses obtained with the reference design.

In a second study, the reduction of the silver content in the ECA composition was evaluated at the module manufacturing level. Nine different ECA pastes were used for that experiment, having silver contents of 60%, >50%, and <50%. Among those with less than 50% silver, two had copper added in their composition in the following ratios: 15:70% Ag to Cu for the first, and 30:60% for the second. The samples were manufactured with one ECA pad configuration that already allowed a 40% ECA reduction, and then the adhesion of the ribbons was measured with a peel force tester. Results showed that the ribbon adhesion was greater than $0.57\,Nmm^{-1}$ for most of the samples, and that only one discarded sample had a lower adhesion, around $0.28\,Nmm^{-1}$. After TCT200, one sample with less than 50% silver content exhibited the best performance by far, in compliance with the

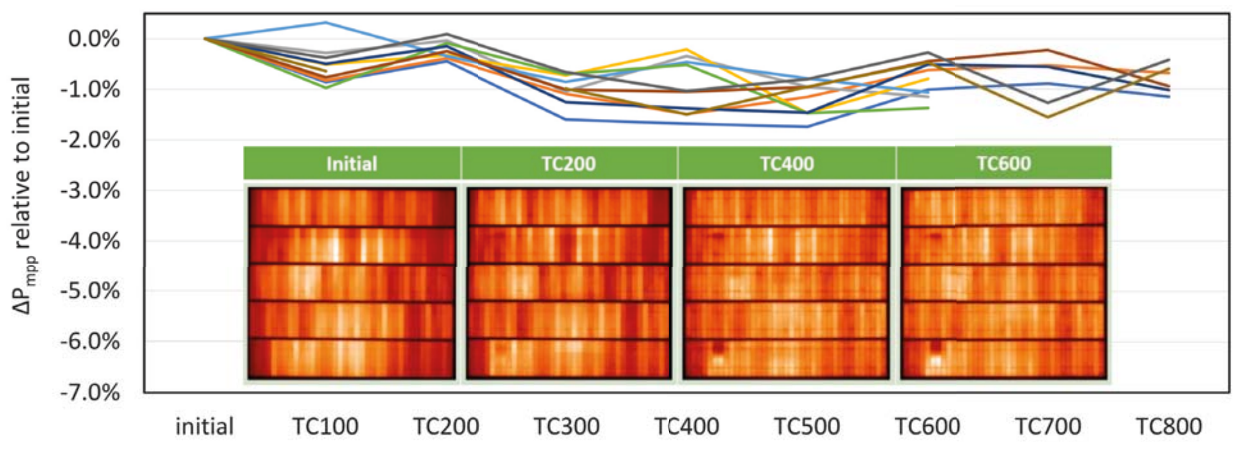

Figure 8. Evolution of P_{mpp} for mini-modules submitted to TCT800 and TCT600. The inset shows the EL images through the accelerated ageing process of a different but related shingled module with five strings bussed in parallel.

IEC norm, with a P_{mpp} loss of around –1.2%.

To conclude, the possible reduction of the quantity of ECA per cell demonstrated by CEA-INES may lead to a significant decrease in silver consumption when the ECAs used have less than 50% silver content. Furthermore, most manufacturers have launched numerous new products in recent years, and an acceleration of further development in ECA technologies is expected with the large-scale industrial implementation of HJT modules. Further improvements in the compatibility of ECA and silver-free wire/ribbon coatings could also lead to a cost reduction factor of a third, enhancing the very promising results already obtained.

HJT reliability

ECA-based interconnections are particularly interesting for high-efficiency architectures, such as HJT solar cells or the latest generations of TOPCon cells, for which low or moderate temperature processes are often required (<200°C for HJT devices, for example). In the case of HJT cells, several tests to study ECA shingling interconnection reliability have recently been conducted at CEA-INES within the framework of the EU's Horizon2020 HighLite project, with consortium partners spanning tool manufacturers, ECA producers and several leading PV research institutes [33].

In one study, strings of HJT shingled cells were embedded into mini-modules and placed into climate chambers for up to 800 thermal cycles, in accordance with the IEC61215-2 norm requirements (–40°C/85°C). As shown in Fig. 8, the P_{mpp} losses after TCT800 were in the range 0.41–1.15% for a first batch of samples. EL images of a different but closely related shingled module are shown in the Fig. 8 inset and provide further qualitative support.

In another test, several quantities of one type of deposited ECA were tested and combined with different solar cell thicknesses (160μm, which is the current standard, and 120μm). Mini-modules were tested up to TCT600, with a maximal degradation in P_{mpp} of 2.6%. The samples that showed the strongest degradation on average (2.6%) were made of 120μm cells with only 1.6mg of ECA per shingle stripe. As expected, those that showed the best reliability (–0.7%) had the larger amount of 6.5mg of ECA per shingle stripe for 160μm-thick cells. Standard quantity deposition of 3.3mg showed equivalent reliability for both thicknesses: close to –1.8% on average after TCT600. Larger strings of 37 shingle stripes were also submitted to thermal cycling tests, and both cell thicknesses showed an average P_{mpp} loss of 2.4% with standard ECA quantity deposition. A PV module made of five large shingle strings bussed in parallel reached a P_{mpp} degradation of less than 2.8% after TCT600.

Although ECA-based shingle interconnection with HJT solar cells is still the subject of R&D efforts, the results obtained to date demonstrate the excellent reliability of the currently developed interconnection technology. Further studies of shingling reliability will be carried out with the aim of improving shingle HJT technology from an economic and environmental point of view, by reducing the quantity of silver used (at the grid metallization and ECA levels) and the solar cell thickness, as well as by increasing the active surface area per module.

Shingling interconnection

ECAs can be used for the direct front-to-rear interconnection of solar cells. This technology is called *shingling*, since the solar cells slightly overlap in a similar way to shingled roof tiles. Shingled solar modules yield an increased power density, as shingling results in an increased overall packing density in the module. Furthermore, the ohmic losses related to the ribbons used to interconnect the solar cells within a conventional solar module are eliminated. These advantages of shingling technology can translate to an absolute gain in module efficiency of up to around 1.9% [34]. Hence, shingled solar modules further reduce the gap between solar cell efficiency and module efficiency.

An important aspect of solar cell interconnections is the thermomechanical stresses exerted on the connection during production and normal operation; for example, it has been shown that solar cells are shifted relative to each other while the laminate is cooling down [35]. In shingling, the ECA bond between the solar cells must ensure both a reliable mechanical and a reliable electrical connection at all times. In particular, ECAs must be able to withstand the shear stresses exerted on shingled joints, as shown in Fig. 9.

"ECAs must be able to withstand the shear stresses exerted on shingled joints."

The schematics in Fig. 9(a) illustrate the deformation modes of the ECA joint (orange) during temperature changes of the PV laminate. The reference temperature is the temperature of the cross-linking reaction of the encapsulant during lamination (~150°C). After lamination, the glass governs the thermal expansion of the solar module. Since in operation solar modules seldom reach temperatures higher than T_{ref}, the relevant deformation mode is $T < T_{ref}$, when solar cells move towards each other.

Finite element simulations of thermal cycling in accordance with IEC 61215 [37] have shown that the strain at –40°C is close to pure shear strain [36], with mean absolute shear strains of $|\varepsilon_{xy}| \cong 6.5\%$ and mean absolute shear stresses of $|\sigma_{xy}| \cong 25$MPa. Although these values are strongly dependent on the material data used in the simulations, the implication is that ECAs in shingled solar modules are subjected to stresses and strains of the same order of magnitude as their strength limits.

In addition to the deformation of the joint itself, the solar cells above and below are affected by

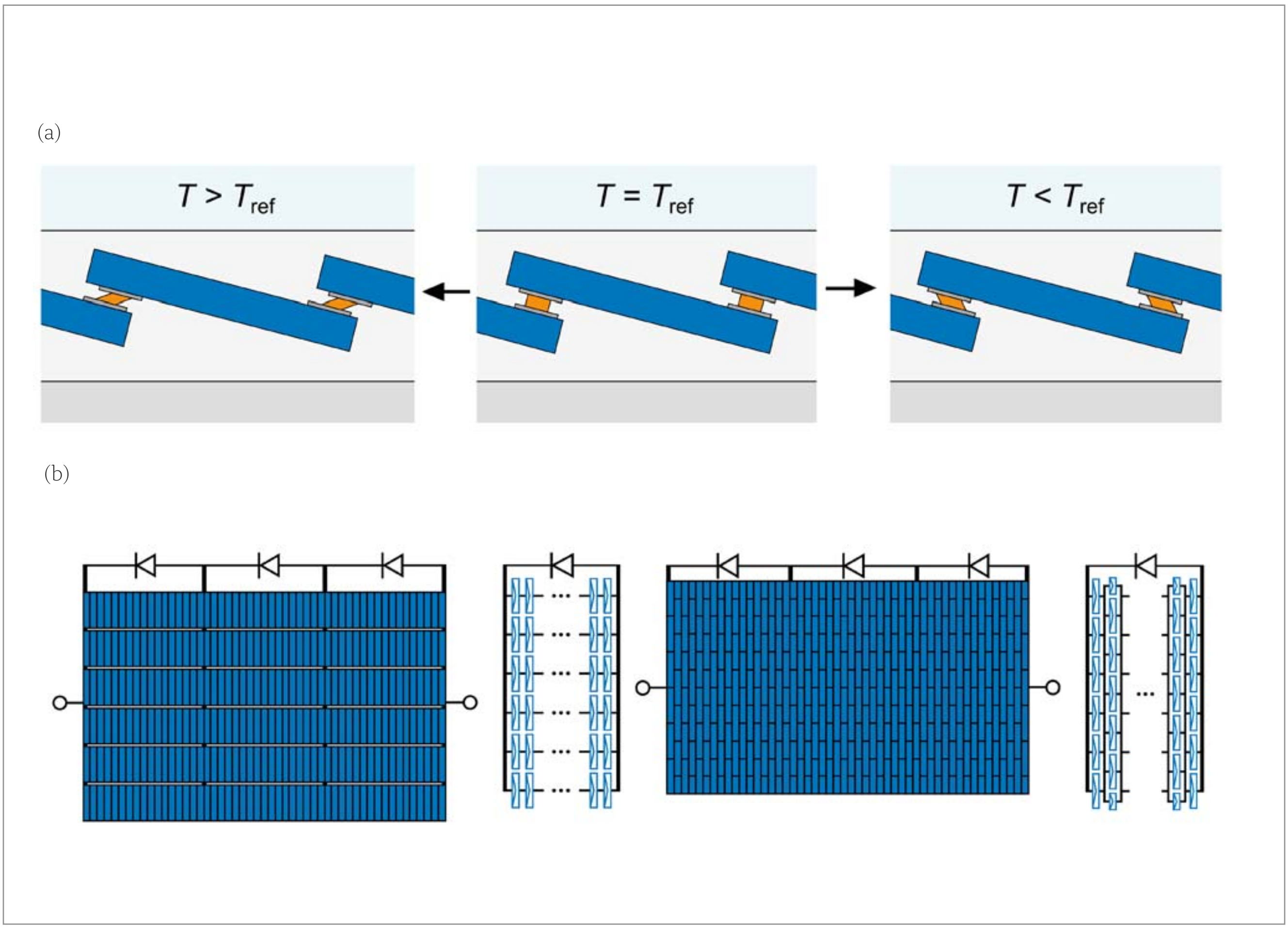

Figure 9. (a) Deformation modes of shingle joints subjected to changes in temperature. For temperatures higher than the stress-free reference temperature T_{ref}, the shingled solar cells move apart, whereas they move towards each other at temperatures less than T_{ref} [36]. (b) Typical interconnection scheme of the shingle string layout and circuit (left), and the shingle matrix layout and circuit (right).

thermomechanical stress. Thermal contraction of the EVA surrounding the joint causes a bending of the solar cells, inducing high tensile stresses on the surface of the solar cell opposing the ECA. These tensile stresses are locally limited to the applied ECA. Characteristic cracking patterns perfectly matching the applied ECA have been found in electroluminescence images after thermal cycling ageing. Because of the asymmetric structure of PV laminates, the highest stresses occur on the solar cell surface facing the backsheet. The defect can occur in monofacial solar cells, but can only be observed in bifacial cells in combination with transparent backsheets, since detection requires electroluminescence techniques. Therefore, it might go unnoticed in conventional laminates with opaque backsheets. So far, it has not been possible to link this cracking mechanism to significant losses in power; however, the mechanism was presented at the 11th SiliconPV 2021 [38].

Besides the thermomechanics of ECA-bonded joints and the as-yet unresolved issue of recombination at the cut cell edges [39], shingled solar cell interconnection opens up possibilities for more sophisticated solar module layouts, such as the shingle matrix interconnection (see Fig. 9(b), right) [40]. Such solar modules are much more resilient with regard to partial shading [41]; consequently, shingled solar modules and especially shingle matrix modules are well suited to vehicle and building integration. M10 Industries now offers a high-throughput shingling stringer, which was developed in conjunction with Fraunhofer ISE within the public German Shirkan project [42], and which is capable of implementing both the linear- and matrix-shingled module concepts.

When shingled modules are produced in a high-volume manufacturing environment, the shingling of strings is achieved using dedicated equipment which is considerably different from that used for the mainstream stringing and tabbing approach. In fact, cells first have to be separated into shingle stripes (for example, by traditional laser scribe and cleave, or using newer techniques such as thermal laser separation); the ECA then has to be deposited (screen/stencil printing or dispensing) before the shingle stripes are arranged in the typical overlapping scheme. Current-generation tools – such as Applied Materials' Sonetto 2.0 – can assemble up to 4,000 full cells per hour in a dual-lane configuration. In practice, five or six shingles are processed simultaneously within a cycle time of 1.8s, equating to 20,000–24,000 shingle stripes per hour, and next-generation tools have already been announced that are capable of 6,000 M12-sized full cells per hour [43].

When depositing ECAs by screen printing, several variables need to be considered in production:

- *Rheology variations:* ECAs should be as stable as possible in terms of rheology variations (thixotropy) over time in order to maintain constant deposits.

- *Temperature and humidity:* environmental changes, such as a temperature increase, may induce partial curing of the ECAs. The risk is higher if the ECA is deposited on the cell and more of the surface is exposed.

- *ECA lifetime on screen:* different chemistries react differently to the rolling mechanism introduced by the printing process.

- *Printing parameters:* accurate controls of print force, speed, distance to the substrate, and stroke are essential to achieving a consistent product.

By stabilizing and controlling all of the above elements, it is possible to achieve suitable production yields, which normally surpass 98.5% (from cells-in to strings-out, including reworking). Because of its unique approach, shingling-based interconnection can be implemented with only relatively minor equipment modifications for large wafers, thin wafers, low-temperature cells, lead-free modules and building-integrated PV (BIPV) applications.

An alternative approach investigated within the ongoing German Hossa research project by a consortium of tool suppliers, module manufacturers and research institutes [44] relies on a modified process order for high-throughput industrial shingling. In this approach, the ECA is applied first to the uncut shingled cells, then the laser scribing is performed adjacent to the deposited ECA, as shown in Fig. 10; in a final step, the stringer separates the cells and assembles the strings. In this way, the difficult processing of many small cell stripes is postponed to a later process step, with significant benefits to process and machine simplification. In order to implement this approach, the ECA has to be optimized with particular regard to the pot life or on-part life, while the laser process needs to be adjusted such that the final properties of the ECA bond remain unaffected. Results have shown that, despite laser-induced changes to the surface and shape of the ECA line (as shown in Fig. 10), this can be achieved when using the correct laser and process parameters, even when lasering very close to the ECA.

Anecdotally, the long-term reliability of shingled modules is exceptional, with several manufacturers offering warranty extensions of at least five years vs. their non-shingled counterparts. Notwithstanding the efforts described below to determine the failure modes and root causes of degradation in shingled modules and other formats that employ ECA for bonding, despite somewhat contradictory results in the published literature, the reasons for such high levels of manufacturer confidence can be readily seen by considering again the data in Figs. 3, 7 and 8. Of note is the fact that several BOM combinations

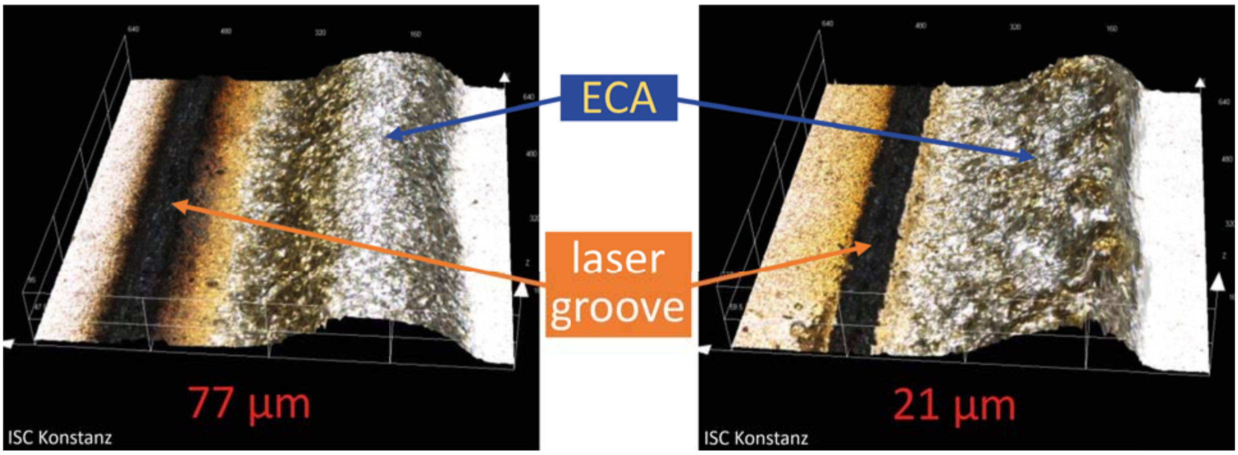

Figure 10. Laser scanning microscope images of laser-etched grooves adjacent to uncured ECA lines, where the separation between laser groove and ECA is 77µm (left) and 21µm (right).

can withstand thermal cycling for periods well in excess of the IEC 61215 pass criterion for TCT (degradation less than 5% with up to 200 cycles); indeed, several combinations showed the potential for only around 1% degradation with up to 700–1,400 cycles. The same combination that exhibited less than 1% degradation in Fig. 3 also exhibited less than 1.5% degradation for up to 4,250h of damp heat testing (data not shown).

Further ECA reliability studies

Currently, the reliability of modules built using ECAs is of great interest in the scientific community, but not many studies have been published and relevant work is ongoing. Additionally, qualification tests for ECAs in PV modules have not yet been developed and implemented [45,46]. Mesquita et al. [47] proved scanning acoustic microscopy (SAM) to be a powerful tool for non-destructively characterizing modules built using ECAs. In their work, the authors could clearly distinguish between defective and non-defective adhesive after accelerated ageing tests. Schiller et al. [48] proposed an accelerated TCT able to give, in a shorter time, results that are similar to the typical IEC TCT. The proposed test might be useful during material development to reduce testing time.

Three ECA formulations have been tested by Bauermann et al. [49], two of which fulfilled the IEC 61215 criteria in terms of power loss after HFT, DHT and TCT. None of the formulations, however, performed comparably to traditional soldered ribbon, possibly because of the negative interaction between adhesive and water. Additionally, the adhesives showed differences depending on the stress applied, thus indicating that a climate-specific application should be considered. Klasen et al. [50] proposed a model able to predict, in comparative studies, mechanical stresses in the joints of shingled solar cells using different geometries.

With regard to the mechanical behaviour and the fracture toughness of the cured resin in high-efficiency cell concepts and reduced cell thicknesses, the consideration of mechanical strain is especially important. Springer et al. [51] recently investigated the viscoelastic properties of different ECA formulations. Chemical composition and cure conditions had a big influence on viscoelastic material properties. Furthermore, the response to dry and damp heat exposure was investigated. Depending on the ECA type, the observations ranged from no change to significant changes in the viscoelastic properties. Damp heat exposure caused embrittlement to a point, where even small strains imposed during dynamic mechanical analysis caused fracture. Moreover, changes in thermal expansion behaviour were detected after ageing. Embrittlement of ECAs has also been reported elsewhere [52].

So far, only a limited number of papers [53–55] dealing with the fatigue behaviour of different types of cell interconnection have been published, and they give contradictory results. Pander et al. [55] found that the use of ECAs in silicon solar cells led to a reduction in strain within the silicon compared to soldering. They also studied fatigue of solar cell interconnectors, and designed the loading profile during the fatigue test so as to achieve the same strain amplitude in the cell gaps as that found in a full-size module simulation under ±1,000Pa, which corresponds to the IEC testing standard [53].

"Modern ECAs are consistently proving themselves to be one of the key technologies in the future of PV."

Dietrich et al. [53] also investigated fatigue of solar cell interconnectors, but chose the test amplitude in such a way that the failure occurred in less than 10,000 cycles; however, the authors did not give details of the load levels applied in their fatigue test. Zarmai et al. [56] studied thermomechanical damage and fatigue life of solar cell solder interconnections, and reported calculated values of 21MPa for the maximum stress concentration in the solder joint. This value was obtained through thermal cycling tests in accordance with IEC 61215 [57].

Oreski et al. [58] investigated the cyclic fatigue behaviour of two different ECA types, and found a significant difference in the resistance to fatigue. One explanation lies in the intrinsic fatigue resistance of the materials, but also the sample preparation may have an impact on the fatigue resistance. Regarding the cyclic fatigue behaviour of the ECA types studied, the S–N curves depicting cyclic stress as a function of cycles to failure are either significantly above the mean stress levels reported for interconnections in PV modules [53,54] or in a similar range to them [56]. The reported values for the number of cycles to failure for soldered bonds are also in a similar range.

For ECA-bonded test modules, a slight power loss after thermal cycling, damp heat and irradiance exposure has been observed [58]. In that study, the power loss was attributed not only to failure of the ECA bond but also to additional factors such as sample preparation and cell damage that was present from the start. In the same study, the compatibility of different ECA formulations and various encapsulation films and ribbon materials was investigated. No harmful interactions were found between the ECA formulations examined and the different encapsulant films after lamination and ageing tests. The main outgassing products were identified as fragments of the hardener. In addition, no migration of silver particles was observed. ECAs were compatible with all tested ribbon types (Cu, Ag, SnAgCu), since no delamination or discoloration after lamination or accelerated ageing tests was observed.

Summary and outlook

Whether in shingling, in low-temperature interconnections or as solder replacement, modern ECAs are consistently proving themselves, through their material performance, process flexibility and reliability in application, to be one of the key technologies in the future of PV. Considering the maturity and inherent material and process limitations of traditional lead and lead-free metal soldering technology compared to the vast range in potential of the filler–adhesive platform offered by ECAs, the trajectory of development is clearly leaning towards ECAs becoming a dominant interconnection medium. Of course, with the currently high rate of progress and innovation in PV, coupled with the ponderous momentum of an industry in which multi-GW factories can take years to plan and build, and not forgetting the financial and economic realities of decision-making in a highly competitive global market, only time will tell if this turns out to be the case.

It is accepted, however, that an exponential increase in PV production output will be required over the next decade to meet national renewable energy targets and international emissions reduction agreements (such as the Paris Climate Accords). That being the case, as well as the natural evolution of PV market share towards higher-efficiency cell concepts, not to mention the inevitable progression towards tandem cells that use silicon and temperature-sensitive thin-film technologies (such as perovskites and GaAs, which are now firmly on the horizon), the future is certainly looking very bright for ECAs.

References

[1] Nicolics, J. & Mündlein, M. 2007, "Electrically conductive adhesives", in *Micro- and Opto-Electronic Materials and Structures: Physics, Mechanics, Design, Reliability, Packaging,* Suhir, E., Lee, Y.C. & Wong, C.P., Eds. New York, USA: Springer, pp. B571–B610.

[2] Battermann, A. 2012, "Joining technology that's fit for the future", *Adhes. Adhes . Sealants,* Vol. 9, pp. 40–43.

[3] Morris, J.E. & Wang, L. 2014, "Isotropic conductive adhesive interconnect technology in electronics packaging applications", in *Adhesion in Microelectronics,* Mittal, K.L. & Ahsan, T., Eds. Hoboken, NJ, USA: John Wiley & Sons, Inc, pp. 173–210.

[4] Li, Y., Moon, K.-S. & Wong, C.P. 2005, "Electronics without lead", *Science*, Vol. 308, No. 5727, pp. 1419–1420.

[5] Yim, M.J. & Paik, K.W. 2006, "Recent advances on anisotropic conductive adhesives (ACAs) for flat panel displays and semiconductor packaging applications", *Int. J. Adhes. Adhes.,* Vol. 26, No. 5, pp. 304–313.

[6] Beier, B. et al. 2001, "Electrical conductive adhesives", *Proc. 17th EU PVSEC,* Munich, Germany, pp. 812–815.

[7] Frisson, L. et al. 2001, "Conductive adhesives as an interconnection technique for very thin solar cells", *Proc. 17th EU PVSEC,* Munich, Germany, pp. 414–416.

[8] Lalaguna, B. et al. 2008, "Evaluation of stress on cells during different interconnection processes", *Proc. 23rd EU PVSEC,* Valencia, Spain, pp. 2705–2708.

[9] Bultman, J.H. et al. 2003, "Fast and easy single step module assembly for back-contacted c-Si solar cells with conductive adhesives", *Proc. 3rd WCPEC,* Osaka, Japan, pp. 979–982.

[10] Scherff, M.L.D. et al. 2006, "10 × 10 cm^2 HIT solar cells contacted with lead-free electrical conductive adhesives to solar cell interconnectors", *Proc. 4th WCPEC,* Waikoloa, Hawaii, USA, pp. 1384–1387.
[11] Schwertheim, S. et al. 2008, "Lead-free electrical conductive adhesives for solar cell interconnectors", *Proc. 33rd IEEE PVSC,* San Diego, California, USA, pp. 1–6.
[12] Späth, M. et al. 2011, "Hetero-junction module technology", *Proc. 26th EU PVSEC,* Hamburg, Germany, pp. 3121–3124.
[13] teamtechnik 2018, "Lower costs, more efficiency: Russian module manufacturer and PV project developer Hevel LLC switches to adhesive technology from teamtechnik for its HJT modules", Press Release, 25 Sep. [https://www.teamtechnik.com/en/news/].
[14] teamtechnik 2018, "Major contract for teamtechnik: Italian PV manufacturer orders stringers for production of high efficiency modules with HJT cells", Press Release, 12 Feb. [https://www.teamtechnik.com/en/news/].
[15] Chunduri, S.K. 2011, "Sticky and cool", *Photon International,* Vol. 2011, No. 11, pp. 158–165.
[16] Yan, F. et al. 2013, "Evaluation of CIGS cell interconnection methods", *Proc. 39th IEEE PVSC*, Tampa, Florida, USA, pp. 2064–2067.
[17] SunPower 2021, "Performance Solar Panels" [https://sunpower.maxeon.com/uk/solar-panel-products/sunpower-performance-solar-panels].
[18] Devoto, M.I. et al. 2021, "Contact resistivity of ECA bonded joints", *AIP Conf. Proc.,* Vol. 2367, No. 1, p. 020011.
[19] Geipel, T. 2018, "Electrically conductive adhesives for photovoltaic modules", Technical Report, Fraunhofer ISE.
[20] Devoto, M.I. et al. 2021, "Measuring the contact resistivity of ECA-based joints", *Proc. 38th EU PVSEC*, Lisbon, Portugal.
[21] Bennett, I.J. et al. 2014, "An overview of developments in foil-based back-contact modules", *Proc. 29th EU PVSEC,* Amsterdam, The Netherlands.
[22] Timofte, T. et al. 2021, "Reliability assessment for industrial soldered and glued BJ-BC solar cell interconnections", *Proc. 38th EU PVSEC,* Lisbon, Portugal.
[23] Sweatman, K.W. et al. 2016, "Controlling voiding mechanisms in the reflow soldering process", *Proc. IPC APEX Expo 2016,* Las Vegas, Nevada, USA.
[24] Habenicht, G. 2009, *Kleben*, Springer.
[25] Haschke, J. et al. 2018, "Silicon heterojunction solar cells", *Sol. Energy Mater. Sol. Cells,* Vol. 187, pp. 140–153.
[26] De Wolf, S. & Kondo, M. 2009, "Nature of doped a-Si:H/c-Si interface recombination", *J. Appl. Phys.,* Vol. 105, No. 10, p. 103707.
[27] Gierth, P. et al. 2013, "Comparison of NiV and polymer paste metallization as low temperature interconnection of high efficiency heterojunction solar cells", *Proc. 28th EU PVSEC,* Paris, France, pp. 464–467.
[28] De Rose, A. et al. 2017, "Low-temperature soldering for the interconnection of silicon heterojunction solar cells", *Proc. 33rd EU PVSEC,* Amsterdam, The Netherlands, pp. 710–714.
[29] Lewis, H.J. & Coughlan, F.M. 2008, "An overview of the use of electrically conductive adhesives (ECAs) as a solder replacement", *J. Adhes. Sci. Technol.,* Vol. 22, No. 8–9, pp. 801–813.
[30] Kaiser, C. et al. 2020, "Reduction of ECA amount for the ribbon interconnection of heterojunction solar cells", *Proc. 37th EU PVSEC* (virtual event), pp. 1086–1090.
[31] Geipel, T. et al. 2019, "Industrialization of the ribbon interconnection of silicon heterojunction solar cells with electrically conductive adhesives", *Proc. 36th EU PVSEC,* Marseille, France, pp. 916–925.
[32] GOPV. EU Horizon2020, Grant Agreement Number 792059.
[33] HighLite. EU Horizon2020, Grant Agreement Number 857793.
[34] Mittag, M. et al. 2017, "Cell-to-Module (CTM) analysis for photovoltaic modules with shingled solar cells", *Proc. 44th IEEE PVSC,* Washington DC, USA.
[35] Eitner, U. 2011, "Thermomechanics of photovoltaic modules", Dr.-Ing. dissertation, Martin-Luther-Universität Halle-Wittenberg, Halle-Wittenberg.
[36] Klasen, N. et al. 2019, "FEM simulation of deformations in strings of shingled solar cells subjected to mechanical reliability testing", *AIP Conf. Proc.,* Vol. 2156, No. 1, pp. 020016-1–020016-11.
[37] IEC 61215-2:2016, "Terrestrial photovoltaic (PV) modules – Design qualification and type approval – Part 2: Test procedures".
[38] Klasen, N. et al. 2021 [submitted], "Root cause analysis of solar cell cracks at shingle joints", *Sol. Energy Mater. Sol. Cells.*
[39] Tune, D. et al. 2020, "Measuring and mitigating edge recombination in modules employing cut cells", *Proc. 37th EU PVSEC* (virtual event).
[40] Klasen, N. et al. 2021 [forthcoming], "Performance of shingled solar modules under partial shading", *Prog. Photovolt: Res. Appl.*
[41] Klasen, N. et al. 2021 [forthcoming], "'Shading Resilience' as a general measure of shading tolerability in PV modules", *IEEE J. Photovolt.*
[42] Shirkan project. BMWi, Funding Ref. No. 03EE1026A.
[43] Taiyang News 2021 [http://taiyangnews.info/technology/day-2-taiyangnews-whats-hot-in-european-solar-rd/].
[44] Hossa project. BMWi, Funding Ref. No. 03EE1014D.
[45] Hu, Y. & French, R.H. 2019, "Degradation and failure mechanisms of PV module interconnects" in *Durability and Reliability of Polymers and Other Materials in Photovoltaic Modules,* Yang, H.E., French, R.H & Bruckman, L.S., Eds. Amsterdam: Elsevier, pp. 119–134.
[46] Oreski, G. et al. 2021, "Designing new materials

for photovoltaics: Opportunities for lowering cost and increasing performance through advanced material innovations", Report IEA-PVPS T13-13:2021, International Energy Agency.

[47] Mesquita, L.V. et al. 2019, "Analysis of shingle interconnections in solar modules by scanning acoustic microscopy", *AIP Conf. Proc.,* Vol. 2147, 090003.

[48] Schiller, C.H. et al. 2019, "Accelerated TC test in comparison with standard TC test for PV modules with ribbon, wire and shingle interconnection", *Proc. 36th EU PVSEC,* Marseille, France, pp. 995–999.

[49] Bauermann, L.P. et al. 2017, "Qualification of conductive adhesives for photovoltaic application – Accelerated ageing tests", *Energy Procedia,* Vol. 124, pp. 554–559.

[50] Klasen, N. et al. 2019, "FEM simulation of deformations in strings of shingled solar cells subjected to mechanical reliability testing", *AIP Conf. Proc.,* Vol. 2156, 020016.

[51] Springer, M. & Bosco, N. 2020, "Linear viscoelastic characterization of electrically conductive adhesives used as interconnect in photovoltaic modules", *Prog. Photovolt: Res. Appl.,* Vol. 28, No. 7, pp. 659–681.

[52] Eitner, U. et al. 2012, "Characterization of electrically conductive adhesives", *Energy Procedia,* Vol. 27, pp. 676–679.

[53] Meier, R. et al. 2016, "Microstructural optimization approach of solar cell interconnectors fatigue behavior for enhanced module lifetime in extreme climates", *Energy Procedia,* Vol. 92, pp. 560–568.

[54] Pander, M. et al. 2013, "Lifetime estimation for solar cell interconnectors", *Proc. 28th EU PVSEC,* Paris, France, pp. 2851–2857.

[55] Pander, M., Schulze, S.-H. & Ebert, M. 2014, "Mechanical modeling of electrically conductive adhesives for photovoltaic applications", *Proc. 29th EU PVSEC,* Amsterdam, The Netherlands, pp. 3399–3405.

[56] Zarmai, M.T. et al. 2017, "Evaluation of thermo-mechanical damage and fatigue life of solar cell solder interconnections", *Robot. Comput. Integr. Manuf.,* Vol. 47, pp. 37–43.

[57] IEC 61215-1:2016, "Terrestrial photovoltaic (PV) modules – Design qualification and type approval – Part 1: Test requirements".

[58] Oreski, G. et al. 2019, "Reliability of electrically conductive adhesives", *Photovoltaics International,* Vol. 42, pp. 38–45

About the Authors

Daniel Tune studied nanotechnology with a major in physics at the Flinders University of South Australia. He graduated with Honours in 2009 then received his Ph.D. in chemistry in 2014. Since 2019 he has been managing R&D projects at ISC Konstanz, with a focus on advanced and alternative PV module concepts.

Torsten Roessler is head of the Conductive Adhesives Team at Fraunhofer ISE. He studied information systems technology at TU Dresden (Germany). He worked with module manufacturer Solon (Berlin) for several years, before joining Fraunhofer ISE to work on his doctoral thesis about ECAs for PV modules.

Dr. Oreski is division manager at the Polymer Competence Center Leoben (Austria). He holds a Ph.D. in polymer engineering and has over 18 years' expertise in quality and reliability testing of polymers for PV.

Carolyn Carriere holds an M.Sc. in physics of materials for energy from the Aix-Marseille University, France. Having previously worked as an engineer at CNRS (France), the University of Sherbrooke 3IT (Canada) and imec (Belgium), she joined the CEA-INES PV research group in 2020 to work on innovative module and interconnection technologies.

Christina Kaiser studied materials science and sustainability methods at the University of Applied Sciences Bonn-Rhein-Sieg, and received her master's in 2019. Since then, she has been with Fraunhofer ISE, working mainly on the characterization of ECAs and the cell interconnection and module integration of HJT solar cells.

Dr. Timofte studied chemistry at the Alexandru Ioan Cuza University in Iași, Romania, and received his Ph.D. in solid state chemistry and material science from the University of Cologne, Germany. Since 2011 he has been active in R&D in the PV sector, working on the characterization and development of solar cells and module components and assembly.

Nils Klasen studied process engineering at the Karlsruhe Institute of Technology (KIT), Germany. In 2017 he started research at Fraunhofer ISE for his Ph.D. on shingled solar cell interconnections. His research focuses on mechanical and electrical reliability, and is funded by a scholarship from the German Federal Environmental Foundation DBU.

Dr.-Ing. Julian Weber studied physics at the University of Konstanz, Germany. The research he carried out at Fraunhofer ISE for his Ph.D. thesis involved laser-assisted diffusion processes for manufacturing silicon solar cells. Since 2021 he has been working at Fraunhofer ISE on solar modules, in particular shingled solar modules.

Bengt Jäckel received his Ph.D. in materials science from TU Darmstadt in 2005. Since 2007 he has been working in the PV industry, holding various positions covering the entire value chain. He currently heads the Reliability of Modules and Systems Team at Fraunhofer CSP as well as the PV Module Group at DKE.

Stephan Großer studied physics and received his Ph.D. in 2008, and worked in the PV industry as a process engineer and researcher. In 2011 he joined Fraunhofer CSP, where he leads a team that focuses on the microstructure diagnostics of materials and devices and the root cause analysis of defects.

Matthias Pander has been working in the Reliability of Solar Modules and Systems Group at Fraunhofer CSP in Halle, Germany, since 2010. He specializes in the field of finite element simulation of PV modules and material modelling, as well as lifetime evaluation.

Dr. Marko Turek received his Ph.D. in the field of condensed matter theory from the University of Regensburg. At Fraunhofer CSP, he leads the Electrical Characterization Team, focusing on loss analysis of solar cells, advanced characterization methods, development of new test methods and data analysis of production data.

Marco Galiazzo received his M.Sc. in telecommunications engineering from the University of Padova, and then joined a start-up as an optical engineer. Since 2008 he has been working for Applied Materials Italy as an R&D manager, coordinating research activities in the fields of solar cell metallization and module manufacturing.

Ignacia Devoto obtained her bachelor's and master's in electrical engineering at the University of Chile in 2018. She is currently pursuing her doctor's in PV engineering, for which she is investigating failure modes in interconnections based on ECAs, and developing mitigation strategies and a methodology to accurately determine the contact resistivity of such joints.

Thomas Fischer received his Dipl. Ing. in mechanical engineering from the University of Magdeburg in 1995, after which he worked as a design engineer at FAM and then as an application engineer at THK. He has been with teamtechnik since 2008, where he is currently head of Mechanical Design & Technology Development. His expertise lies in solar cell soldering and the ECA stringing process.

Ingo Ullmann holds an engineering diploma in materials and surface technology, and has been involved in process and development engineering for over 20 years. Since 2017 he has been working in the Module Development Department at ISC Konstanz, where he specializes in shingled solar cells and conductive adhesive applications.

Dominik Rudolph studied microsystems engineering in Freiburg, Germany, and graduated with a Diploma in 2008. Since 2009 he has been working at ISC Konstanz, where he is currently a project manager and process engineer in the field of metallization and laser processes for silicon solar cells.

Andreas Halm studied physics at the University of Konstanz. He joined ISC in 2008, working on industrial solar cells fabricated from SoG-Si, and then worked his way up the value chain as far as module integration. He currently leads the Module Department, and is a member of the board of directors.

Enquiries
Daniel Tune
International Solar Energy Research Center
ISC Konstanz
Germany

Email: daniel.tune@isc-konstanz.de

Advertisers and web index

ADVERTISER	WEB ADDRESS	PAGE NO.
3D-Micromac	www.3d-micromac.com	55
Aiko Cells	en.aikosolar.com	Outside Back Cover
EUPVSEC	www.photovoltaic-conference.com	57
Exateq	www.exateq.de	29
h.a.l.m	www.halm.de	43
Henkel	www.henkel.com/	59, 61, 63
Intersolar	www.intersolar.de	Inside Back Cover
JA Solar	www.jasolar.com	Inside Front Cover
Kontron AIS	www.kontron-ais.com/en/	7
Meco Equipment Engineers	www.besi.com	47
Mondragon Assembly	www.mondragon-assembly.com	31
Nagase ChemteX America Corp	www.nagasechemtex.com/	66
Photovoltaics International	www.pv-tech.org/photovoltaics-international/	77
PV Manufacturing & Technology Quarterly Report	www.marketresearch.solarmedia.co.uk	72
PV Tech Premium	www.pv-tech.org/pv-tech-premium/	36
Sentech Instruments	www.sentech.com	15
SNEC PV Power Expo 2022	www.snec.org.cn	19
Von Ardenne	www.vonardenne.biz	39

To advertise within Photovoltaics International, please contact the sales department: Tel +44 (0) 20 7871 0122

inter
solar
connecting solar business

The World's Leading Exhibition Series
for the Solar Industry

INTERSOLAR EVENTS 2022

www.intersolar-events.com

JANUARY 13–15, 2022, LONG BEACH, USA
www.intersolar.us

MARCH 7–9, 2022, DUBAI, UAE
www.intersolar.ae

MAY 11–13, 2022, MUNICH, GERMANY
www.intersolar.de

AUGUST 23–25, 2022, SÃO PAULO, BRAZIL
www.intersolar.net.br

SEPTEMBER 6–8, 2022, MEXICO CITY, MEXICO
www.intersolar.mx

DECEMBER 2022, MUMBAI, INDIA
www.intersolar.in

INTERSOLAR SUMMITS WORLDWIDE
www.intersolar-summit.com

FOLLOW US